ADVANCES IN GEOPHYSICS, VOLUME 21

THE INFLUENCE OF MOUNTAINS ON THE ATMOSPHERE

RONALD B. SMITH

Department of Geology and Geophysics
Yale University
New Haven, Connecticut

1. AN INTRODUCTION TO MOUNTAIN EFFECTS

It is often said that if the Earth were greatly reduced in size while maintaining its shape, it would be smoother than a billiard ball. From this viewpoint the mountains on our planet seem insignificant, and it makes us wonder how they manage to have such a strong influence on our wind and weather. One answer to the dilemma is that the atmosphere itself is

ISBN 0-12-018821-X

very shallow—a density scale height of about 8.5 km—so that many mountains reach to a significant fraction of its depth. This argument, however, underestimates the mountain effect. The real answer is that our atmosphere is exceedingly sensitive to vertical motion—and for two reasons.

First, its strong stable stratification gives the atmosphere a resistance to vertical displacement. Buoyancy forces will try to return vertically displaced air parcels to their equilibrium level even if such restoration requires a broad horizontal excursion or the generation of strong winds. Second, the lower atmosphere is usually so rich in water vapor that slight adiabatic ascent will bring the air to saturation, leading to condensation and possibly precipitation. As an example, the disturbance caused by a 500-m high mountain (i.e., a very small fraction of the atmospheric depth) could well include (a) broad horizontal excursions of the wind as it tries to go around rather than over the mountain, (b) severe downslope winds as air that has climbed the mountain runs down the lee side, and (c) torrential orographic rain on the windward slopes.

The intention of this article is to review the meteorological phenomena that are associated with topography. This topic is of course only one of several subdisciplines within physical and dynamical meteorology, but it is one which scientists should be familiar with as they struggle to understand the workings of the atmospheric system. This review will not supersede previous works such as "The airflow over mountains" by Queney *et al.* (1960) as it is in many ways less detailed. On the other hand, the range of phenomena and scales included here is broader than in previous reviews. Because of the lack of detail, the experts in the various areas will probably find little for them except a widened awareness which comes from seeing their specialty placed into a broader setting.

The study of airflow past mountains is complicated by the wide range of scales that must be considered. The nature of the disturbance caused by a narrow hill will be quite different from that caused by a broad plateau, even if the terrain height and other factors are the same. This is so because there are several natural length scales in the atmospheric system with which the mountain width (say, L) can be compared. These include (with scale increasing):

1. the thickness of the atmospheric boundary layer
2. the distance of downwind drift during a buoyancy oscillation
3. the distance of downwind drift during the formation and fallout of precipitation
4. the distance of downwind drift during one rotation of the Earth
5. the Earth radius

The ratios of the mountain width to each of the natural length scales are important in determining the physical regime of the flow. This idea is emphasized in the present article by treating the effects of boundary layers and buoyancy (length scales 1 and 2) in Section 2, the effect of the Earth's rotation (length scale 4) in Section 3, and the effect of the Earth's curvature (length scale 5) in Section 5. The section on orographic rain (Section 4) includes mountain scales both shorter and longer than the natural cloud physics length scale (length scale 3).

In the past several years there have been some remarkable advances in the understanding of mountain flows and yet there are many outstanding problems. A partial list of these will serve to illustrate the vigor and breadth of the subject. Theoretically and observationally the distinction between trapped lee waves and vertically propagating mountain waves is now clear. In most cases, however, it has still proved impossible to predict these waves accurately. In spite of recent work on large-amplitude waves and wave breaking, the connection with downslope wind storms is still unclear. The studies of flow around realistic mesoscale mountains ($L \sim$ 100–500 km) has just begun. New theoretical results have invalidated the "textbook" descriptions of vortex stretching over broad mountains. The strong variation in rainfall amount between the top and bottom of small hills now has been demonstrated but the physical cause is undetermined. There is mounting evidence that much of the presumed stable orographic rain may in fact be generated by closely spaced convection, triggered by orographic lifting. Numerical simulations indicate that the general circulation of the atmosphere may be strongly influenced by the major mountain systems. The midlatitude westerlies are deflected into standing waves which produce zonal variations in climate and, by transporting heat northward, reduce the frequency and strength of cyclonic storms.

2. The Flow over Hills and the Generation of Mountain Waves

The flow over small-scale mountains or hills (100 m to 50 km wide) can be considered without including the Coriolis force. One would expect however that the influence of buoyancy forces and the turbulent Reynolds stresses acting in the boundary layer will be important. Two natural length scales thus arise: first, the distance of downwind drift during a buoyancy oscillation (U/N) $\approx$ 1 km, and second, the thickness of the boundary layer, $\delta \approx$ 300 m. Of course, all these parameters U,N,δ depend ultimately on the Coriolis force, but the local problem is usually

considered to be well posed if these parameters are known. For a narrow hill (say, $L = 100$ m $\ll U/N$) the characteristic time for the flow, that is, the time it takes an air parcel to cross the hill, is much less than the buoyancy period, and the buoyancy forces can be neglected. If there were no boundary layer or if the boundary layer were very thin, this "narrow hill" flow would be closely analogous to the irrotational (i.e., potential) flow much studied in engineering aerodynamics. In fact, in the atmosphere, there is a thick preexisting boundary layer, and the disturbance caused by a narrow hill is for the most part confined within the boundary layer. Thus the aerodynamic analogy is not a good one.

For wider hills ($L \sim 1$ km and greater) the boundary layer thickness becomes smaller in relation to the scale of the flow. At the same time, the buoyancy force associated with the atmosphere's static stability becomes more important. The flow outside the boundary layer cannot be considered irrotational, and internal gravity waves become possible. For still wider mountains ($L \sim 10$ km) the boundary layer seems vanishingly thin, and the buoyancy forces dominate to the extent that the vertical accelerations become relatively small and the pressure field is nearly hydrostatic. Finally, for mountains wider than about 50 km (depending on the wind speed) the Coriolis force begins to become important. This added complication will not be considered in this section but will be treated in some detail in the following section on mesoscale flows.

The cornerstone of this subject seems to be the huge body of literature on the theory of inviscid mountain waves. There have in fact already been several reviews of this subject (e.g., Queney *et al.*, 1960; Miles, 1969; Musaelyan, 1964; Eliassen, 1974; Vinnichenko *et al.*, 1973; Kozhevnikov, 1970), and the existence of these somewhat lessens the demands on this section. In response to this we will back off and attempt a less detailed overview of the subject. A more detailed discussion will be necessary only on matters of continuing controversy or points that have only recently been clarified.

It is also important to keep in mind that a theoretical understanding of the inviscid problem is probably not sufficient. The interaction of the inviscid flow with the turbulent boundary layer and the turbulent regions of wave breakdown aloft could completely change the flow just as in aerodynamics where the separation of a thin boundary layer completely invalidates the potential flow solution. More on this point later.

2.1. Buoyancy Forces

In order to understand the transition from small-scale irrotational flow to larger scale, buoyancy-dominated hydrostatic flow, we examine the

vertical momentum equation for an inviscid fluid

$$\rho \frac{Dw}{Dt} = -\frac{\partial p}{\partial z} - \rho g \tag{2.1}$$

Consider a parcel of fluid of density ρ_P surrounded by a fluid of density ρ. If the surroundings are not accelerating, the pressure field will be hydrostatic

$$\frac{\partial p}{\partial z} = -\rho g \tag{2.2a}$$

$$p = p_0 - \rho g z \tag{2.2b}$$

where p_0 is an arbitrary reference pressure. Any object placed in such a linear pressure field feels a net force equal to its volume times the pressure gradient [this follows from the derivation of (2.1) or from Archimedes Law]. The net force on the parcel is the sum of the net pressure force and the gravitational force

$$\rho g = \rho_P g = g(\rho - \rho_P) \tag{2.3}$$

and this is the so-called buoyancy force. If the parcel is less dense than its surroundings, the buoyancy force will act upward and vice versa.

One important property of the buoyancy force is that it can create vorticity in the fluid by applying a torque about the center of mass of a fluid parcel. It is well known that the gravitational force cannot create vorticity as it is a "potential" force field and always acts through the center of mass. The buoyancy force, however, includes a pressure force term and it is this, that can create vorticity.

The alert reader will have already noticed a weakness in the above parcel agreement. If there is a net buoyancy force acting on the parcel then it will be accelerating and the fluid nearby the parcel will also be accelerating to keep out of the way. Thus our assumption that the surrounding fluid is hydrostatic is incorrect and the clear definition of buoyancy force fades slightly. If the parcel could be persuaded to hold its shape (e.g., a sphere), the effect of the accelerations could be easily accounted for by using the hydrodynamic theory of "added mass" but this too is an abstraction. The best way to resharpen our view of buoyancy is to consider its effect on a consistent field of fluid motion, and this will be done later when we consider the motion field induced by mountains.

The generation of density differences can occur in two ways, either by a local heating or cooling, or by moving an air parcel from one environment to another. In the latter case, the resulting density variation can be

associated either with the differing properties of the "source" environment or with density alterations during the displacement, for example, adiabatic expansion. For either of the above mechanisms (i.e., heating/cooling or displacement) the resulting density variation can be computed easily by assuming that the parcel has come to pressure equilibrium with its new environment. Any pressure imbalance would be quickly eliminated by the generation and propagation away of acoustic waves. The potential temperature

$$\theta = T(P/P_0)^{\kappa} \tag{2.4}$$

(P_0 is an arbitrary reference pressure, κ is the ratio of R/c_p for the gas in question) is especially useful as it is conserved during adiabatic lifting or sinking. Any parcel A having a higher potential temperature than some remote environment B ($\theta_A > \theta_B$) will, when brought into environment B (i.e., brought to the pressure P_B), be warmer ($T_A > T_B$) and less dense ($\rho_A < \rho_B$) than its environment and will experience an upward buoyancy force. This parcel argument can also be used to show (as is done in most meteorology texts) that an environment in which potential temperature increases with height ($d\theta/dz > 0$) is stable since any vertical displacement will result in a restoring buoyancy force.

2.2. *The Theory of Two-Dimensional Mountain Waves*

2.2.1. The Governing Equations. The theoretical description of mountain waves begins with the following set of equations (restricted here to two dimensions):

the horizontal momentum equation:

$$\rho \frac{Du}{Dt} = -\frac{\partial p}{\partial x} \tag{2.5}$$

the vertical momentum equation:

$$\rho \frac{Dw}{Dt} = -\frac{\partial p}{\partial z} = -\rho g \tag{2.6}$$

the equation of continuity:

$$\frac{D\rho}{Dt} = -\rho \nabla \cdot \vec{u} \tag{2.7}$$

an equation describing adiabatic, reversible changes (derived from the first law of thermodynamics, the definition of specific heat, and the

perfect gas law):

$$\frac{Dp}{Dt} = c^2 \frac{D\rho}{Dt}, \qquad c^2 = \gamma RT \tag{2.8}$$

the perfect gas law:

$$p = \rho RT \tag{2.9}$$

With these equations we can examine the small perturbations produced by a mountain on a basic state of horizontal hydrostatic flow described by

$$\bar{U}(z),\ T(z) \qquad \text{specified}$$

$$\bar{W}(z) = 0$$

and $\bar{p}(z)$, $\bar{\rho}(z)$ determined from

$$d\bar{p}/dz = -\bar{\rho} g \tag{2.10}$$

and

$$\bar{p} = \bar{\rho} R \bar{T} \tag{2.11}$$

Each variable will be represented as a sum of the basic value and a perturbation

$$\begin{aligned} u(x, z) &= \bar{U}(z) + u'(x, z) \\ w(x, z) &= 0 + w'(x, z) \\ \rho(x, z) &= \bar{\rho}(z) + \rho'(x, z) \\ p(x, z) &= \bar{p}(z) + p'(x, z) \\ T(x, z) &= \bar{T}(z) + T'(x, z) \end{aligned} \tag{2.12}$$

We have assumed further that the flow will eventually come to a steady state and it is this state that we seek.

Upon substituting (2.12) into the governing equations and linearizing, we obtain the following equations for the perturbation quantities:

From (2.5):

$$\bar{\rho}\left(\bar{U}\frac{\partial u'}{\partial x} + w'\frac{d\bar{U}}{dz}\right) = -\frac{\partial p'}{\partial x} \tag{2.13}$$

From (2.6):

$$\rho\left(\bar{U}\frac{\partial w'}{\partial x}\right) = -\frac{\partial p'}{\partial z} - \rho' g \tag{2.14}$$

From (2.7):

$$\bar{U}\frac{\partial \rho'}{\partial x} + w'\frac{d\bar{\rho}}{dz} = -\bar{\rho}\left(\frac{\partial u'}{\partial x} + \frac{\partial w'}{\partial z}\right) \tag{2.15}$$

From (2.8):

$$\bar{U}\frac{\partial p'}{\partial x} + w'\frac{d\bar{p}}{dz} = \bar{c}^2\left(\bar{U}\frac{\partial \rho'}{\partial x} + w\frac{d\bar{\rho}}{dz}\right) \tag{2.16}$$

which can be written as

$$\frac{\bar{U}}{\bar{\rho}}\frac{\partial \rho'}{\partial x} = w'\left(\frac{-1}{\bar{\rho}}\frac{d\bar{\rho}}{dz} + \frac{g}{\bar{c}^2}\right) - \frac{\bar{U}}{\bar{\rho}\bar{c}^2}\frac{\partial p'}{\partial x} \tag{2.17}$$

(a) (b) (c) (d)

This last equation warrants special attention as it describes the formation of density anomalies which in turn [through Eq. (2.14)] produce buoyancy forces. The left-hand side (a) is the rate of change of density encountered by an observer moving horizontally downstream at a speed $\bar{U}(z)$. The right-hand side represents the causes for the observed density variations. Term (b) represents the lifting of denser air into a less dense environment, but this is strongly modified by term (c), the adiabatic expansion of the parcel as it is lifted. Terms (b) and (c) can be combined to read

$$\frac{1}{\bar{\theta}}\frac{d\bar{\theta}}{dz} = \beta \tag{2.18}$$

which is a measure of the static stability. The final term (d) is a correction for any lack of pressure equilibration. For fast acoustic waves this term is of central importance, but for lower frequency motions, such as considered here, it is negligible. That is not to say that there are no pressure variations but only that these variations are not important in the generation of density anomalies. As shown by Queney *et al.* (1960) the retention of term (d) substantially complicates the analysis, but if $\bar{U}^2 \ll \bar{c}^2$(e.g. $10^2 \ll 300^2$) it many be neglected. In this limit the continuity equation is simplified [substitute (2.17) into (2.15)] to

$$\frac{\partial u'}{\partial x} + \frac{\partial w'}{\partial z} = \frac{g}{\bar{c}^2}w \tag{2.19}$$

so that the divergence in the velocity field is clearly associated with the adiabatic ascent of air parcels.

The previous equations can be reduced among themselves to obtain a

single equation for the vertical velocity $w(x, z)$

$$w'_{xx} + w'_{zz} - \bar{S}w'_z + \left(\frac{\beta g}{\bar{U}^2} + \frac{\bar{S}\bar{U}_z}{\bar{U}} - \frac{\bar{U}_{zz}}{\bar{U}}\right) w' = 0 \tag{2.20}$$

with the subscripts denoting differentiation. The coefficient $\bar{S}$ is defined by

$$\bar{S} \equiv \frac{d}{dz} \ln \bar{\rho}(z) \tag{2.21}$$

and has been called the heterogeneity by Queney (1947). $\bar{S}$ is not related to the generation of buoyancy forces as it does not include the effect of adiabatic expansion but instead describes the effect of density variations in the divergence of the velocity field [Eq. (2.19)] and the vertical variation in inertia in the momentum equations (2.13) and (2.14). The first term involving $\bar{S}$ in (2.20) cannot be neglected even if $\bar{S}$ is small as it will always result in an amplification of the disturbance in the far field. It can be neatly accounted for by introducing the new dependent variable

$$\hat{w} \equiv [\bar{\rho}(z)/\bar{\rho}(0)]^{1/2} w' \tag{2.22}$$

The square of this new variable is proportional to the energy of the wave disturbance (see Eliassen and Palm, 1960). Equation (2.20) then becomes

$$\hat{w}_{xx} + \hat{w}_{zz} + l^2(z)\hat{w} = 0 \tag{2.23}$$

with

$$l^2(z) \equiv \frac{\beta g}{\bar{U}^2} + \frac{\bar{S}\bar{U}_z}{\bar{U}} - \frac{1}{4}\bar{S}^2 + \frac{1}{2}\bar{S}_z - \frac{\bar{U}_{zz}}{\bar{U}}$$

This equation is the central tool for theoretical studies of small-amplitude, two-dimensional mountain waves. In practice, the coefficient $l^2(z)$ is usually dominated by the first term, that is, the buoyancy force term $\bar{\beta}g/\bar{U}^2$; although in regions of strong shear the term $\bar{U}_{zz}/\bar{U}$ may become important. The neglect of the $\bar{S}$ terms is equivalent to making the Boussinesq approximation—that density variations are only important as they effect the buoyancy. In this case Eq. (2.23) may be easily interpreted as a vorticity equation with (upon multiplying through by $\bar{U}$) $\bar{U}(w_{xx} + w_{zz})$ being the rate of change of vorticity following a fluid particle; $\bar{\beta}gw/\bar{U}$ being the rate of vorticity production by buoyancy forces; and $-\bar{U}_{zz}w$ being the rate of production of perturbation vorticity by the redistribution of background vorticity ($\sim \bar{U}_z$). In the case of $l^2(z) = 0$, we have

$$\nabla^2 \hat{w} = 0 \tag{2.24}$$

which states that the flow is irrotational.

2.2.2. The Flow over Sinusoidal Topography. It is helpful at this point to examine the flow of a semi-infinite stratified atmosphere over sinusoidal topography (see Queney, 1947). The choice of sinusoidal topography simplifies the solution, thereby clarifying the underlying physics, and also paves the way for the use of Fourier methods in the next section.

Consider the flow of uniform incoming wind speed $\bar{U}(z) = \bar{U}$ and Brunt—Vaisala frequency $N^2 = \bar{\beta}g$, over terrain described by $z = h(x) = h_m \sin kx$, where h_m and $k = 2\pi/\text{wavelength}$ describe the height and spacing of the ridges. At the ground the flow is assumed to follow the terrain so that the streamline slope equals the terrain slope

$$\frac{w}{u} = \frac{w'}{\bar{U} + u'} = \frac{dh}{dx} \qquad \text{at} \quad z = h(x) \tag{2.25}$$

For small amplitude topography (and disturbance u') this simplifies to

$$w' = \hat{w} = \bar{U}(dh/dx) \qquad \text{at } z = 0 \tag{2.26}$$

so

$$\hat{w}(x, 0) = h_m k \cos kx \tag{2.27}$$

We will look for solutions (here using real functions and variables) of the form

$$\hat{w}(x, z) = \phi_1(z) \cos kx + \phi_2(z) \sin kx \tag{2.28}$$

so the equation for these ϕ functions becomes from (2.23)

$$\phi_{zz} + (l^2 - k^2)\phi = 0 \tag{2.29}$$

The k in (2.29) will be the same as the terrain wave number in (2.27), in order to satisfy (2.27).

In this equation the sign of the term in parentheses is of central importance. We must consider two cases: first, the case of closely spaced ridges (together with weak stability and high wind speed) such that

$$k^2 > l^2 \tag{2.30}$$

For example, if N and U are chosen to have typical values of 0.01 sec^{-1} and 10 m/sec respectively, then condition (2.30) will be satisfied for topographic wavelengths

$$\lambda = 2\pi/k < 6.3\,\text{km}$$

In this case the term in parentheses in (2.29) is negative and the solution is

$$\phi(z) = A \exp[(k^2 - l^2)^{1/2} z] + B \exp[-(k^2 - l^2)^{1/2} z] \tag{2.31}$$

The first term represents an unlimited growth of the disturbance energy away from the terrain, which should be considered as source of the disturbance. This runs counter to our intuition and to laboratory experience and must be regarded as unphysical. Therefore we set $A = 0$ and the solution becomes [from (2.31), (2.28), (2.27)]

$$\hat{w}(x, z) = h_m k \exp[-(k^2 - l^2)^{1/2} z] \cos kx \tag{2.32}$$

The other variables u', p', T, ρ can be easily determined from $\hat{w}(x, z)$ by using the original equations (2.13)-(2.17). The streamline pattern corresponding to (2.32) is shown in Fig. 1a.

The other possibility is

$$k^2 < l^2 \tag{2.33}$$

which corresponds to more widely spaced ridges or alternatively, greater stability and slower wind speed. Here the term in parentheses in (2.29) is positive and the solution is

$$\phi(z) = A \sin(l^2 - k^2)^{1/2} z + B \cos(l^2 - k^2)^{1/2} z \tag{2.34}$$

Combining this with (2.28) and using a trigonometric identity gives the

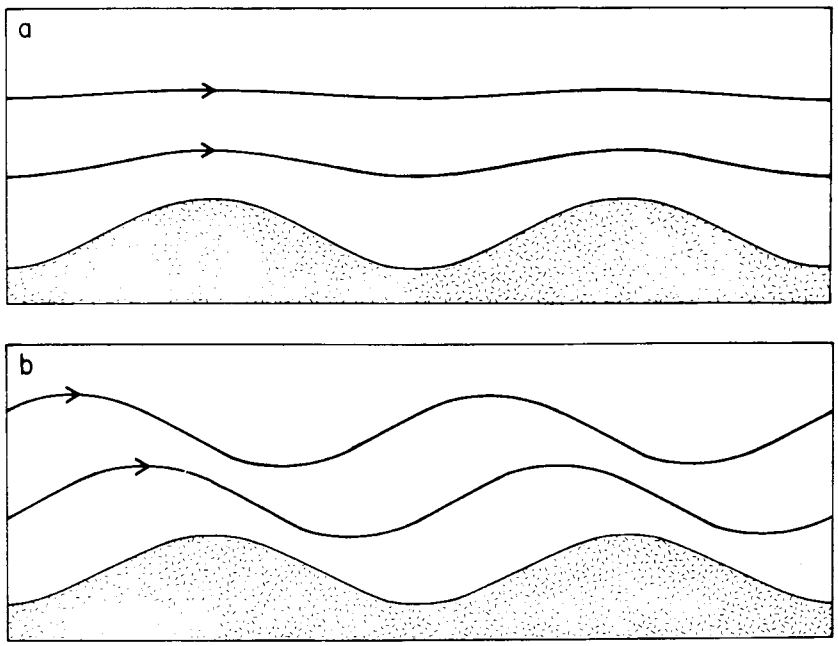

FIG. 1. The steady inviscid flow over two-dimensional sinusoidal topography. (a) Little or no influence of buoyancy, $Uk > N$. The disturbance decays upward with no phase line tilt. (b) Strong buoyancy effects, $Uk < N$. The disturbance amplitude is constant with height while the lines of constant phase tilt strongly upstream.

vertical velocity in convenient form

$$\begin{aligned}\hat{w}(x, z) = {} & C\cos[kx + (l^2 - k^2)^{1/2}z] \\ & + D\cos[kx - (l^2 - k^2)^{1/2}z] \\ & + E\sin[kx + (l^2 - k^2)^{1/2}z] \\ & + F\sin[kx - (l^2 - k^2)^{1/2}z]\end{aligned} \tag{2.35}$$

where the upward and downward propagating waves are now recognizable. The lower boundary condition (2.27) requires $E + F = 0$ as well as

$$C + D = h_m k \tag{2.36}$$

and as before, the remaining indeterminacy between E and F, and C and D requires the use of an upper boundary condition.

As shown by Eliassen and Palm (1960), disturbance energy can be transferred from one region of the fluid to another by doing work at the boundary between the two regions. In an inviscid electrically neutral fluid, as we have here, this work is done by pressure forces acting together with displacements across the boundary. Thus the vertical flux of energy across a horizontal surface is

$$\int_{-\infty}^{\infty} p'w'\,dx \tag{2.37}$$

Eliassen and Palm also show that for $\bar{U}^2 \ll \bar{c}^2$ the vertical flux of energy, averaged over a wavelength, can be written in terms of the field of vertical velocity

$$\overline{p'w'} = \frac{\bar{U}\bar{\rho}}{k^2}\,\overline{w_x' w_z'} \tag{2.38}$$

A comparison of this with the solution (2.35) shows that the C and E terms, with phase lines tilting to the left, produce an upward energy flux (i.e., p' in phase with w'). The opposite is true for the D and F terms. Physically we regard the irregular terrain as the source of the disturbance energy so in the absence of energy production or reflection aloft, terms D and F must be regarded as unphysical and we set $D = F = 0$. This gives $E = 0$ and $C = h_m k$ so that

$$\hat{w}(x, z) = h_m k\cos[kx + (l^2 - k^2)^{1/2}z] \tag{2.39}$$

The streamlines for this are shown in Fig. 1b. Note that in the above argument it is not sufficient to require that the net energy flux be upward, as this only demands $C + E > D + F$. Instead we must require that

there be no components of the flow which radiate energy downward. This "radiation condition" will be discussed again in the next section.

The difference between the two types of flow $k^2 > l^2$ or $k^2 < l^2$ is striking and deserves discussion. In the case of closely spaced topography the flow is qualitatively similar to irrotational flow (i.e., $l^2 = 0$) in that the phase lines are vertical and the disturbance decays with height. This flow is inherently nonhydrostatic as the w'_{xx} term in (2.20) carries the influence of the vertical accelerations and it is this term which allows the disturbance to decay vertically. In fact there is a crude balance between the vertical decay of the pressure disturbance and the vertical accelerations. As $k^2 \to l^2$ this balance is increasingly altered by buoyancy forces and the vertical penetration of the disturbance increases.

When $k^2 < l^2$ the intrinsic frequency of the motion $\bar{U}k$ (i.e., the frequency experienced by a fluid parcel moving through the stationary pattern) is less the N, the Brunt-Vaisala (or buoyancy) frequency, and internal gravity waves are therefore possible. These waves propagate vertically and thus the disturbance does not decay upward. The phase lines tilt forward into the mean wind, and as we have seen this is connected with the propagation of energy vertically away from the topography that produces the wave.

Vertical accelerations play only a modifying role in this wave motion. For the case $l^2 \gg k^2$ we can ignore the k^2 term in (2.29) and this is equivalent to making the hydrostatic assumption in (2.14). In this case the vertical wave number of the disturbance is

$$(l^2 - k^2)^{1/2} \approx l \tag{2.40}$$

which depends only on the characteristic of the airstream, not on k.

Note that with $l^2 > k^2$ the flow near the hills is asymmetric with low speed and high pressure on the windward side and high speed and low pressure on the leeward side. Thus there is a pressure drag on the ridges and this momentum is transported vertically by the waves. The amplitude of this "wave drag" averaged over a wide area is

$$\bar{\rho}\,\overline{u'w'} = \bar{\rho}\,\bar{U}^2 k(l^2 - k^2)^{1/2} h_m^2 \quad \text{per unit area} \tag{2.41}$$

2.2.3. Isolated Topography. Although much of the interesting physics of mountain waves was captured in the foregoing constant l^2, sinusoidal terrain model, there are still new concepts which arise in the flow over a single ridge and still more when we allow $l^2(z)$ to vary. Following Lyra (1943), Queney (1947), and Queney *et al.* (1960), we express all disturbance variables in terms of a one-sided Fourier integral. For example, the

vertical velocity is written as

$$\hat{w}(x, z) = \mathrm{Re} \int_0^\infty \tilde{w}(k, z) e^{+ikx}\, dk \tag{2.42}$$

substituting this into (2.23) gives an expression for $\tilde{w}(k, z)$

$$\tilde{w}_{zz} + [l^2(z) - k^2]\tilde{w} = 0 \tag{2.43}$$

The lower boundary condition (2.26) becomes

$$\tilde{w}(k, 0) = \bar{U}(0) ik \tilde{h}(k) \tag{2.44}$$

where $\tilde{h}(k)$ is the Fourier transform of the mountain shape,

$$\tilde{h}(k) = \frac{1}{\pi} \int_{-\infty}^{\infty} h(x) e^{-ikx}\, dx \tag{2.45}$$

For the case of $l^2 = \text{const}$, the solution to (2.43) is for $k^2 > l^2$

$$\tilde{w}(k, z) = \tilde{w}(k, 0) \exp[-(k^2 - l^2)^{1/2} z] \tag{2.46}$$

and for $k^2 < l^2$

$$\tilde{w}(k, z) = \tilde{w}(k, 0) \exp[i(l^2 - k^2)^{1/2} z] \tag{2.47}$$

In each case the arbitrariness in the sign of the exponent allowed by (2.43) has been eliminated by using an upper boundary condition. In the evanescent case the solution is assumed to decay rather than grow as $z \to \infty$, while in the propagating case the positive sign is chosen in the exponential so that the phase lines tilt upstream and energy is propagated upward. In this case of constant $\bar{U}$, it is slightly more convenient to solve directly for the vertical displacement of a streamline $\eta(x, z)$ where

$$w' = \bar{U}(\partial \eta / \partial x) \tag{2.48}$$

Then using (2.42), (2.44), (2.46), and (2.47)

$$\begin{aligned} \eta(x, z) = [\rho_0/\rho(z)]^{1/2} \mathrm{Re} \int_0^l h(k) \exp[i(l^2 - k^2)^{1/2} z] \exp(ikx)\, dk \\ + \int_l^\infty \tilde{h}(k) \exp[-(k^2 - l^2)^{1/2} z] \exp(ikx)\, dk \end{aligned} \tag{2.49}$$

For the purpose of illustration it has become standard practice (after Queney, 1947) to consider a bell-shaped mountain described by

$$\tilde{h}(x) = h_m a^2/(x^2 + a^2) \tag{2.50}$$

which has a particularly simple Fourier transform

$$\tilde{h}(k) = h_m a e^{-ka} \tag{2.51}$$

The height of the ridge is h_m, and a is a measure of its width. The function $\tilde{h}(k)$ happens to be real because the ridge is symmetric. The type of flow predicted by (2.49) with (2.51) depends on the dimensionless quantity al which is proportional to the ratio of the time it takes for a fluid particle to cross the ridge, to the period of a buoyancy oscillation $2\pi/N$. Even with the choice (2.50) the exact evaluation of (2.49) is readily done only for the two limiting cases $al \gg 1$ or $al \ll 1$.

For the narrow mountain, weak stability, and strong winds, al is small and the first integral in (2.49) becomes small; while the second becomes

$$\begin{aligned} \eta(x, z) &= [\rho_0/\rho(z)]^{1/2} \operatorname{Re}\left[h_m a \int_0^\infty e^{-ka}\, e^{-kz}\, e^{ikx}\, dk \right] \\ &= [\rho_0/\rho(z)]^{1/2} h_m a \operatorname{Re}\left[\frac{-1}{-(a+z) + ix} \right] \end{aligned} \tag{2.52}$$

and taking the real part

$$\eta(x, z) = \left[\frac{\rho_0}{\rho(z)} \right]^{1/2} \frac{h_m a (a+z)}{(a+z)^2 + x^2} \tag{2.53}$$

Note that as $z \to 0$, $\eta(x, z) \to h(x)$ given by (2.50) as it should. In this $al \ll 1$ limit, the buoyancy force is not important and the flow is irrotational. This same flow field could have been constructed from potential flow theory by placing a doublet slightly below the ground. The streamline pattern is shown in Fig. 2.

In the opposite extreme case, $al \gg 1$, buoyancy effects dominate and the flow is hydrostatic. Mathematically, $\tilde{h}(k)$ is small in the range $l <$

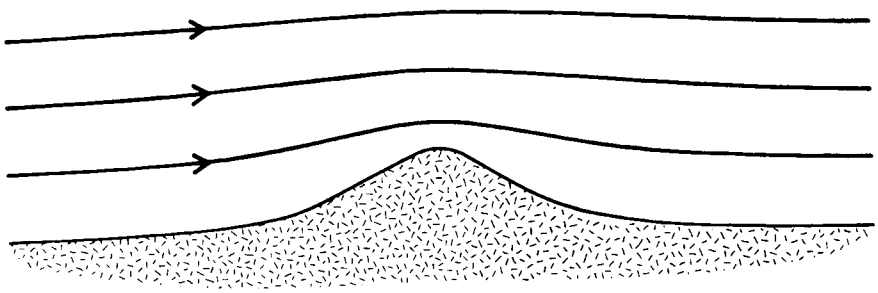

FIG. 2. The steady flow of a homogeneous fluid over an isolated two-dimensional ridge, given by (2.53). From the spacing of the streamlines, it is evident that the highest speed and the lowest pressure will occur at the top of the ridge.

$k < \infty$, so the second integral in (2.49) makes no contribution. Then

$$\eta(x, z) = [\rho_0/\rho(z)]^{1/2} \operatorname{Re}\left[h_m a \int_0^\infty e^{-ka}\, e^{ilz}\, e^{ikx}\, dk \right] \tag{2.54}$$
$$= [\rho_0/\rho(z)]^{1/2} h_m a \operatorname{Re}\left[\frac{-1}{-a + i(lz + kx)} \right]$$

taking the real part

$$\eta(x, z) = \left[\frac{\rho_0}{\rho(z)} \right]^{1/2} h_m a \frac{(a \cos lz - x \sin lz)}{a^2 + x^2} \tag{2.55}$$

This flow (shown in Fig. 3) is best described as a field of nondispersive

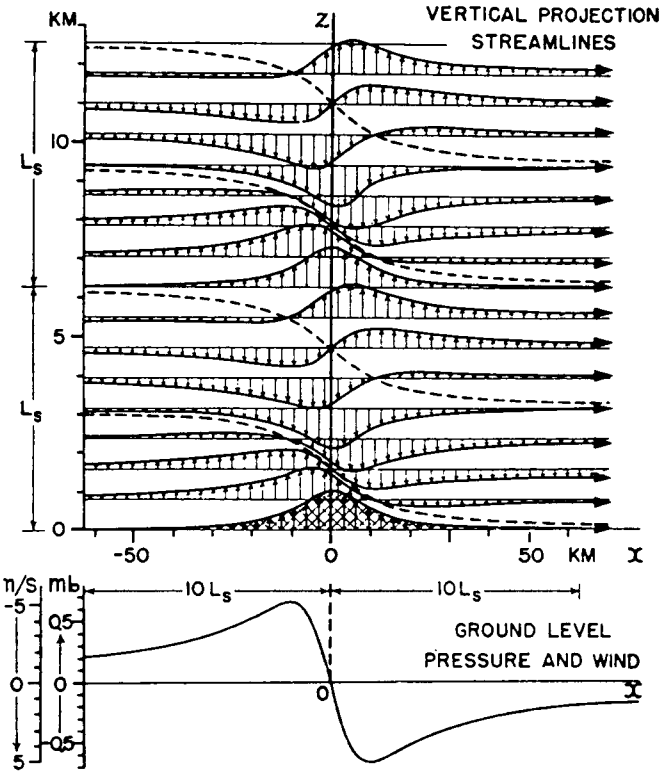

FIG. 3. Buoyancy-dominated hydrostatic flow over an isolated two-dimensional ridge, given by (2.56). The disturbance is composed of vertically propogating internal gravity waves of the sort shown in Fig. 1b. The evident upstream tilt of the phase lines indicates that disturbance energy is propagating upward away from the mountain. The maximum wind speed and minimum pressure occur on the lee slope of the ridge. The mountain height h_m = 1 km, the half-width a = 10 km, the mean wind speed U = 10 m/sec, the Brunt-Vaisala frequency N = 0.01 sec^{-1}, and the vertical wavelength $L_s = 2\pi U/N$ = 6.28 km. (From Queney, 1948.)

vertically propagating waves. The flow is periodic in the vertical so that at $z = \pi/l$ the streamline shape is the inverted ridge shape $h(x)$ and at $z = 2\pi/l$ the ridge is reformed upright. This is true for any ridge shape, not just $h(x)$ given by (2.50). The upstream tilt of the phase lines, which we required of the individual Fourier components, is still very noticeable in the composite flow. This asymmetry to the flow, which is associated with the vertical propagation of wave energy, has a number of implications. From the distance between the streamlines in Fig. 3 it is apparent that the wind speed is low on the windward slope of the ridge and faster on the leeward slope. From Bernoulli's equation, this requires a pressure difference across the ridge—high pressure upwind and lower pressure downwind. The primary reason for windward-side high pressure is the thickened layer of dense cool air just above the mountain, but this in turn is related to the radiation condition aloft.

The pressure difference results in a net drag on the mountain which can be computed either as the horizontal pressure force on the mountain

$$D = \int_{-\infty}^{\infty} P'(x, z = 0) \frac{dh}{dx} dx \tag{2.56}$$

or equivalently, as the vertical flux of horizontal momentum in the wave motion

$$D = \rho(z) \int_{-\infty}^{\infty} u'w' dx \tag{2.57}$$

For the bell-shaped mountain, the drag per unit length is (using 2.55 and 2.56)

$$D = \frac{\pi}{4} \rho_0 N U h_m^2 \tag{2.58}$$

This momentum is transferred to a level where the wave breaks down—a process not included in the linearized model. Mountain wave drag is discussed in more detail by Sawyer (1959), Eliassen and Palm (1960), Blumen (1965), Miles (1969), and Bretherton (1969) among others. Direct measurements of mountain drag using (2.56) or (2.57) have been attempted by Lilly (1978) and Smith (1978a).

The increase in wind speed on the lee slope is an especially interesting facet of the model. It has been invoked as an explanation for severe downslope winds found occasionally in the lee of mountain ranges. Frequently the strong lee-side winds are warm and dry, replacing colder air, and in this case it is proper to call the wind a föhn or foehn (chinook is the local name in the northwest United States; it is called the Santa Ana

in California). There has been a good deal of work concerning the relationships between the föhn, the downslope wind storm (these two are not necessarily the same), and the generation of mountain waves. Descriptions of the föhn phenomena can be found in Defant (1951), Stringer (1972), Godske *et al.* (1957), Brinkman (1970, 1971), Holmes and Hage (1971), and Beran (1967). The application of mountain wave theory to this problem can be found crudely treated in Holmes and Hage (1971), Beran (1967), and in more complete form in Vergeiner (1971, 1976) and Klemp and Lilly (1975). Other theories of the generation of strong lee-side winds, such as the hydraulic theories of Kuettner (1958) and Houghton and Isaacson (1970) and the trapped lee-wave theories (see Holmes and Hage, 1971), appear to be less well founded—but will be discussed later.

It is clear from the discussion above that the qualitative description and interpretation of mountain wave theory hinges crucially on the use of the correct radiation condition aloft. In 1949, R. Scorer wrote what is now considered to be a classic paper describing the physics of trapped lee waves (a subject that will be treated later in this review). As a sidelight to his treatment he computed the vertically propagating wave field—just as we have done here—but using an incorrect radiation condition. In the controversy that followed (see Scorer, 1958; Corby and Sawyer, 1958; Palm, 1958a) the physical arguments of Lyra (1943) and Queney (1947) involving friction, of Palm (1958a) concerning the approach to steady state, and of Eliassen and Palm (1954, 1960) concerning the vertical flux of energy, clearly carried the day. The use of the radiation condition prohibiting downcoming energy is now standard among researchers of this subject. Unfortunately there is still some confusion on this point among researchers in other fields who wish to use the results of mountain wave theory. One of Scorer's (1949) figures, showing downstream (and therefore incorrect) phase line tilt has been reproduced in reviews such as Queney *et al.* (1960), Vinnichenko *et al.* (1973), Kozhevnikov (1970), Stringer (1972), and Scorer (1978). Confusion on this point is also evident in studies of the föhn (Beran, 1967; Holmes and Hage, 1971), orographic rain (Atkinson and Smithson, 1974), and blocking (Scorer, 1978). Recently the wider understanding of the concept of group velocity and the favorable comparison of theoretical solutions with numerical and laboratory experiments have eliminated most of the remaining confusion. Scorer (1978), however, seems to cloud the issue by discussing the radiation condition as if it were only one of several equally plausible choices.

The calculation of the inverse Fourier integral (2.49) for the solution of stratified flow over a bell-shaped ridge is more difficult in the case of

$al \sim 1$. In this case buoyancy forces are important but they do not dominate to the extent that the flow can be considered hydrostatic. This problem has been studied in detail by Queney (1947) using the asymptotic properties of Bessel functions and by Sawyer (1960) using numerical integrations. In this section we will apply directly the asymptotic technique of stationary phase to determine the nature of the flow far from the mountain.

The second integral in (2.49) containing the evanescent components will rapidly tend to zero as $z \to \infty$ because of the exponential decay of the integrand. At large $| x |$ this integral will again tend to zero as the rapid oscillations in e^{ikx} will cause cancellation of the contributions from the different wave numbers. The same kind of cancellation will occur in the first integral in (2.49) with one important difference. This integral can be written as

$$I = \int_0^\infty h(k) e^{i\phi(k)}\, dk \tag{2.59}$$

where the phase function

$$\phi(k) \equiv (l^2 - k^2)^{1/2} z + kx \tag{2.60}$$

For the most part, with either large $| x |$ or z, $\phi(k)$ is a rapidly varying function, but there is an obvious exception to this. Taking

$$\frac{\partial \phi}{\partial k} = \frac{-kz}{(l^2 - k^2)^{1/2}} + x = 0 \tag{2.61}$$

shows that $\phi(k)$ is approximately constant in the region near k^* defined by (2.61)

$$\frac{z}{x} = \frac{(l^2 - k^{*2})^{1/2}}{k^*} \tag{2.62}$$

Thus, far from the mountain, at any specified point (x, z), there is a range of wave numbers near k^* given by (2.62), whose contributions to the disturbance will not cancel themselves out. The noncanceling wave number k^* is constant along a straight line with slope given by (2.62), emanating from the origin where the mountain is located. The physical interpretation of this is that waves of that wave number k^* are generated by the mountain and are propagating away in the direction given by (2.62). Note from (2.62) that as $z > 0$, $k > 0$ waves will only be found for $x > 0$, that is, downstream of the obstacle. To evaluate the integral (2.59) we expand $\phi(k)$ in a Taylor series near k^*

$$\phi(k) = \phi(k^*) + \tfrac{1}{2}\phi_{kk}\hat{k}^2 \tag{2.63}$$

where $\hat{k} = k - k^*$. The only contribution to the integral (2.59) comes from k near k^* so approximately

$$I = \tilde{h}(k^*) \exp[i\phi(k^*)] \int_{-\infty}^{\infty} \exp[(i/2)\phi_{kk}\hat{k}^2]\, d\hat{k} \tag{2.64}$$

The definite integral in (2.64) can be simplified by the change of variable (this is equivalent to using the method of steepest descent)

$$\beta = \left(\frac{-i}{2}\phi_{kk}\right)^{1/2} \hat{k} \tag{2.65}$$

with the result that

$$\begin{aligned} I &= \tilde{h}(k^*) e^{i\phi(k^*)} \frac{\sqrt{\pi}}{[(-i/2)\phi_{kk}]^{1/2}} \\ &= \tilde{h}(k^*) e^{i\phi} \frac{(1+i)\sqrt{\pi}}{(\phi_{kk})^{1/2}} \end{aligned} \tag{2.66}$$

then

$$\eta(x, z) = [\rho_0/\rho(z)]^{1/2}\sqrt{\pi}\, \mathrm{Re}\left\{ \frac{\tilde{h}(k^*)}{(\phi_{kk})^{1/2}} e^{i\phi(k^*)}(1+i) \right\} \tag{2.67}$$

together with (2.45), (2.62), and $\phi_{kk} = -l^2 z/(l^2 - k^{*2})^{3/2}$. For the symmetric bell-shaped ridge (2.50), (2.67) becomes

$$\begin{aligned} \eta(x, z) = &- \left[\frac{\rho_0}{\rho(z)}\right]^{1/2} (2\pi)^{1/2} \left[\frac{(l^2 - k^{*2})^{3/2}}{l^2 z}\right]^{1/2} h_m a. \\ &e^{-k^* a} \cos\left[(l^2 - k^{*2})^{1/2} z + k^* x - \frac{\pi}{4}\right] \end{aligned} \tag{2.68}$$

with $k^*(x, z)$ given by $k^* = l/[(z/z)^2 + 1]^{1/2}$. This approximate form is not useful near the mountain or directly above the mountain (large z/x and small k^*) because of the assumptions used to obtain (2.68). It does however clarify the nature of the nonhydrostatic waves which trail behind the vertically propagating hydrostatic waves discussed earlier in the $al \gg 1$ case (see Fig. 3). As we look up along a sloping line of fixed z/x we find waves of constant wave number and decreasing amplitude. As we look further downwind at a given level (fixed z, decreasing z/z) we find shorter waves with k approaching l (i.e., $\to 2\pi U/N$). The upstream tilt of the phase lines is obvious just as it was for the long hydrostatic waves, but the tilt decreases as we move downstream to shorter waves. The decrease in wave amplitude with height $1/\sqrt{z}$ is associated with the fact

that the wave energy is progressively dispersed over a wider horizontal area.

These results are consistent with the concept of group velocity. In a stagnant stratified fluid the dispersion relation for (time varying) internal gravity waves is (see, for example, Turner, 1973)

$$\sigma^2 - N^2k^2/|k|^2, \qquad |k| = (k^2 + m^2)^{1/2} \tag{2.69}$$

where σ, k, m are the frequency and horizontal and vertical wave numbers. The horizontal phase speed is

$$C_{P_x} = \mp N/|k| \tag{2.70}$$

and the group velocity, which describes the direction and efficiency of wave energy propagation, is

$$\vec{C}g = \mp\left(\frac{N}{|k|} + \frac{Nk^2}{|k|^3}\right)\vec{i} \pm \frac{Nkm}{|k|^3}\vec{k} \tag{2.71}$$

In the study of steady mountain waves we are interested in the waves that first, have a component of their group velocity directed upward away from the mountain and second, have a phase velocity (relative to the fluid) equal and opposite to the mean flow U (see Fig. 4). Only in this way can the waves stand steady against the stream. This second condition requires that

$$C_{P_x} = -U \tag{2.72}$$

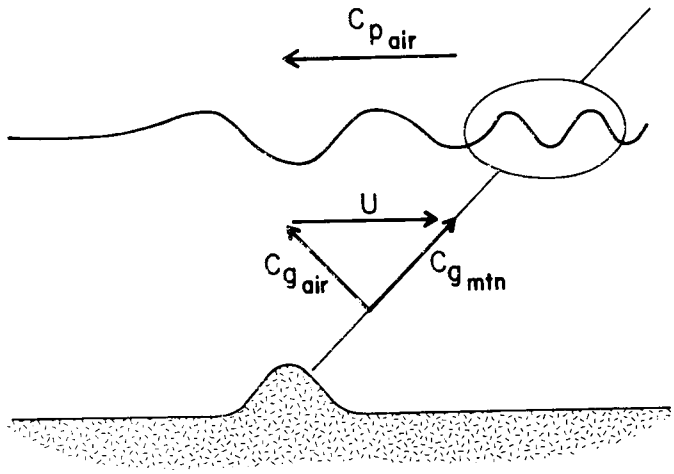

FIG. 4. A diagram illustrating the nature of steady mountain waves. The upstream phase speed of the wave is exactly equal and opposite to the freestream speed. The wave energy propogates upward and upstream relative to the air, but is advected into the lee by the mean wind. Relative to the mountain, the disturbance energy propagates upward and downstream.

With this choice, and going into a mountain fixed reference frame, the vertical and horizontal components of the group velocity become

$$U\frac{k}{m} \quad \text{and} \quad U\frac{k^2}{m^2} \tag{2.73}$$

The ratio of these two expressions is the slope along which a packet of waves produced at the mountain would propagate

$$\text{slope} = m/k \tag{2.74}$$

and using $m = (l^2 - k^2)^{1/2}$ this is exactly what was derived using the method of stationary phase (2.62). The purpose of the preceding analysis was to give a physical interpretation to the train by nearly periodic waves found aloft (Fig. 5). It is appropriate to consider these as a "dispersive tail" of nonhydrostatic waves with k less than, but not much less than l. If the mountain is too broad and smooth to create any of these shorter

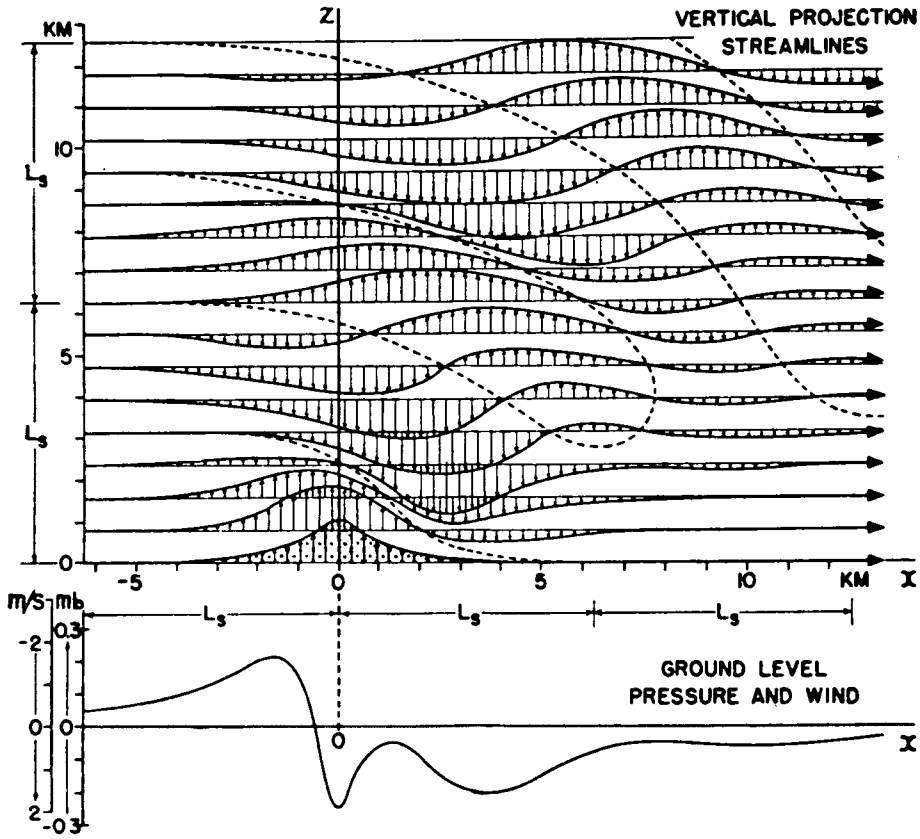

FIG. 5. The flow over a ridge of intermediate width ($al = 1$) where the buoyancy forces are important, but not so dominant that the flow is hydrostatic. The dispersive character of the nonhydrostatic waves (k less than, but not much less than N/U) is evident as they trail behind the ridge. Parameters are as in Fig. 3 except $a = 1$ km. (From Queney, 1948.)

waves ($al \gg 1$) then the flow will be as pictured in Fig. 3. It seems fair to call these trailing waves "lee waves" as they appear downstream of the mountain, but as we shall see there is another type of mountain wave for which this name is more suitable.

2.2.4. Trapped Lee Waves. Scorer (1949) pointed out that the theoretical description of the "dispersive tail" bears little resemblance to the long trains of waves which often cause lee-wave clouds in the lower atmosphere (see Fig. 6). By contrast with Fig. 5, these observed lee waves do not decay downstream but the amplitude of the disturbance does fall off rapidly with height. Scorer showed that under conditions

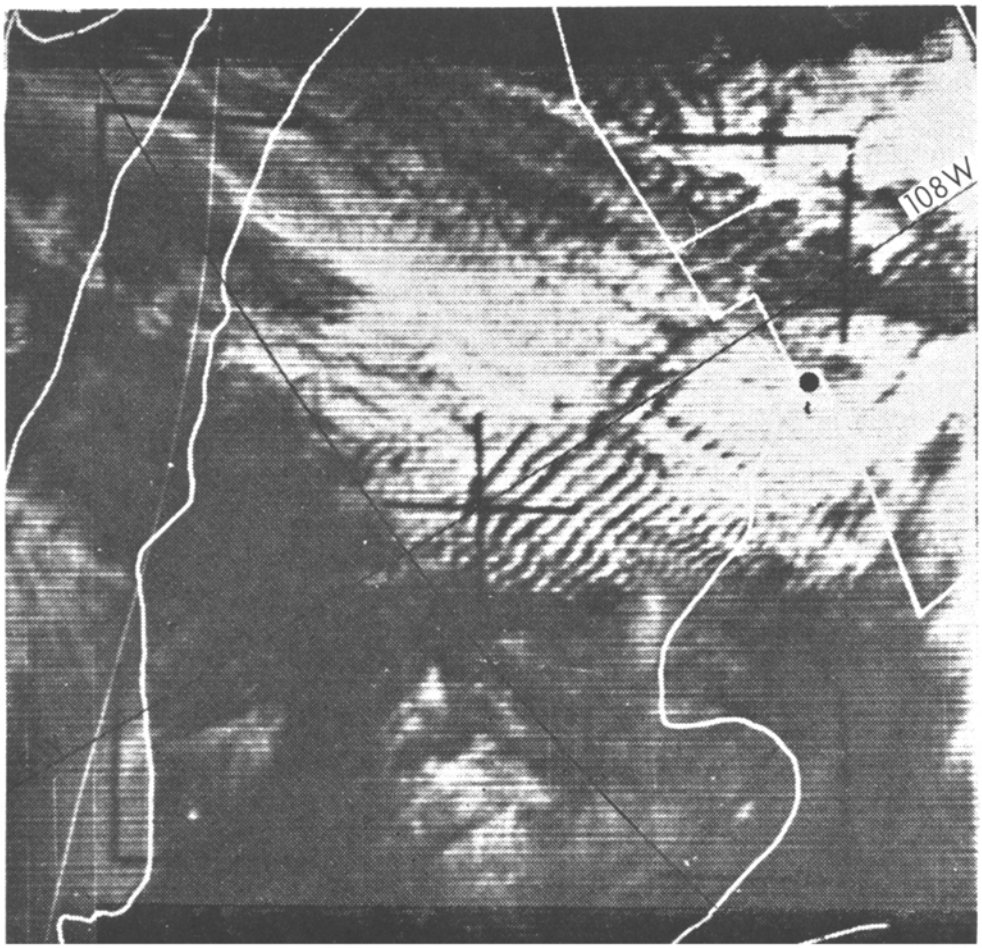

FIG. 6. Photograph of clouds forming in the crests of trapped lee waves over northern Mexico, southern Arizona, southern New Mexico, and western Texas. Clouds originate at the Sierra Madre Occidental Mountains in Mexico. Wavelength near central cross is 21 km. Taken from TIROS VI orbit at 1706 GMT, 15 November 1962. (From Nicholls, 1973.)

where the parameter $l^2(z)$ decreased rapidly with height, the atmosphere could support a new kind of mountain wave—the trapped lee wave or resonance wave. This realization triggered a decade of active theoretical research on the effect of l^2 variations and provided a framework for understanding the atmospheric observations.

As before, we consider the equation governing the field of vertical motion $w(x, z) = [\rho_0/\rho(z)]^{1/2}\hat{w}(x, z)$

$$\hat{w}_{xx} + \hat{w}_{zz} + l^2(z)\hat{w} = 0 \tag{2.75}$$

with

$$l^2(z) \approx \frac{N^2}{U^2} - \frac{U_{zz}}{U} \tag{2.76}$$

and use the Fourier representation

$$\hat{w}(x, z) = \mathrm{Re}\int_0^\infty \hat{w}(k, z)e^{ikx}\, dk \tag{2.77}$$

Then $\tilde{w}$ must satisfy

$$\tilde{w}_{zz} + [l^2(z) - k^2]\tilde{w} = 0 \tag{2.78}$$

The linearized lower boundary condition is

$$\tilde{w}(k, 0) = ikU_0\tilde{h}(k) \tag{2.79}$$

where $\tilde{h}(k)$ is the Fourier transform of the mountain shape. We wish to consider waves that do not propagate vertically but instead obey the upper boundary condition

$$\hat{w}(k, z) \to 0 \quad \text{as} \quad z \to \infty \tag{2.80}$$

Combining (2.77) and (2.79) gives

$$w(x, z) = \left[\frac{\rho_0}{\rho(z)}\right]^{1/2} \mathrm{Re}\int_0^\infty ikU_0\tilde{h}(k)\frac{\tilde{w}(k, z)}{\tilde{w}(k, 0)}\, e^{ikx}\, dk \tag{2.81}$$

where ratio $\tilde{w}(k, z)/\tilde{w}(k, 0)$ is to be determined from (2.78) and (2.80). In general, with a nonconstant $l^2(z)$, $\tilde{w}(k, z)$ is so complicated that it is impossible to perform the integral (2.81) exactly. Nonetheless it is still possible to obtain an expression for the flow far from the mountain by using asymptotic techniques. In fact we can proceed quite far without having to specify the mountain shape $h(x)$ or the structure of the incoming atmosphere $N(z)$, $\bar{U}(z)$. According to the Riemann–Lebesgue lemma the integral (2.81) will go to zero as $x \to \infty$ if the kernel is well behaved. It follows that the only nonvanishing disturbance as $x \to \infty$ must come

from portions of the integral nearby to where $\tilde{w}(k, 0) = 0$. Just as in the previous section, this allows (2.81) to be approximated by

$$w(x, z) \simeq \left[\frac{\rho_0}{\rho(z)}\right]^{1/2} \mathrm{Re}\left[ik_n U_0 \tilde{h}(k_n) \exp(ik_n x)\, \tilde{w}(k_n, z) \left(\frac{\partial \tilde{w}}{\partial k}\bigg|_{k_n}\right)^{-1} \cdot \int_{-\infty}^{\infty} \frac{\exp(i\hat{k}x)}{\hat{k}}\, d\hat{k}\right] \tag{2.82}$$

where k_n is any of the special wave numbers such that

$$\tilde{w}(k_n, 0) = 0 \tag{2.83}$$

and nearby to k_n, $\tilde{w}(k, 0)$ has been expressed as a Taylor series

$$\tilde{w}(k, 0) = 0 + \frac{\partial \tilde{w}}{\partial k}\bigg|_{k_n} \hat{k} \tag{2.84}$$

with $\hat{k} = k - k_n$. The integral in (2.82) can be evaluated by closing the path of integration at infinity and then computing the residues of the singularities inside. For $x > 0$ the contributions from the extended path will vanish if the path is taken upward enclosing the first and second quadrants. For $x < 0$ it must go downward enclosing the third and fourth quadrants. The final result can now be seen to depend crucially on whether the integral path along the real axis is taken just over or just under the singularity at k_n. The former choice will result in waves upstream of the mountain and none downstream. The latter choice will put all the waves downstream. Scorer correctly chose to put the wave downstream, and the physical basis for this choice will be discussed shortly. We have then, at large $|x|$

$$w(x, z) \approx 0 \qquad \text{upstream} \tag{2.85}$$

$$w(x, z) = \left[\frac{\rho_0}{\rho(z)}\right]^{1/2} \cdot \mathrm{Re}\left[ik_n U_0 \tilde{h}(k_n) \exp(ik_n x) \tilde{w}(k_n, z) \left(\frac{\partial \tilde{w}_0}{\partial k}\bigg|_{k_n}\right)^{-1} 2\pi i\right] \qquad \text{downstream} \tag{2.86}$$

or taking the real part

$$w(x, z) = \left\{-\left[\frac{\rho_0}{\rho(z)}\right]^{1/2} 2\pi U_0 k_n \left(\frac{\partial \tilde{w}_0}{\partial k}\bigg|_{k_n}\right)^{-1} |\tilde{h}(k_n)|\right\} \cdot \tilde{w}(k_n, z) \cdot \cos(k_n x + \phi) \tag{2.87}$$

where

$$|\tilde{h}(k_n)| = [\tilde{h}(k_n) \cdot \tilde{h}(k_n)^*]^{1/2} \tag{2.88}$$

The phase angle ϕ given by

$$\phi = -\tan^{-1}(\tilde{h}_i/\tilde{h}_r) \tag{2.89}$$

is zero if the mountain is symmetric making $\tilde{h}(k_n)$ real.

The contributions to the amplitude (i.e., term in braces) in (2.87) are physically clear (see Corby and Wallington, 1956) except for the $(\partial w/\partial k)$ factor. This term can be reexpressed by multiplying (2.78) both for k and k_n, by $w(k_n)$ and $w(k)$, respectively, and integrating from $z = 0$ to ∞. Integrate by parts once, subtract the two equations, and take the limit as $k \to k_n$ to obtain

$$\left.\frac{\partial w_0}{\partial k}\right|_{k_n} = 2k_n\bar{z}^3, \qquad \bar{z}^3 \equiv \int_0^\infty \frac{w^2(k_n, z)\, dz}{(\partial w/\partial z\,|_{z=0})^2} \tag{2.90}$$

In this way the sensitivity of the airstream to topographic forcing from below is represented solely in terms of $w(k_n, z)$. Computational experience has shown (see Smith, 1976) that the length $\bar{z}$ is roughly the distance from the ground to the height where the lee-wave energy is concentrated, which in turn is close to the level of maximum $l^2(z)$. Thus lee waves associated with a stable layer near the ground are sensitive to topographic forcing. Other interpretations of $\bar{z}$ are also possible.

The remaining part of the theoretical lee-wave problem is the determination of the lee-wave wavelength (or k_n) and the associated vertical structure function $\tilde{w}(k_n, z)$. The simplest cases in the literature are the two-layer model of Scorer (1949), the Couette linear shear flow model ($l \sim 1/z$) of Wurtele (see Queney *et al.*, 1960), the exponential model ($l \sim \bar{e}^{Cz}$) of Palm and Foldvik (see Foldvik, 1962), and the sharp inversion case (see, for example, Smith, 1976). With the advent of computers, more realistic $l^2(z)$ profiles can be treated (see Sawyer, 1960; Vergeiner, 1971; Smith, 1976).

Theoretically there is one obvious requirement for the existence of true trapped lee waves. Looking at (2.78) we note that at any level where $k > l$ the vertical accelerations dominate over the buoyancy forces and the function $\hat{w}(k, z)$ will behave exponentially. Conversely, where $k < l$, buoyancy dominates and $\hat{w}(k, z)$ will be trigonometric—always curving back toward zero. If $k < l$ at high levels, the upper boundary condition $\hat{w}(k, \infty) = 0$ cannot be met as the solution will continue to oscillate. If $k > l$ at all levels, the exponential form of the solution cannot satisfy the $\hat{w}(k, z) = 0$ condition at both $z = 0$ and $z = \infty$. Thus the necessary

(but not sufficient) condition for a wave number k to be a k_n with $\tilde{w}(k_n, 0) = 0$, is that $k^2 > l^2(z)$ aloft but $k^2 < l^2(z)$ over some lower levels. This is the basis for *Scorer's condition for the existence of lee waves, namely, $l^2(z)$ decreasing strongly aloft*. In practice this is associated with [looking now at (2.76)] a strongly stable layer in the low atmosphere and/or strongly increasing wind speed with height.

There are two helpful ways to think about lee waves. The first is to consider the analogy with the standing waves found downstream of an obstacle in a running river or stream. The stable air–water interface is equivalent to the stable layer required by lee-wave theory. With this analogy in mind we can attempt to understand why the waves are found only *downstream* of the obstacle. Just as in the vertically propagating waves, the key is to consider the obstacle as the source of the wave disturbance. For water waves it is known that the phase velocity (i.e., speed of crest motion) is greater than the group velocity (rate of energy propagation). Now in a standing wave the phase velocity must be equal in magnitude and opposite in direction to the mean stream U. It follows that the speed U will be greater than the group velocity and the transport of wave energy will be dominated by the advection due to the mean velocity U. Then, with the obstacle acknowledged as the source of the wave energy, the wave energy must be found downstream. Note that this last result is not universally true. Some types of wave motion, for example capillary waves on the surface of a liquid, have a larger group velocity than phase velocity, and standing waves of this sort will be found upstream of the obstacle.

Another way to help understand the lee wave is to consider the movement of wave packets in an atmosphere with a decreasing $l^2(z)$ (see Bretherton, 1966). In the stable lower atmosphere the generated wave (with $k^2 < l^2$) propagates up and to the right as discussed before. Eventually it reaches a level where $k^2 > l^2$. The wave cannot propagate in such a region, and the wave energy is totally reflected back toward the Earth. The wave energy bounces up and down between the ground and the low $l^2(z)$ region aloft, forming a standing wave pattern in the vertical (i.e., no phaseline tilt).

Both the vertically propagating waves and the trapped lee waves can occur together. An example of this is shown in Fig. 7. The clear distinction between these two wave types begins to fade as we consider atmospheres with more complicated structure. Two examples of mountain waves with intermediate qualities were found in the solutions of Sawyer (1960), and both of these are associated with the presence of a stable stratosphere aloft. If l^2 in the stratosphere is greater than anywhere below, Scorer's criterion cannot be satisfied and trapped lee waves, in

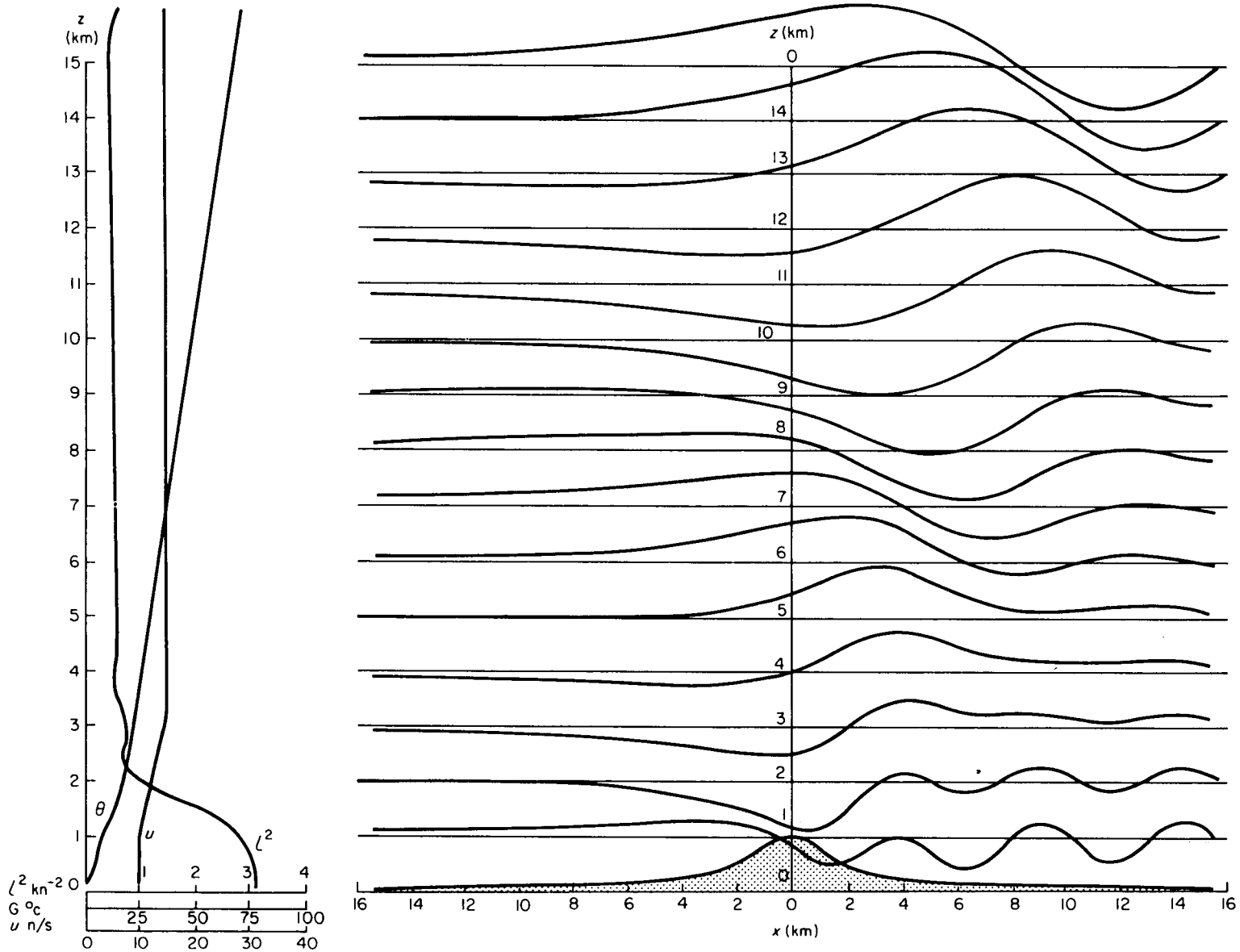
z (km)
15
14
13
12
11
10
9
8
7
6
5
4
3
2
1
θ
u
ℓ²
ℓ² kn⁻² 0 1 2 3 4
G °c 25 50 75 100
u n/s 0 10 20 30 40
z (km)
0
14
13
12
11
10
9
8
7
6
5
4
3
2
1
0
16 14 12 10 8 6 4 2 0 2 4 6 8 10 12 14 16
x (km)

the strict sense, are impossible. Still, if there is a thick middle-upper tropospheric layer with small l^2 above a stable layer, it is possible to have a partially trapped or "leaky" lee wave with a structure very similar to that obtained without a stratosphere (see Corby and Sawyer, 1958; Bretherton, 1969). Such a wave will, however, decay slowly downstream, and in the stratosphere the disturbance will have the form of a small-amplitude vertically propagating wave with a nonzero energy flux. Mathematically the singular wave number k_n has moved slightly off the real axis, and this allows for the decay downstream and for the vertical propagation of wave energy through the low l^2 middle-upper troposphere.

The second way in which a stratosphere can result in a wave with intermediate characteristics does not require a low-level stable layer. If the change in stability across the tropopause is abrupt, a vertically propagating wave will be partially reflected back toward the Earth. The reflected wave energy will continually rebound between the Earth and tropopause, losing a certain fraction of its energy each time, because the downward reflection is only partial. If this process occurs in the dispersive part of the spectrum (i.e., $k^2 \sim l^2$) the result will be a periodic-looking lee wave which decays downstream.

2.2.5. Other Effects of Variable $l^2(z)$. One effect of $l^2(z)$ variation has been described in the previous subsection—the trapping of waves in a high l^2 waveguide. Others will be considered in this subsection.

If the Scorer parameter $l^2(z)$ is a slowly varying function of z, then we can expect to find a solution to (2.78) in the form

$$\tilde{w}(k, z) = a(k, z)e^{i\Phi(k,z)} \tag{2.91}$$

where ϕ is the phase function and $a(k, z)$ is a slowly varying amplitude function (Bretherton, 1966). Substituting (2.91) and (2.78) gives, for the rapidly varying part

$$-a \cdot \phi_z^2 + [l^2(z) - k^2]a = 0 \tag{2.92}$$

or

$$\phi(k, z) = \int_0^{z'} [l^2(z') - k^2]^{1/2}\, dz \tag{2.93}$$

FIG. 7. The flow over a ridge where the background wind speed and stability vary with height. High above the mountain, the disturbance is composed of vertically propagating waves with tilted phase lines as in Fig. 5. In the lower atmosphere, trapped lee waves are evident extending well downstream. These waves have no phase line tilt. Trapped lee waves occur in this case as the Scorer condition—that $l^2(z)$ decrease strongly with height—is satisfied by the incoming flow. (From Sawyer, 1960.)

and for the slowly varying parts

$$2a_z\phi_z + a\phi_{zz} = 0 \tag{2.94}$$

or

$$a^2\phi_z = a^2[l^2(z) - k^2]^{1/2} = \text{const} \tag{2.95}$$

For long hydrostatic waves the above relations are simplified to

$$\phi(z) = \int_0^{z'} l(z')\, dz' \tag{2.96a}$$

and

$$\tilde{a}^2 l = \text{const} \tag{2.96b}$$

An alternative way to derive these relationships is to use the result of Eliassen and Palm (1960) that the vertical flux of energy is proportional to $U(z)$, together with the expression for the energy flux in a upward-going wave in a uniform medium [see the expression for the group velocity (2.71)]. From this second derivation, the special characteristics of the slowly varying medium are more clearly revealed. Locally, the wave must behave as it would in a uniform medium, and the changes in l^2 must be so gradual that no down-going waves are produced by reflection. A further condition for the validity of (2.96) is that $l^2 > k^2$ everywhere. If l^2 drops below k^2, strong reflection (and trapping) can occur even though l^2 is slowly varying. The solution in the neighborhood of these $l^2 = k^2$ "turning points" can be expressed in terms of Airy functions.

Qualitatively [from (2.96b)] the amplitude of the vertical velocity a in a mountain wave is reduced in regions of strong static stability (e.g., the stratosphere) and increased in regions of high wind speed (e.g., the jet stream). The amplitude of the vertical displacement [$\sim a/U(z)$] is reduced in regions of high wind speed as the fluid particles spend less time in the updraft and downdraft regions. This behavior is evident in the measurements of streamline patterns over the Rockies by Lilly and Zipser (1972). The wave activity appears strong above and below the jet stream and weakest in the jet core, in spite of the fact that the vertical energy flux is largest there.

When appreciable changes in $l^2(z)$ occur over a height comparable or smaller than a vertical wavelength, partial reflection will occur. Eliassen and Palm (1960) computed the fraction of energy reflected by discontinuous changes in l^2. Blumen (1965) and Klemp and Lilly (1975) have shown how partial reflections from the tropopause can considerably alter mountain drag and the severity of the lee side downslope winds. These phenomena will either be amplified or attenuated depending on the height

to the tropopause in relation to the vertical wavelength of the mountain wave.

A most interesting and important situation occurs when the component of the mean wind perpendicular to the ridge [i.e., $U(z)$] reverses above some height $z = D$. Near $z = D$ the mean wind $U(z)$ approaches zero, sending the Scorer parameter to infinity. Booker and Bretherton (1967) were able to show that a small-amplitude wave would be absorbed at such a critical level if the local background Richardson number were large. Bretherton *et al.* (1967) showed experimentally that little, if any, wave energy reaches the region of reversed flow aloft. Jones and Houghton (1971) compute the time development of the mean flow as it is influenced by the absorption of wave momentum. The acceleration of the mean flow near $z = D$ appears to decrease the Richardson number locally. Breeding (1971) and Geller *et al.* (1975) have studied the local structure of the critical levels. Their results, and the estimates of Smith (1977) using the "slowly varying" solutions (2.96), suggest that nonlinearity may be important at or just before the critical level even if the incident wave is of small amplitude. The possibility of getting significant reflection from a critical level was suggested by Breeding (1971), and this has been confirmed by the numerical experiments of Klemp and Lilly (1978). This whole issue must be considered unsolved, and the simple results of Booker and Bretherton (1967) cannot be accepted yet as representative of real flows.

2.3. Observations of Mountain Waves

There have been a large number of observations of mountain waves and in particular lee waves. Reviews of some of these observations can be found in Queney *et al.* (1960), Nicholls (1973), Musaelyan (1964), Vinnichenko *et al.* (1973), and Yoshino (1975). A partial list of some of the most easily available studies is given in Table I.

A number of authors have attempted to verify aspects of linear theory by comparison with observations. In regard to lee waves, the use of Scorer's criterion has proved successful, at least in a statistical sense, for predicting the occurrence of lee waves. On a case-to-case basis, however, there are still many discrepancies. The lee-wave wavelength has been used as a basis of comparison by many authors (see Corby, 1957; Corby and Wallington, 1956; Wallington and Portnall, 1958; Sawyer, 1960; Foldvik, 1962; Pearce and White, 1967; Berkshire and Warren, 1970; Vergeiner, 1971; Smith, 1976; Cruette, 1976). Such comparisons have been generally successful but not completely convincing because

TABLE I. OBSERVATIONS OF MOUNTAIN WAVES

Lee Waves

England
- Corby (1957)
- Cruette (1976)
- Foldvik (1962)
- Manley (1945)
- Starr and Browning (1972)

United States (*Appalachians*)
- Colson *et al.* (1961)
- Fritz (1965)
- Fritz and Lindsay (1964)
- Lindsay (1962)
- Smith (1976)

(*Cascades*)
- Fritz (1965)

(*Rockies*)
- Vergeiner (1971)
- Vergeiner and Lilly (1970)

(*Sierras*)
- Holmboe and Klieforth (see Queney *et al.* 1960)
- Nicholls (1973)
- Viezee *et al.* (1973)

Scandinavia
- Döös (1961)
- Foldvik (1954)
- Larrson (1954)
- Smirnova (1968)

Alpine Region and France
- Cruette (1976)
- Förchtgott (1957, 1969)
- Gerbier and Berenger (1961)
- Kuettner (1958)

South America
- Döös (1962)
- Fritz (1965)
- Sarker and Calheiros (1974)

Soviet Union
- Kozhevnikov *et al.* (1977) the Urals
- See Vinnichenko *et al.* (1973)

Middle East and India
- De (1971)
- Doron and Cohen (1967)

Mars
- Leovy (1977)

(*continued*)

TABLE I.—*Continued*

Larger Scale Vertically Propagating Waves
United States (*Rockies*)
Lilly *et al.* (1974)
Lilly and Kennedy (1973)
Lilly and Lester (1974)
Lilly (1978)
For other areas in the United States see Nicholls (1973)
Canada (*Rockies*)
Lester (1976)
Orographic Clouds (in General)
Conover (1964)
Hallet and Lewis (1967)
Ludlam (1952)

the lee-wave wavelength seldom varies by more than a factor of two or three (i.e., 6 km to 20 km) and it is always difficult to obtain a $l^2(z)$ profile at the same place and time of the lee-wave observation. The general tendency for the wavelength to increase with wind speed has been confirmed by observation (see Corby, 1957; Sawyer, 1960; Fritz, 1965; Cruette, 1976) and is now being used to estimate wind speed from satellite pictures of lee-wave clouds. Trains of lee-wave clouds have also been observed behind craters in the atmosphere of Mars and may eventually be used to estimate the wind speed and stability of that atmosphere.

The comparison of predicted and observed lee-wave amplitudes is more difficult. The prediction requires knowledge of the size and shape of the mountain that is generating the wave, and in mountainous terrain this is not always obvious (see Smith, 1976). The empirical estimation of lee-wave amplitude cannot normally be done from wave cloud observation alone, but requires direct aircraft or balloon measurement. Such a comparison has been completed by Holmboe and Klieforth (see Queney *et al.*, 1960), Vergeiner (1971), Foldvik (1962), and Smith (1976). The first two of these studies concerned very large mountains (Sierra Nevada and Front Range) where the linear theory would not be expected to hold. Foldvik studied the waves over complex terrain, and the wave source could not clearly be identified. Smith measured the waves produced by a low straight section of the Blue Ridge in the Appalachians, and reported amplitudes four times larger than theoretically predicted. This discrepancy is confirmed in the laboratory and explained by the early onset of nonlinearity in $l^2(z)$ profiles with thin, strongly stable layers.

Certainly the most extensive measurements of the longer, vertically

propagating waves are those by Lilly and collaborators (1973, 1974, 1978) in the Rocky Mountain Front Range region. Using aircraft measurements (Fig. 8), the qualitative predictions of linear theory—that is, penetration of the disturbance to great height, forward tilt of the phase lines, downward flux of momentum—have been confirmed. Some observations of the breakdown of waves to turbulence have also been described. The great vertical extent of the disturbance is also evident in the formation of orographic cirrus (Ludlam, 1952) and mother-of-pearl clouds (Hallet and Lewis, 1967). The outstanding qualitative questions concern the degree to which the flow is two-dimensional and steady and the degree of upstream low-level blocking. The question as to the steadiness and the three-dimensional structure of the wave field can now be treated using the remote sensing methods of Reynolds *et al.* (1968), Starr and Browning (1972), and Viezee *et al.* (1973).

The theory of mountain waves also predicts mountain drag. Lilly and Kennedy (1973) have indirectly measured this drag by computing the vertical flux of momentum in the observed waves. They find that during

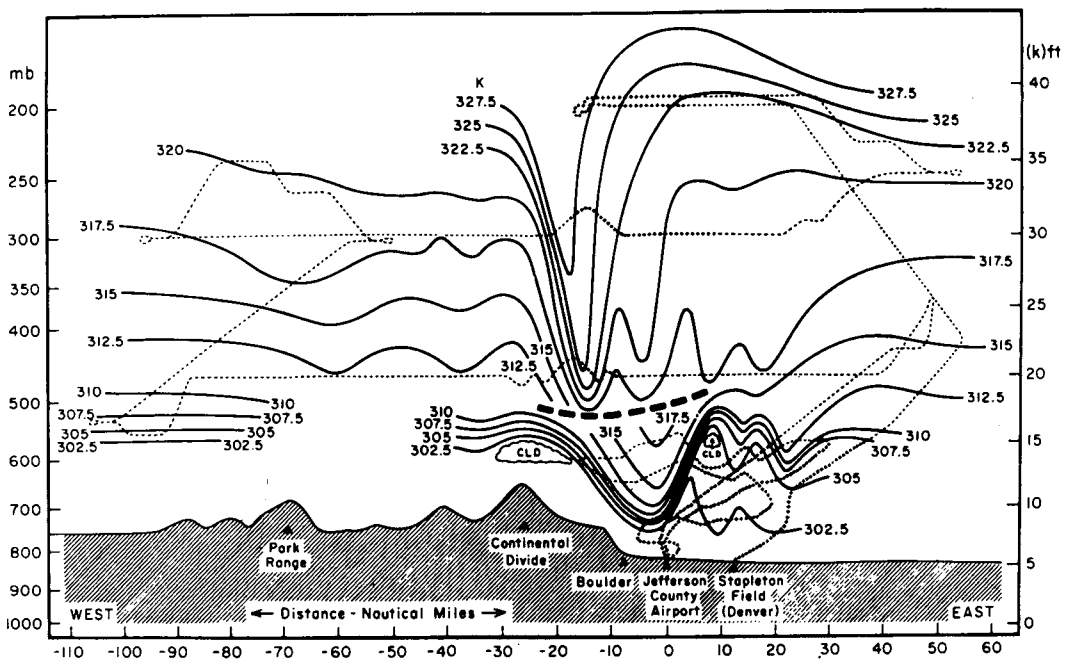

FIG. 8. Cross section of the potential temperature field (K) along an east-west line through Boulder, as obtained from research aircraft on 11 January, during a downslope windstorm in Boulder. To the extent that the flow is steady and adiabatic, these isentropes are good indicators of the streamlines of the air motion. Note that while the predicted vertically propagating nature of the disturbance is evident from its great vertical extent and from its tilted phase lines, the amplitude is much larger than predicted from linear theory (see Fig. 3). (From Lilly and Zipser, 1972.)

severe downslope wind events, the mountain drag on the Colorado Front Range can be an appreciable fraction of the total surface drag around the Earth in a latitude belt. Direct measurements of mountain drag have recently been accomplished (Lilly, 1978; Smith, 1978) by recording the surface pressure on each side of a mountain.

2.4. *The Three-Dimensional Flow over Isolated Hills*

2.4.1. Three-Dimensional Vertically Propagating Waves. All of the foregoing discussion has been concerned with the two-dimensional problem of flow over an infinitely long ridge. Most mountains on the Earth, however, are of a more irregular shape, and even the naturally occurring long ridges do have finite length. Furthermore it appears that there may be some fundamental theoretical differences between the two- and three-dimensional flows. Thus for both practical and theoretical reasons, we must attempt to understand the three-dimensional mountain flow problem. There has been much less theoretical and experimental work on the three-dimensional mountain wave problem, and at the present time there are still a good many unanswered physical questions.

One approach to the problem has been to extend the small-amplitude linearized theory to three dimensions. This approach has been used by Wurtele (1957), Scorer (1956), Crapper (1959, 1962), Trubnikov (1959), and Blumen and McGregor (1976) to study the orographic disturbance in an atmosphere with little vertical structure. Probably the most straightforward analysis is the study of Wurtele (1957; see also pp. 88–91 in Queney *et al.*, 1960). The field of vertical velocity $w(x, y, z)$ is written as a double Fourier integral according to

$$w(x, y, z) = \mathrm{Re} \int_{-\infty}^{\infty} \int \tilde{w}(k, l, z) e^{i(kx+ly)}\, dk\, dl \tag{2.97}$$

For the case of constant Scorer parameter $k_s = N/U$

$$\tilde{w}(k, l, z) = \tilde{w}(k, l, 0) e^{imz} \tag{2.98}$$

where magnitude of the vertical wave number m is given by

$$m^2 = \frac{k^2 + l^2}{k^2} (k_s^2 - k^2)$$

and the correct sign is chosen to prevent downward radiation; $\mathrm{sgn}(m) = \mathrm{sgn}(k)$. As in the two-dimensional theory, the vertical velocity near the ground can be written in terms of the mountain profile $z = h(x, y)$

according to

$$w(x, y, z = 0) = U(\partial h/\partial x) \tag{2.99}$$

Wurtele simplified his problem by choosing topography in the form of semi-infinite plateau of height h with narrow width $2b$ in the cross-flow (i.e., "y") direction. In this case the vertical velocity vanishes near the ground except near the origin $x = y = 0$ and

$$w(x, y, z = 0) \approx 2Uhb\ \delta(x)\ \delta(y) \tag{2.100}$$

Even with this choice, the integral (2.97) is still intractable, and Wurtele resorts to the method of stationary phase to investigate the region far from the mountain; $k_s x$, $k_s y$, $k_s z$ all large. At the level $k_s z = 2$, the theory predicts that the regions of updraft take on a horseshoe shape and are located some distance downstream of the mountain. Wurtele points out the relationship between this result and the observation of horseshoe-shaped wave clouds in the lee of Mt. Fuji (Abe, 1932).

Crapper (1959, 1962) has extended the work of Wurtele by allowing for more realistic mountain shapes but is again forced to use asymptotic techniques which are valid only in the far field of flow. Crapper (1962) finds that the nature of the far-field flow depends in an intricate way on the presence of curvature in the mean velocity profile, but no clear physical explanation for this is evident. Trubnikov (1959) has a similar approach to the three-dimensional mountain flow problem, but his results are expressed only formally, in terms of unevaluated integrals. Scorer's (1956) solutions for the stratified flow over an isolated mountain should probably be disregarded as the incorrect radiation condition was used.

One fundamental difference between the two- and three-dimensional problems is the direction in which wave energy propagates away from the mountain. It was shown earlier that in two dimensions, as the mountain becomes wider and the flow more nearly hydrostatic, the group velocity (relative to the mountain) becomes directed vertically with the result that the wave energy is found directly above the mountain. This result *does not* carry over to three dimensions. Some of the hydrostatic waves generated by an isolated mountain lie downstream of the mountain and to the side, tending to form trailing wedges of vertical motion. This is shown in Fig. 9.

2.4.2. Three-Dimensional Trapped Waves. The three-dimensional problem, just like the two-dimensional problem, changes considerably when the Scorer parameter decreases with height rapidly enough to permit the existence of trapped lee waves. This situation was first studied

by Scorer and Wilkinson (1956) and later by Palm (1958), Sawyer (1962), Crapper (1962), and more recently by Gjevik and Marthinsen (1977).

The three-dimensional development of trapped waves in the atmosphere is similar in many respects to the occurrence of surface waves behind a ship moving in calm water. The wave pattern is generally contained within a wedge with apex at the mountain. The waves within the wedge are of two types. The *transverse* waves lie approximately perpendicular to the flow direction and physically are composed of waves that have attempted to propagate approximately into the wind but have been advected to the lee. These waves are analogous to the trapped lee waves found in the two-dimensional problem. When, for example, the wind is faster than the phase speed of the fastest trapped wave, lee waves disappear in the two-dimensional problem and the transverse waves will disappear from the three-dimensional problem.

The other type of wave—the *diverging* wave—has crests that meet the incoming flow at a rather shallow angle. These crests are composed of waves that have not attempted to buck the stream but have propagated laterally away from the mountain and have been advected into the lee. At high wind speeds these waves continue to exist and respond only by aligning their wave crests more closely with the free stream direction in order to keep their upstream phase speed equal to the free stream velocity.

Both types of waves are evident in Fig. 10 which shows the cloud patterns associated with flow past Jan Mayen.

2.4.3. Three-Dimensional Flow at a Low Froude Number. Another approach to the problem of stratified flow past an isolated three-dimensional mountain is to consider the limit of very slow speeds and strong stratification so that the Froude number

$$\text{Fr} \equiv U/(N \cdot L) \tag{2.101}$$

is small. Intuitively it is clear that in this limiting situation there will be little vertical motion and the fluid particles will deflect horizontally to move around the mountain while remaining in horizontal planes. As the Froude number is increased, vertical deflections will occur, and Drazin (1961), using an expansion in Fr, has devised a method of computing these vertical deflections. According to Drazin, the cause of the deflection is the vertical difference in the pressure field associated with the two-dimensional potential flow occurring in each horizontal plane. On an object with fore-aft symmetry, the potential flow pressure field will be symmetric (i.e., high pressure of the front and back, low pressure on the

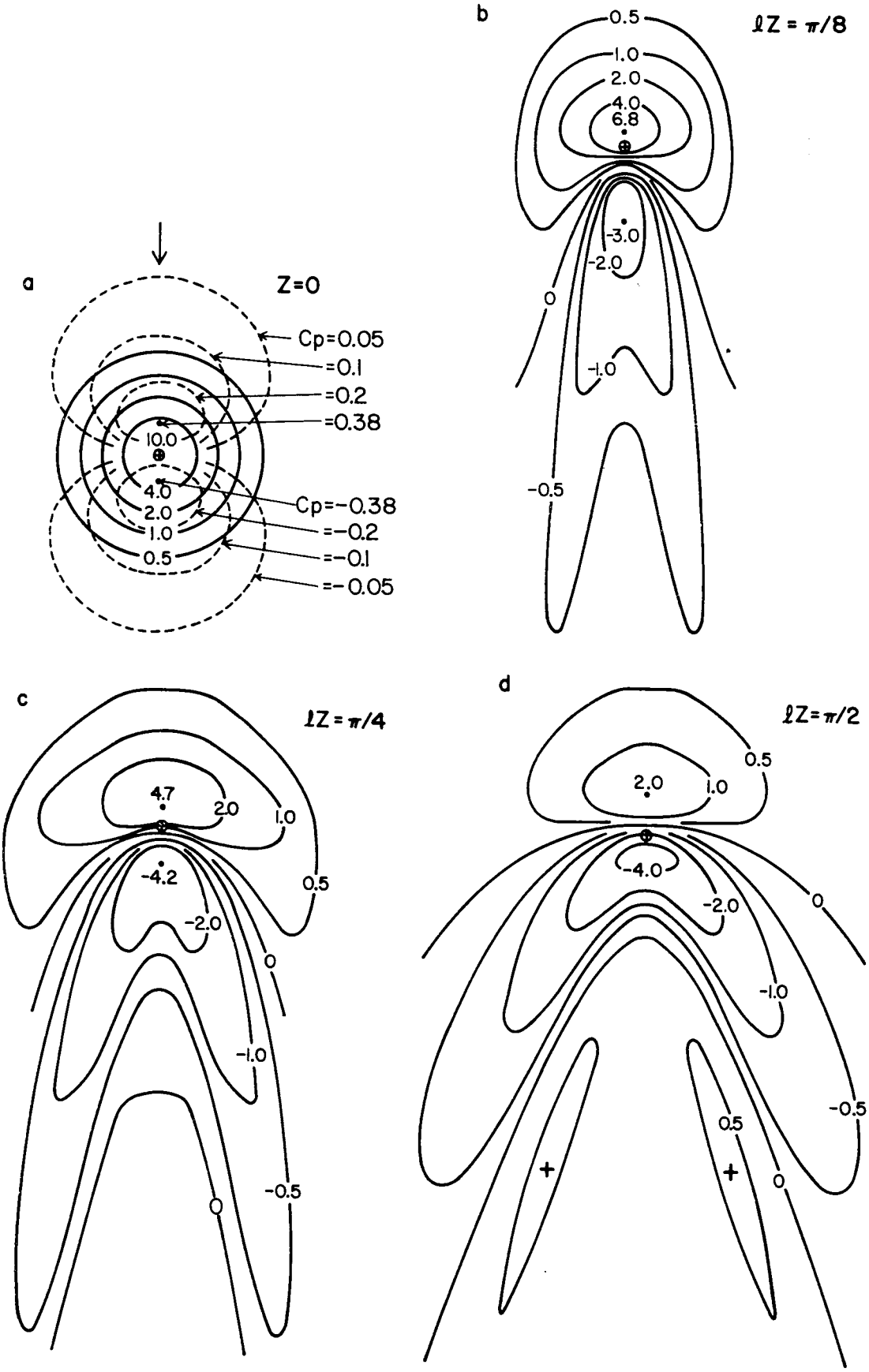
a
Z=0
Cp=0.05
=0.1
=0.2
=0.38
10.0
4.0
2.0
1.0
0.5
Cp=-0.38
=-0.2
=-0.1
=-0.05
b
ℓZ = π/8
0.5
1.0
2.0
4.0
6.8
-3.0
-2.0
0
-1.0
-0.5
c
ℓZ = π/4
4.7
2.0
1.0
-4.2
0.5
-2.0
0
-1.0
-0.5
0
d
ℓZ=π/2
0.5
2.0
1.0
-4.0
-2.0
0
-1.0
-0.5
0.5
+
+
0

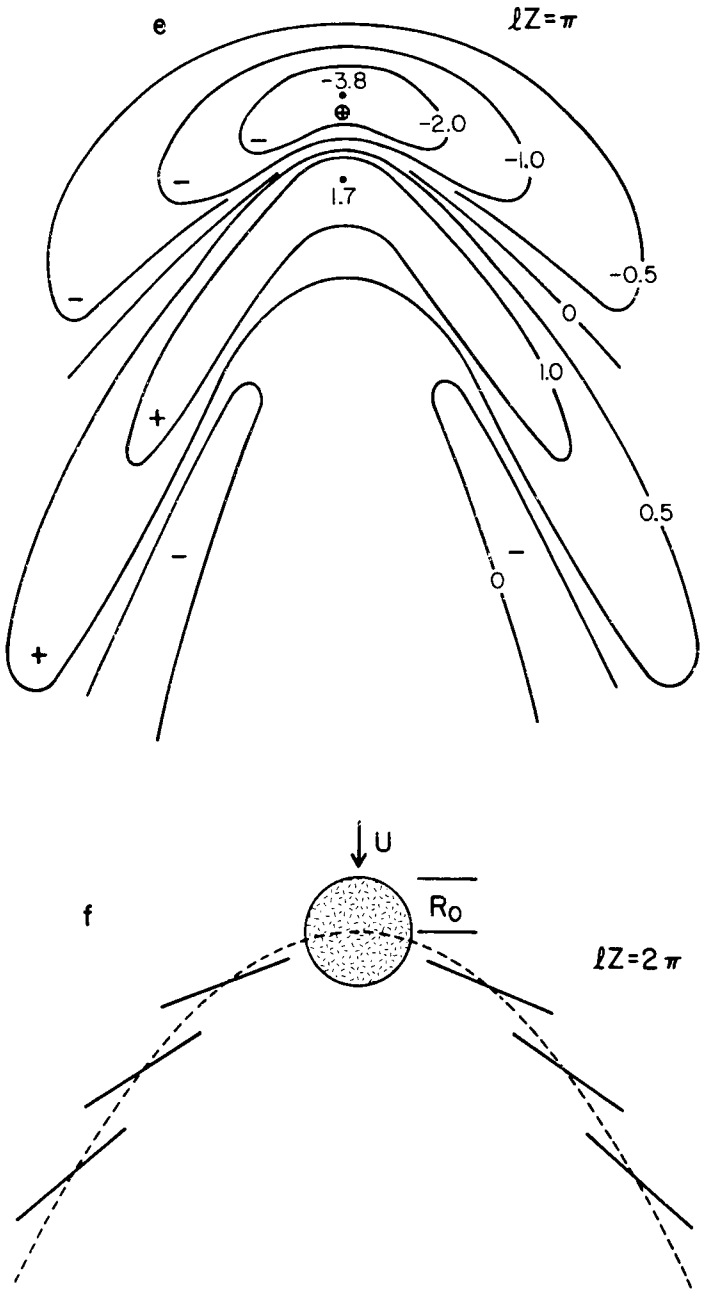

FIG. 9. The buoyancy-dominated, hydrostatic flow over an isolated mountain with circular contours [$h(x, y)$ given by (3.19)]. (a) The topographic contour of the mountain (solid lines) and the surface pressure field (dashed lines) $C_p \equiv p'/\rho UNh_m = -u'/Nh_m$. (b)-(e) Contours of the vertical displacements of the isentropic surfaces at the heights $lz = \pi/8$, $\pi/4$, $\pi/2$, π, determined by evaluating (2.97) numerically using a two-dimensional Fast Fourier Transform algorithm. (f) A schematic representation of the disturbance far from the mountain at $lz = 2\pi$, determined by asymptotically evaluating (2.97) using the method of stationary phase. The wave crests and troughs (solid lines) point back at the mountain, while the wave energy at each level is confined to the region near the parabola $y^2 = (k_s R_0 z)x$ (shown dashed). This parabola becomes progressively wider at higher levels. (From Smith, 1980.)

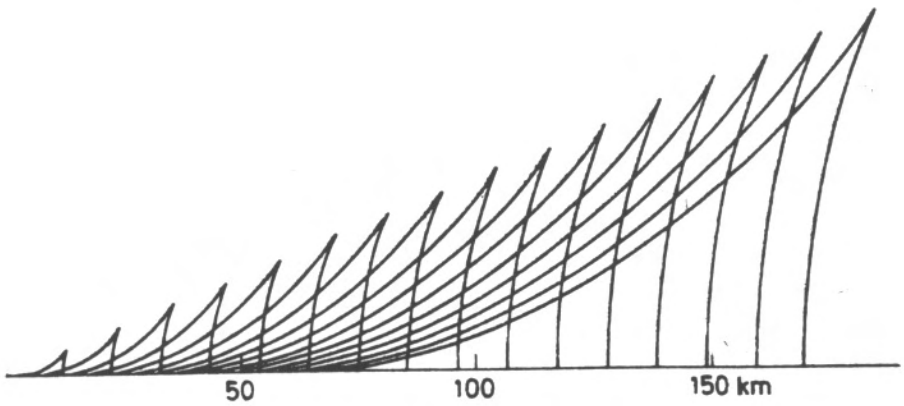

(a)

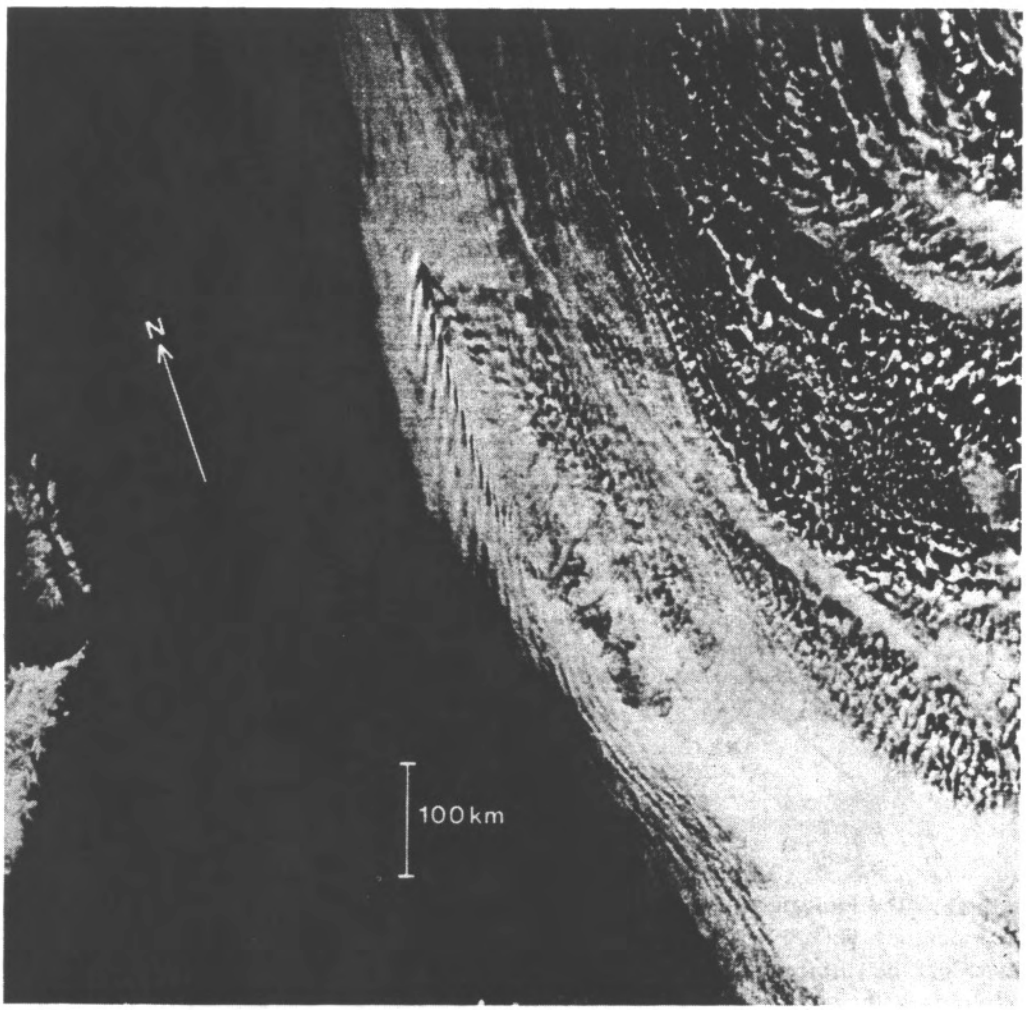

(b)

FIG. 10. Trapped gravity waves behind an isolated mountain. (a) The computed wave crests for a case with both diverging and transverse waves present. (b) Satellite VHRR-photography showing the wave pattern (primarily diverging waves) induced by the island Jan Mayen. (From Gjevik and Marthinsen, 1978.)

sides), and this is also true of the vertical deflection computed by Drazin's method. Riley *et al.* (1975) have checked these theoretical predictions in the laboratory by slowly towing obstacles through a stratified fluid. They find that as soon as the Froude number is increased enough that vertical deflections are noticeable, those deflections are strongly asymmetric. Slight lifting is observed upstream and strong sinking in the lee.

There are two possible explanations for this discrepancy between theory and experiment. Riley *et al.* suggest that one should take into account the fact that in a slightly viscous fluid the potential flow solution is often replaced by separated flow with low pressure in the lee. The lee-side low pressure causes drag on the obstacle (the resolution of D'Alembert's paradox) and in the stratified model would cause a drawing down of flow surfaces in the lee. The other explanation is just to realize that the laboratory observation is qualitatively consistent with the predictions of linear theory for inviscid flow over small-amplitude topography, as discussed earlier. In that case the lee-side low pressure and downward deflection are associated with the generation of mountain waves and wave drag. The inviscid wave drag mechanism is not described by Drazin's Froude number expansion. One way to explain this is to note that mathematically the drag turns out to be exponentially small for small Froude number and thus cannot be described by a power series expansion. Alternatively, note that while the full equations can describe wave motion, the equations generated from the expansion in Froude number cannot.

There is one other interesting phenomenon that can occur when the Froude number is low—the periodic shedding of vortices. The resulting vortex "streets" have been observed in the cloud patterns downstream of isolated islands. This subject has been reviewed by Chopra (1973). For more recent work on this phenomena the reader can refer to descriptions and laboratory results of Brighton (1978).

Recently there have been a number of attempts to model numerically the three-dimensional flow over and around mountains, for example, Onishi (1969), Zeytounian (1969), Vergeiner (1975, 1976), Danard (1977), Mahrer and Pielke (1977), Warner *et al.* (1978), and Anthes and Warner (1978). A detailed description of the techniques and results of the studies would take us too the far afield—especially so because for the most part (1) the numerical models are full of complex and interrelated parameterizations; (2) the boundary conditions are not the same as in the theoretical studies; and (3) little attempt has been made to compare the numerical results with the earlier theoretical results. Still there seems to be rapid progress occurring which soon will make an impact on our understanding of three-dimensional stratified flows.

2.5. *Large-Amplitude Mountains and Blocking*

The earlier discussion in this section has been based on the assumption that the linearized equations of motion give a satisfactory description of the flow. This assumption may seem to gain some support from the fact that most of the Earth's terrain features are rather gentle, that is, with small slope (h/L). In a stratified fluid, however, there are length scales other than the mountain width (L) with which the mountain height (h) can be compared. It turns out that linear theory begins to break down when h becomes comparable to either the inversion height, if one exists, or in a continuously stratified atmosphere, the vertical wavelength of hydrostatic disturbances $\lambda_z = 2\pi U/N$. In practice this usually means that any mountain greater than 0.5 to 1.0 km in height will produce disturbances too large for linear theory, even if the slope of the surface is quite small. The breakdown of linear theory is significant because it may be associated with new phenomena, for example, wave steepening and breaking and possibly blocking—the stagnation of low-level air ahead of the mountain. The present discussion of finite amplitude effects will be brief and rather cursory. This is partly because there have already been a number of reviews of this subject (Yih, 1965; Miles, 1969; Gutman, 1969; Kozhevnikov, 1970; Long, 1972) and partly because many of the available studies are of questionable relevance due to either a restriction to two dimensions or the imposition of a rigid-lid upper boundary condition.

The recent interest in finite-amplitude mountain waves originated with the three papers of R. R. Long (1953, 1954, 1955). In the first and third of these papers, Long discussed the steady flow of an incompressible, continuously stratified fluid and pointed out that there is a special class of upstream profiles for which the governing equations become exactly linear. The simplest of these cases is when the dynamic pressure $\frac{1}{2}\rho U^2$ and the vertical density gradient $\partial\bar{\rho}/\partial z$ are constant with height. Within the accuracy of the Boussinesq approximation this reduces to the case of constant wind and stability which was studied earlier using linear theory (e.g., Queney, 1947). This special case, together with the belief that the upstream flow can be specified *a priori*, constitutes "Long's model." Long's approach has been extended by Yih (1960) to widen the class of exactly linear flows and by Claus (1964) to allow compressibility, but most interest has centered on obtaining solutions for Long's simplest case. The difficulty here is that while the equation for the interior motion is of a simple type, the boundary condition at the mountain surface is still of a difficult nature. Long (1955) obtained solutions using an inverse method and compared the theoretical derived flow fields with laboratory

observation. The agreement showed by Long stands as one of the cornerstones of the subject even though the rigid upper lid, used in his experiments and theory, prevents direct application to the atmosphere.

The rigid-lid problem, however, has continued to receive considerable attention as a fundamental problem in fluid mechanics (Yih, 1960; Drazin and Moore, 1967; Grimshaw, 1968; Davis, 1969; Benjamin, 1970; Segur, 1971; McIntyre, 1972; Baines, 1977). The basic thrust of this research has been to investigate the way in which Long's model breaks down, either by the occurrence of instability and turbulence or by the alteration of the upstream flow (i.e., blocking). These phenomena are of considerable importance for the atmosphere, but much of this work may have to be extended, by eliminating the rigid lid, before it can be applied to the atmosphere.

Solutions to Long's model in an unbounded atmosphere (using a radiation condition) were first obtained by Kozhevnikov (1968) and Miles (1968), and later by Huppert and Miles (1969), Janowitz (1973), and Smith (1977). The nature of these solutions are reviewed by Miles (1969). As the height of the mountain is increased, the basic structure of the flow field remains the same. In the regions of up motion, the streamlines steepen (see Fig. 11) more rapidly than predicted by linear theory. This steepening has been linked to the nonlinear lower boundary condition by Smith (1977). Eventually when the mountain height reaches a critical value the streamlines become locally vertical. Further increase in mountain height will cause overturning—regions where denser fluid is temporarily lifted above lighter fluid. This, it is thought, will allow convective instability to occur locally, and the rigid-lid experiments of Long (1955) and Baines (1977) seem to confirm this idea. The wave drag also increases more rapidly than predicted by linear theory (Miles, 1969). There does not seem to be a strong tendency for blocking of the flow upstream. The flow speed just ahead of the mountain is much reduced, just as in linear theory, but it resists going to zero until long after reversed flow regions have formed aloft (as an example, see Miles, 1971). The surface level flow thus does not seem to encounter any special difficulty in surmounting the obstacle.

It would be a mistake to try to generalize these qualitative results of Long's model. It is now widely recognized that the special cases for which the governing equations are exactly linear are not only mathematically special, they are also physically special. In flows with variable $U(z)$ and $N(z)$, new nonlinear effects may arise just as new phenomena appeared in the linear theory of lee-wave flow in structured atmospheres.

The only other case for which analytic finite-amplitude mountain flow solutions are available is the situation where the incoming flow is com-

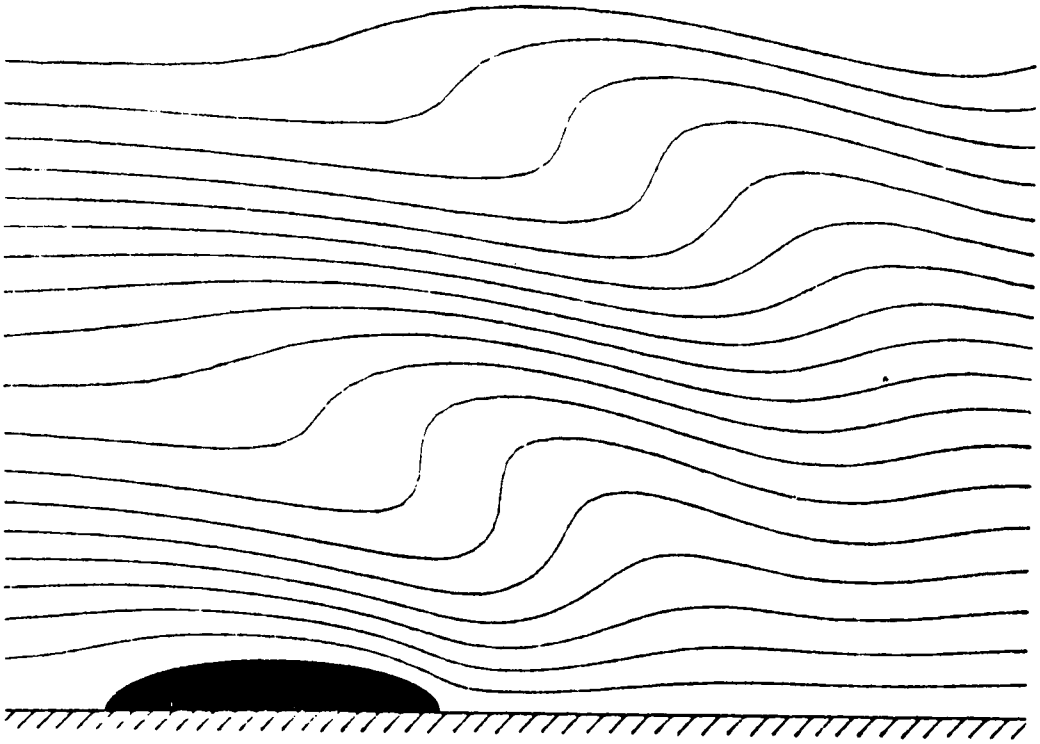

FIG. 11. The finite amplitude flow over a semielliptical ridge computed from Long's model. The intense nonlinear forward steepening of the streamlines is due to the fact that the parameter $h_m l = h_m N/U$ (= 0.93 here) is approaching unity. (From Huppert and Miles, 1969.)

posed of a finite number of layers (usually one or two), each of constant density (Long, 1954; Houghton and Kasahara, 1968; Houghton and Isaacson, 1970; Long, 1970). The effect of stable stratification is modeled by the decrease in density going upward from layer to layer. In the case of a single layer, this decrease in density (in the laboratory this is water to air) is extreme, leading to a free surface condition. The model is made tractable by assuming hydrostatic balance throughout each layer as they pass over the mountain. The hydrostatic assumption is not terribly restrictive as (i) many atmospheric flows are nearly hydrostatic and (ii) the qualitative nature of the Long's model solutions discussed above are rather insensitive to this assumption. The major drawback of this approach is that with a finite number of layers there must always be a homogeneous uppermost layer of infinite thickness preventing any vertical radiation of wave energy. Thus all waves are totally reflected back toward the surface just as they were in the rigid-lid models discussed earlier. Knowing the importance of the radiation condition, this aspect of the layered models may seem fatal, but it can be argued that it is

equally important to model correctly the discontinuous nature of $N(z)$ at, for example, a thin subsidence inversion, and its associated nonlinear effects. Thus for some upstream profiles the layer models may give a better representation of the flow than the unbounded Long's model. Furthermore, some new phenomena arise in layered models such as upstream influence and internal hydraulic jumps. The internal hydraulic jumps (see Yih and Guha, 1955), in fact, play a central role in the layered models because lee-wave radiation and vertical radiation have been eliminated by the hydrostatic and the reflective conditions. Thus the dissipation within the jump is the only way the system can be irreversible and this in turn allows for flow asymmetry (e.g., strong downslope winds) and mountain drag.

The hydraulic approach to the mountain flow problem has been pursued quite vigorously in the Soviet Union. Most of those studies have included the effect of Coriolis force (Khatukayeva and Gutman, 1962; Sokhov and Gutman, 1968; Gutman and Khain, 1975; Ramenskiy *et al.*, 1976).

The final and perhaps potentially the most powerful method for understanding nonlinear mountain flow is the direct numerical solution of the governing equations. Recent attempts to model the two-dimensional flow over a finite-amplitude ridge include Foldvik and Wurtele (1967), Granberg and Dikiy (1972), Furukawa (1973), Mahrer and Pielke (1975), Deaven (1976), Clark and Peltier (1977), Klemp and Lilly (1978), and Anthes and Warner (1978). Along with the advantages of this technique come a series of drawbacks which have plagued investigators. Because of limited computer memory and speed it is impossible to calculate the flow in a semi-infinite domain, leading to the necessity of specifying nearby boundary conditions—both inflow and outflow conditions and an upper "radiation" condition. The upper radiation condition can be directly applied only when the flow variables are expressed as additive Fourier components. In the finite difference models then, this condition can only be simulated by adding a "sponge" region above the region of interest in which the vertically propagating waves are dissipated—hopefully without reflection—by a gradually increasing viscosity (see Clark and Peltier, Klemp and Lilly, and Warner and Anthes). Other limitations on the numerical models are imperfect spatial resolution and the possibility of coding errors and numerical instability. Perhaps the strongest limitation is that while solutions and understanding often go hand in hand in analytical work, this is seldom the case with numerical simulation. The numerical solutions must be cleverly diagnosed to reveal the underlying processes.

The recent numerical work of Clark and Peltier (1977) and Klemp and

Lilly (1978) have shed some light on the problem of what happens when a vertically propagating mountain wave becomes so steep that it causes a local reversal of the flow aloft. By parameterizing the small-scale turbulence, which apparently occurs by local instability, the larger scale mountain wave flow can continue to be calculated even after the critical breaking criterion is exceeded. Both pairs of investigators find that a region of slowly moving turbulent air is generated aloft and that this region seems to cause a partial reflection of the vertically propagating wave energy. This partial reflection increases the intensity of the mountain-induced disturbance in the lower atmosphere and increases the mountain drag. The details of this process are still unclear. It seems likely that this or some closely related phenomena may be the important factor in producing severe downslope wind storms such as reported by Lilly and Zipser (1972) and as shown in Fig. 8. The numerical models have also reproduced some of the aspects of low-level blocking, but the two-dimensional restriction probably prevents a true simulation of the blocking phenomena.

The blocking of low-level air is one of the most important ways in which mountains affect the air flow. The tendency for the surface level flow to slow as it approaches a mountain is described by the linearized theories of mountain flow. It is probably fair to say that this windward-side slowing is due to the difficulty that the heavy surface air has in running upslope. This, by the same token, explains the large velocities on the lee side as heavy air runs downhill. At the same time we must remember that according to linear theory, this upslope–downslope asymmetry also requires the generation of waves that propagate away to infinity. Thus the blocking phenomena cannot be considered a strictly local phenomena.

The linear theory cannot, of course, be used to investigate complete blocking as this immediately implies that the disturbance has become as large as the mean flow. This aspect of the finite-amplitude mountain flow problem has attracted a good deal of attention theoretically and in the laboratory. A brief list of the different types of "blocking" or more generally "upstream influence" is as follows:

1. Sheppard (1956) used Bernoulli's equation to estimate the speed that an incoming flow must have to overcome the background stability and reach the mountain top. To close the system of equations Sheppard had to assume that the pressure of a parcel as it rises is always equal to the environmental pressure far from the mountain. This leads to the approximate condition

$$U > Nh \tag{2.102}$$

if the flow is to reach the top. It is interesting to note that the parameter hN/U appearing in (2.102) is the same parameter that enters as a measure of the nonlinearity in hydrostatic mountain flows (Smith, 1977; Miles, 1969). Miles finds that a lower value of $hN/U = 0.67$ as opposed to (2.102) marks the onset of overturning above a broad mountain of ellipsoidal cross section.

Sheppard's condition (2.102) seems physically reasonable but there is little else to recommend it—especially as it contains no information as to what form the blocking will take. A further problem is that in practice it is difficult to determine the appropriate values of N and U as these are likely to vary quite strongly near the surface.

2. One conception of the blocking phenomena is to consider it as the separation of the boundary layer or as the reversal of the slow moving flow in the boundary layer by the adverse pressure gradient upstream of the mountain (Scorer, 1955, 1978).

3. In the fully three-dimensional flow near an isolated mountain or a ridge with ends or gaps, absolute blocking of the low-level flow is not possible. The layer of dense air may pile up slightly ahead of the mountain, but this can be relieved by airflow around the mountain or through gaps in the ridge. The tendency for the flow to go around is described both in the linear theory and in the low Froude number model of Drazin (1961) described earlier.

4. In two-dimensional flow with a rigid lid, there is the possibility that for specified upstream conditions [i.e., $U(z)$, $N(z)$] there may be no steady-state solution to the governing equations. There is an analogy between this problem and the "choking" phenomena in the one-dimensional flow of a compressible gas into a strongly converging nozzle. In both cases a transient flow occurs in which a wave front moves upstream, altering the incoming flow in such a way as to make a steady state flow possible near the mountain. This situation has been investigated for continuous stratification by Long (1955), Drazin and Moore (1967), Grimshaw (1968), Benjamin (1970), Baines (1977), and in layered flows by Long (1954), Houghton and Kasahara (1968), Houghton and Isaacson (1970), and Long (1970). The "choking" seems to be associated with the reflective upper boundary condition and occurs when the Froude number of the flow is near unity. It is not then simply that the incoming flow is too slow to run up the mountain.

5. The last type of blocking to be described here is the upstream influence that occurs naturally when the free stream is started from rest. Even if a steady state flow may have been possible with the intended upstream conditions, the start-up process can generate long waves which move upstream, altering the flow that approaches the mountain (Mc-

Intyre, 1972). Like the choking phenomena this type of upstream influence seems to depend on a reflective upper boundary condition and thus may not be important for the atmosphere. It has been observed in the laboratory by Baines (1977) and A. Foldvik (personal communication), although there is the possibility that the observed upstream wave may have been generated by viscous or turbulent redistribution of momentum near the mountain.

2.6. The Observed Barrier Effect of Mountains—The Föhn and Bora

The barrier effect of mountains is well documented in several parts of the world. In some regions the low-level flow is diverted horizontally around or through gaps in the mountains. As an example, the strong wintertime westerly winds in southern Wyoming (Dawson and Marwitz, 1978) probably represents air that was blocked by the Front Range. The mistral—a cold wind blowing off the continent in southern France—is able to avoid barriers by flowing down the Rhône Valley. Cool, moist Pacific air is able to move eastward through high passes in the Andes (Lopez and Howell, 1967). Low-level air originating in North America penetrates the central American highlands near Tehuantepec (Godske *et al.*, 1957).

In other situations the cold low-level air can be contained by an unbroken mountain chain for several days. Examples including the trapping of polar air north of the Brooks Range in Alaska (Schwerdtfeger, 1975), the containment of the Scandinavian anticyclone by the Scandinavian mountains, and the damming effect of the southern Appalachians (Richwien, 1978). It occasionally happens that after the barrier effect has persisted for some time, the large-scale pressure gradient will change, forcing the air from one side of the mountain to move over the crest and down the other side. When this happens, the lee slope environment may experience a sudden change in temperature and humidity as the old air mass is replaced by an air mass of different origin. Following Yoshino (1975, p. 393) we can classify these overflow events according to the change in temperature that accompanies the onset of the fall wind (i.e., heavy air moving downslope). "In my opinion . . . the definitions of the föhn and bora should be made in the simplest way as follows: The föhn wind is a fall wind on the lee side of the mountain range. When it blows, the air temperature becomes higher than before on the lee side slope. The bora is also a fall wind on the lee side of a mountain range, but when it begins, the air temperature becomes lower than before on the lee side slope." The föhn phenomenon is common in the Alps (see, for example,

Defant, 1951; Godske *et al.*, 1957; Yoshino, 1975; Vergeiner, 1976), and on the eastern slopes of the Rockies where it is called a chinook (see, for example, Brinkman, 1970, 1971; Holmes and Hage, 1971). In California it is an easterly wind and the local name is the Santa Ana (Serguis *et al.*, 1962).

The definition of the föhn as a warm downslope wind makes no attempt to distinguish the reason for its warmth. It could be (1) a warm source region, (2) warming by the release of latent heat as the air ascends over the mountain (i.e., the Hahn mechanism), or (3) the blocking of low-level air and the descent of higher potential temperature air from above (see Critchfield, 1966, pp. 130–131). In many cases the condensation occurring during stable lifting over a mountain is not sufficient to explain the large temperature difference between the two sides of the mountain. This suggests either that blocking is occurring or that the condensation is increased by convection over the mountain, triggered by orographic ascent. In this regard the reader should refer to Section 4 on the subject of orographic rain.

The most well-known occurrence of the bora is in the northern Adriatic near Trieste and south along the Yugoslavian coast (Yoshino, 1975, 1976). Air cooled over Eurasia spills over the highlands between the Alps and the Balkans and descends to the sea. The mistral flowing between the Pyrenees and Alps and the Tehuantepec fall wind south of the Sierra Madres in Mexico are also bora-type fall winds (see Godske *et al.*, 1957).

2.7. The Influence of the Boundary Layer on Mountain Flows

The theories of airflow past mountains assume for the most part that the flow is inviscid, neglecting the presence of the thick turbulent atmospheric boundary layer. There have, however, been attempts to understand the nature of the boundary layer as it flows over simple topography (Counihan *et al.*, 1974; Taylor and Gent, 1974; Jackson and Hunt, 1975; Deaves, 1976; Taylor *et al.*, 1976; Taylor, 1977a,b). These studies have so far been restricted to small hills where the effects of buoyancy forces could be neglected. It follows that this type of flow may have something in common with the subject of potential flow.

In order to model the flow in the boundary layer it is necessary to take into account (a) the shearing nature of the undisturbed flow; (b) the turbulence, both as it influences and is influenced by the mean flow; and (c) the degree of roughness of the surface (e.g., the roughness length z_0). The complexity of this situation requires that some form of numerical computation be used to solve the governing equations.

The results of these computations (see, for example, Fig. 12) show a qualitative resemblance to potential flow. The wind speed (at a standard level) reaches a maximum near the top of the hill and the pressure has its minimum value there. This is true in spite of the fact that Bernoulli's equation does not strictly hold. Similar computations done for flow across

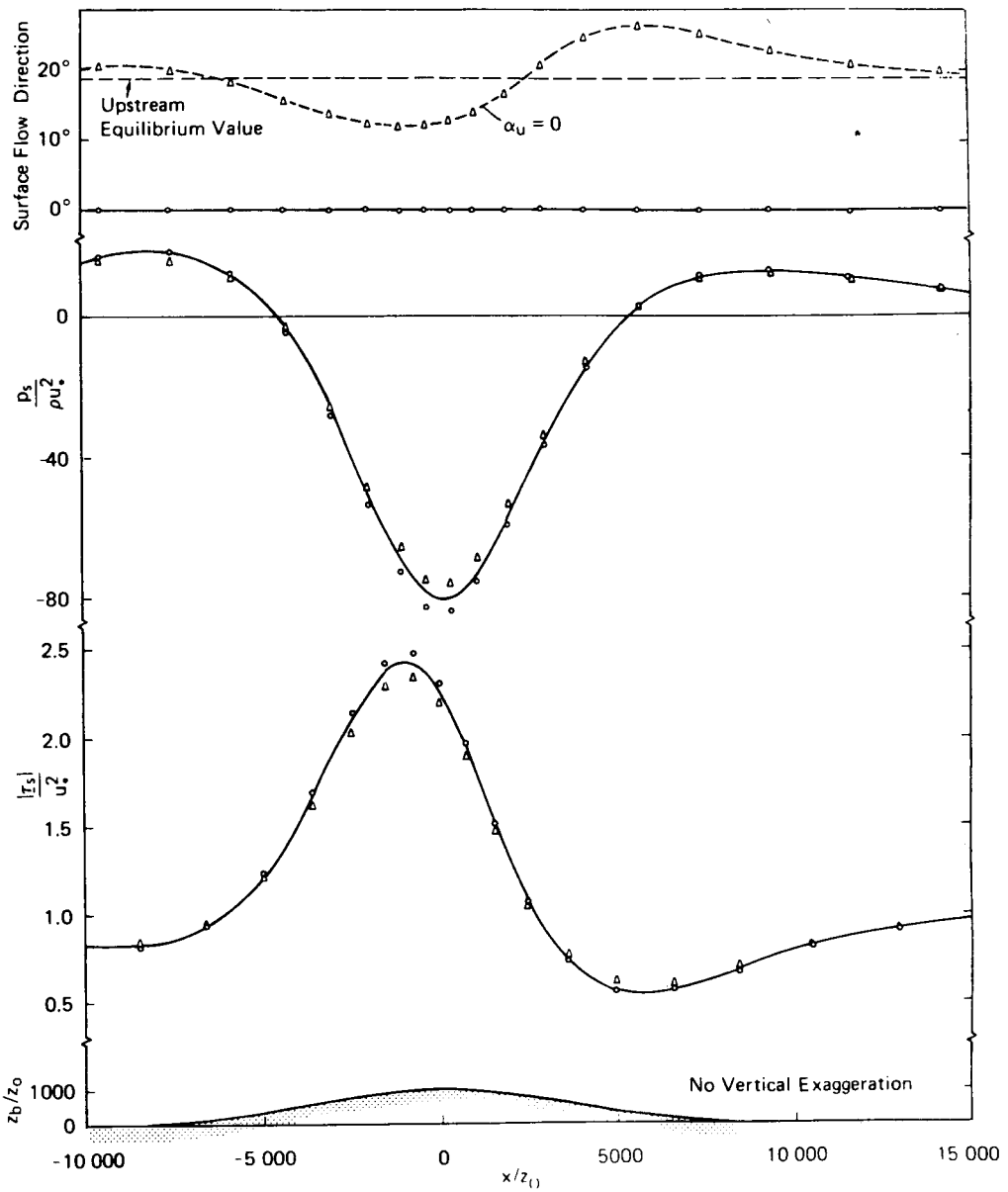

FIG. 12. The computed flow over a small ridge, immersed in a turbulent Ekman layer. The skin friction (and the wind speed near the ground) reaches a maximum just upstream of the crestline while the pressure has a minimum just downstream. To a first approximation the flow resembles inviscid, irrotational flow (see Fig. 2), but upon close inspection, the influence of the preexisting thick turbulent boundary layer is apparent. (From Taylor, 1977b.)

shallow valleys show a strong reduction in wind speed and a pressure maximum in the valley bottom. Qualitatively both the hill and valley results are in agreement with the measurements reviewed by Yoshino (1975, pp. 262-268) and with common experience; that is, hill tops are more exposed to the wind, while topographic lows are sheltered.

A more quantitative examination of the computer results reveals, as expected, some deviation from potential flow behavior. There is a slight asymmetry to the pressure field on the ridge leading to a net drag. There is also a sheltered region which extends a considerable distance downstream. The reduction in surface shear stress in this region partially cancels the drag due to pressure forces as it affects the net areal drag.

The numerical models have not yet been extended to include cases of abrupt topography, leading to separation. The great body of work on this subject in engineering aerodynamics may not be applicable here because of the lack of a thick turbulent boundary layer upstream. The laboratory model of the flow around Mt. Fuji by Soma (1969) did include this effect however. The modeling of the flow past a windbreak (see, for example, Seginer, 1972) is also relevant here.

There has also been a good deal of speculation on the role of the boundary layer in flows where buoyancy forces are obviously important. One question is whether the rotor—a turbulent recirculating region found under the crests in a train of lee waves—is an example of boundary layer separation. This controversy is mentioned in Queney *et al.* (1960), and since that time several other observations have appeared in the literature (Gerbier and Berenger, 1961; Förchtgött, 1969; Lester and Fingerhut, 1974).

2.8. Slope Winds and Mountain and Valley Winds

Whenever the surface temperature differs from the temperature of the air above (due to radiative heating and cooling, or horizontal advection), heat will be transferred from one medium to the other. This will quickly establish a layer of air near the surface which, while more closely matching the soil temperature, will differ from the air still higher up. If this occurs on a sloping surface, the buoyancy forces associated with the temperature variations will cause the layer to accelerate up or down the slope. The acceleration will continue until the frictional resistance becomes equal to the buoyancy forces and a steady-state slope wind is established. A further requirement for steady state is that the rate of heating or cooling the air parcels must be matched by the rate at which these parcels move into regions of warmer or cooler environmental temperature so that their temperature anomaly remains constant. This is

possible if the lapse rate in the vicinity of the mountain slope is a stable one. These requirements for steady state can be written as

$$g \sin(\alpha) \frac{\theta'}{\theta} + \nu \frac{\partial^2 u'}{\partial z^2} = 0 \tag{2.103a}$$

and

$$-\bar{\theta} S \sin(\alpha)\, u' + k \frac{\partial^2 \theta'}{\partial z^2} = 0 \tag{2.103b}$$

after Prandtl (see Defant, 1951). In (2.103a) g is gravitational acceleration, $\bar{\theta}$ and θ' are the background and perturbation potential temperature, u' is the induced slope wind, ν and k are the diffusivities of momentum and heat, S is the stability $d\ln\bar{\theta}/dz$, and the z coordinate in (2.103) is directed perpendicularly to the slope α. If the temperature perturbation at the ground can be specified as ΔT, then the boundary condition is

$$\theta' = \Delta T \qquad \text{at} \qquad z = 0$$

together with the no slip condition

$$u' = 0 \qquad \text{at} \qquad z = 0$$

and the condition that the disturbance decay far above the slope

$$\theta',\, u' \qquad \text{vanish as} \quad z \to \infty$$

With all coefficients taken as constant, the solution is

$$\theta'(z) = \Delta T e^{-z/l} \cos z/l \tag{2.104a}$$

$$u'(z) = (g/N)(k/\nu)^{1/2} \Delta T/\bar{\theta}\, e^{-z/l} \sin z/l \tag{2.104b}$$

with $N^2 = gS$ and l, a measure of the thickness of the layer of moving air, given by

$$l \equiv \left(\frac{4k\nu}{N^2 \sin^2 \alpha} \right)^{1/4} \tag{2.105}$$

This solution can be criticized on a number of grounds, for example, the slope of the terrain (α) has been presumed to be constant both in the downslope and cross-slope directions, and the transport of heat and momentum have been parameterized by specifying the eddy diffusion coefficients k and ν. Nevertheless, the "slope wind" solution (2.104) is useful as it illustrates the type of momentum and heat balance that might be realized in nature.

Probably the best direct application of the slope wind solution is to the nearly continuous katabatic winds which run down the slopes of the great

ice domes of Greenland (Nansen, 1890) and Antarctica (Mawson, 1915). Lettau (1966) has compared (2.104) against observations of an antarctic katabatic wind and found reasonable qualitative agreement for suitably chosen values of k and ν. The profile he studied was characterized by a wind maxima of 3 m/sec at 5 m above the surface corresponding to $l \approx$ 7 m and a temperature anomaly at the surface $\Delta T \approx -10°C$.

The slope wind has also been observed locally in more complex terrain (see, for example, Bergan, 1969).

When the slope changes in the downstream direction, the balances described by Eqs. (2.103) are altered and the horizontal advection of momentum and heat [terms not included in (2.103)] become important. Gutman (1969) has solved the nonlinear two-dimensional steady state equations in a region of changing slope and finds, among other things, that air is expelled from or drawn into the slope boundary current in the vicinity of slope changes. This must occur of course, because the mass flux in the fully developed boundary current depends on the local slope. Using these ideas it is possible to understand how the air in a closed valley can be cooled or warmed by a loss or gain of heat at the valley walls. The divergences in the boundary layer cause slow vertical motion in the interior which, because of the background stratification, results in slow cooling or warming. This situation is closely analogous to the "spin-up" of a rotating fluid by Ekman layer pumping.

If the change in surface slope occurs very abruptly and the katabatic wind is strong, the local flow may be dominated by advection of momentum and heat leading to nonlinear phenomena such as a hydraulic jump. Ball (1956) and Lied (1964) have investigated the abrupt transition that occurs when the antarctic katabatic wind reaches the edge of the continent. Locally they ignore the loss of heat and momentum to the surface by turbulent diffusion, thereby reducing the problem to simple hydraulics. He was able to show that the Froude number computed for the katabatic wind upstream is supercritical and thus the deceleration of the flow is expected to occur by means of an abrupt hydraulic jump—in agreement with the observed flow.

In most mountainous regions the terrain is dissected by numerous river or glacially cut valleys. The slope wind solution may be applicable to some degree on the valley walls, but for the most part the flow is dominated by the tendency of the currents to concentrate in the valleys. The sides of the valley and smaller adjoining valleys then act as "tributaries," swelling the current of cold air moving down the valley (the mountain wind) or the warm air moving up the valley (the valley wind).

The dissected nature of the terrain is also important in decoupling the winds in the valley from the synoptic-scale winds aloft, presumably

through the mechanism of separation. Thus, in many deep valleys the wind climate is almost totally determined by the mountain and valley wind phenomena. (See, for example, Grønås and Sivertsen, 1970, for Norway; Jensen *et al.*, 1976, for Greenland; MacHattie, 1968, for Alberta, Canada; Defant, 1951; Yoshino, 1975, p. 276, for several other areas.)

Generally speaking it is the difference between the surface temperature and the air temperature that determines whether a mountain or valley wind will occur, and this in turn depends on the time of day, season of the year, and latitude. In the midlatitude Alps there is often a strong diurnal variation—mountain winds at night and valley winds during the day. Farther north in Norway, the mountain wind blows for almost the entire day in winter, while the valley wind dominates in the summer. In valleys with modern glaciers, the surface temperature is nearly always cooler than the air above, leading to the continuous "glacier wind" blowing downslope across the glacier or through downward-leading crevasses and caves in the ice.

Because of its influence on local climate, the mountain-valley wind cycle has received considerable attention, but there are still fundamental questions concerning (1) the existence of a reversed wind above the valley floor, and (2) the details of the transition between the valley wind and mountain wind which may occur, for example, at sunrise and sunset. A reversed current aloft could occur in many ways: (a) the weak return current in (2.104b) caused by eddy momentum transport and excess adiabatic cooling, (b) the continuation of the upper part of a deep valley wind after the wind near the surface has reversed, (c) a true "return" current in which the air flows one way in the mountain or valley wind and then returns aloft to satisfy the continuity equation, and (d) the synoptic-scale wind which may happen to be opposed to the wind in the valley.

Detailed models of the wind reversal at sunrise and sunset have been put forth by Defant (1951), Urfer-Henneberger (1964), and Sterten (1963). The observations of Wilkins (1955) also bear on this question. The common point in these models seems to be that the slope winds on the valley sides respond rather quickly to the changes in solar insolation. The winds in the central valley, especially away from the surface, respond more slowly. This is shown in Fig. 13.

Another unanswered question is why the warm valley wind or a warm upslope wind does not detach itself from the surface and rise vertically. Certainly it could release potential energy faster if it did so. The answer to this dilemma may be that the atmosphere above is stably stratified and air must continue to receive heat from the surface if it is to rise. On the

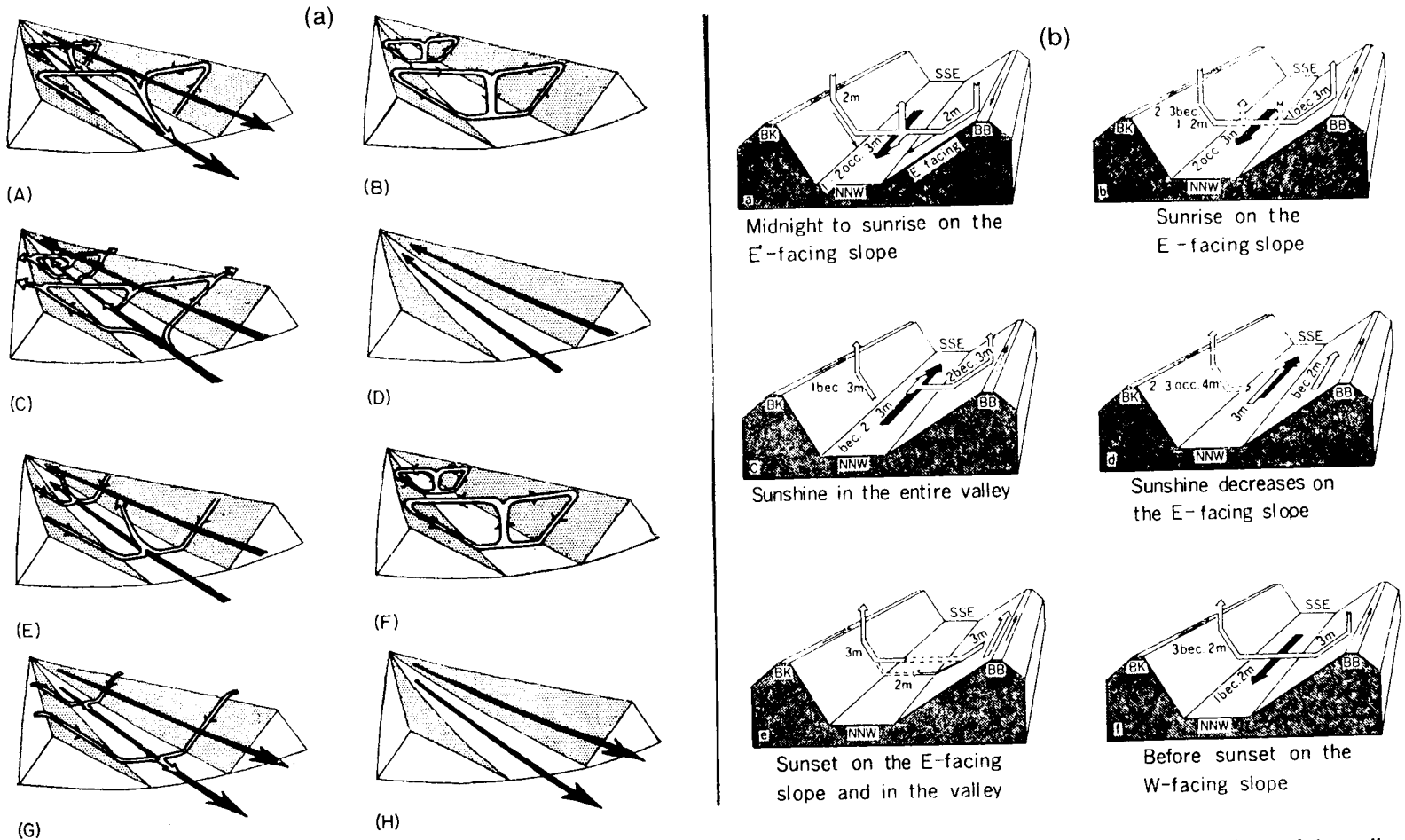

FIG. 13. Two views of the diurnal cycle of mountain and valley winds and the interaction with slope winds on the steep sides of the valley. The slope winds respond quickly to changes in solar insolation, while the wind in the valley responds more slowly. (a) The model proposed by Defant (1951) assumes the valley is uniformly heated by the sun: (A) sunrise, (B) forenoon, (C) early afternoon, (D) late afternoon, (E) evening, (F) early night, (G) middle of night, (H) late night to morning. (b) The model of Urfer-Henneberger (1964) takes into account the difference in insolation between the sunlit and shaded slopes.

other hand, if the surface was strongly heated and of gentle slope, direct parcel ascent (i.e., penetrative convection) could occur.

3. The Flow near Mesoscale and Synoptic-Scale Mountains

In this section we will consider the perturbation to the wind flow caused by a mountain of intermediate scale where the rotation of the Earth cannot be neglected. As an example, let us say that a mountain has a width of from 100 km to 500 km, so that an air parcel moving with the wind at say 10 m/sec will take 10^4 sec (~3 hr) or 5×10^4 sec (~15 hr) to cross the mountain. To estimate the relative importance of fluid accelerations relative to the Earth to those associated with the Earth's rotation (i.e., the Coriolis force) we must compare the transit time of an air parcel with the rotation period of a Foucalt pendulum located at the appropriate latitude $T = 2\pi/2\Omega \sin \phi$. For midlatitudes on the Earth this is about 12 hr, and we conclude that in the horizontal equations of motion both types of accelerations may be the same order of magnitude. Mountains in this size range are quite common on the Earth's surface. Probably any surface irregularity that would be called a large mountain or a mountain range would be included. Examples include the Scandinavian mountain range (width ~ 300 km), the Alps (width ~ 250 km), and the Canadian Rockies (width ~ 400 km). In all these examples the influence of the Coriolis force on the perturbed flow is too large to be ignored, yet too small to allow the assumption of geostrophic balance.

Throughout this section we shall be working between two well-defined limiting situations. With small mountains (width ~ 50 km) the Coriolis force can be ignored while the hydrostatic assumption can still be considered as valid. The flow over synoptic-scale orography (width ~1000 km) may be assumed to be nearly geostrophic. The types of flow occurring in these two situations are quite dissimilar, and one of the challenges of this section is to see if we can understand how the flow transitions from one type to the other as the Coriolis force becomes progressively more important. In the first case (see Fig. 3) the flow is asymmetric (even for a symmetric mountain), the perturbation extends to great altitude, and there is a drag on the mountain. The perturbation caused by the broad mountain on the other hand (see Fig. 17) is symmetric (if the mountain is), decreases with height, and causes no drag on the mountain. The mountain wave situation is discussed in another section of this review, but the broad mountain, quasi-geostrophic limiting case must be discussed here in detail before we can proceed further.

3.1. *Quasi-geostrophic Flow over a Mountain*

Consider the steady flow of a stratified rotating fluid over a mountain. This irregular surface of the ground will be assumed to be a stream surface to the flow. That is, the flow cannot penetrate the ground. We will assume also that the flow approaching the mountain is barotropic so that the potential temperature is constant along the ground. Then, if the potential temperature is constant following a fluid particle and if the surface of the mountain is completely covered by fluid that has come from upstream, it follows that *the mountain surface will coincide with the surface of constant potential temperature* (see Fig. 14).

This result is of crucial importance to the nature of the flow field near the mountain. Note that there are several ways that this condition could be violated: (a) baroclinic flow upstream, (b) transient effects or permanent blocking which prevent the particles with upstream properties from fully penetrating the region of interest, and (c) diabatic effects. Further, the observational evidence does not strongly defend this assumption. The lapse rate measured along a mountain slope is usually substantially less (in magnitude) then the adiabatic lapse rate (see Yoshino, 1975; Peattie, 1936, for a review of these observations), indicating that $\theta \neq$ const along the surface. This criticism can be turned aside by arguing that this variation in θ is due to heating of the air near the ground. There still might be a surface just outside the boundary layer which closely parallels the mountain shape and on which the condition $\theta =$ const is satisfied.

More disturbing are the aerological observations which occasionally seem to show isentropic surfaces, outside the boundary layer, intersecting a mountain. For the most part, however, the radiosonde network is not dense enough to determine the true shape of θ-surfaces in mountainous terrain. In the following analysis we will assume that the θ-surfaces follow the terrain. It is clear, however, both that the validity of this

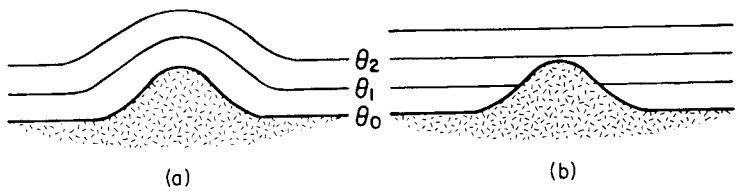

FIG. 14. Two possible configurations for the isentropic surfaces near a mountain. (a) The isentropic surfaces are pushed up, paralleling the ground surface. (b) The mountain penetrates up through horizontal θ-surfaces. If there is flow, it must be going around the mountain. The former model is used as a lower boundary condition in most mathematical models of mountain flow.

assumption is doubtful and that the breakdown of the assumption will fundamentally change the nature of flow.

The next important result involves the nature of the wind field near the mountain. If the flow is geostrophically balanced

$$\rho f u = -\frac{\partial P}{\partial y} \tag{3.1a}$$

$$-\rho f v = -\frac{\partial P}{\partial x} \tag{3.1b}$$

The hydrostatic assumption is written as

$$-\rho g = \frac{\partial P}{\partial z} \tag{3.2}$$

To simplify the analysis we will treat the air as a Boussinesq fluid by neglecting its compressibility and neglecting the influence of density variations on the inertia [i.e., the left-hand side of (3.1)] of a fluid particle (see, for example, Batchelor, 1967). In the absence of compressibility the density of a fluid particle is constant

$$D\rho/Dt = 0 \tag{3.3}$$

If the background flow is stratified $\bar{\rho}(z)$, Eq.(3.3) can be used to show that a local density perturbation ρ' can be produced by raising or lowering a fluid particle a distance η into a different density environment.

$$\rho' = -\frac{\partial \bar{\rho}}{\partial z}\eta \tag{3.4}$$

Now combining (3.1), (3.2), (3.4) gives

$$-\rho f \frac{\partial u}{\partial z} = g\frac{\partial \bar{\rho}}{\partial z}\eta_y \tag{3.5a}$$

$$+\rho f \frac{\partial v}{\partial z} = g\frac{\partial \bar{\rho}}{\partial z}\eta_x \tag{3.5b}$$

which is a Boussinesq version of the more general thermal wind equation. It displays the connection between the vertical wind shear ($\partial u/\partial z$, $\partial v/\partial z$) and the slope of the surfaces of constant ρ (or θ in the atmosphere). This can be put in a more compact form by introducing the stream function

$$\psi_x \equiv v, \qquad \psi_y \equiv -u \tag{3.6}$$

and the integrating (3.5) to obtain

$$\psi_z = -(N^2/f)\eta \tag{3.7}$$

where

$$N^2 = -\frac{g}{\bar{\rho}}\frac{\partial \bar{\rho}}{\partial z} \qquad \left(= \frac{g}{\theta}\frac{\partial \bar{\theta}}{\partial z} \quad \text{in the atmosphere}\right)$$

Near the mountain surface the distribution of uplift of θ-surfaces $\eta(x, y)$ is just equal to the orographic height $h(x, y)$ so the pattern of vertical wind shear is known immediately.

$$\psi_z = -(N^2/f)h(x, y) \qquad \text{near the ground} \tag{3.8}$$

To solve for the wind itself the entire flow field must be considered. We can reason intuitively as follows: Near a region of raised θ-surfaces in a stable geostrophically balanced atmosphere, Eq. (3.8) requires that we have either cyclonic motion which becomes stronger with height or anticyclonic motion which weakens with height. Intuitively we feel that a disturbance produced by a mountain ought to be strongest near the mountain, so it is natural to choose the latter alternative. Thus the flow around the mountain is identical to the textbook description of a "cold anticyclone," with the only difference being that it is the solid mountain surface, rather than the cold air near the ground, that is responsible for the upwarping of the θ-surfaces (see Fig. 15). The expression "mountain anticyclone" is chosen to refer to the qualitative aspects of the flow.

To understand the detailed structure of the mountain anticyclone the concept of conservation of circulation is needed. Consider a column of fluid at point a confined between two isentropic surfaces θ_1, θ_2 (Fig. 16). The absolute circulation $\Gamma_a \equiv \oint_c \bar{v}_{ab} \cdot dS$, which can be written $(\zeta + f)A$,

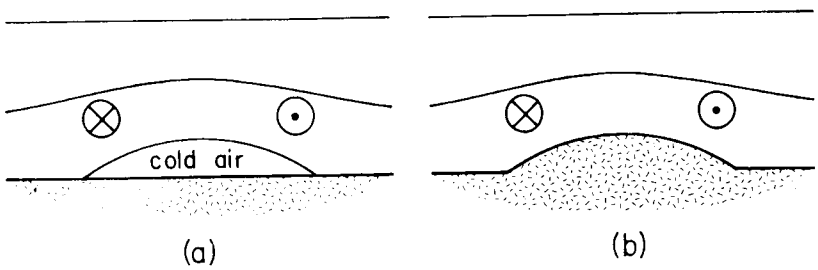

FIG. 15. The upwarping of isentropic surfaces near the ground caused by (a) a cold air mass at the surface or (b) a region of high ground. If the unwarping decreases with height and if the flow is geostrophically balanced, there must be an anticyclonic circulation—either (a) a cold-core anticyclone or (b) a mountain anticyclone.

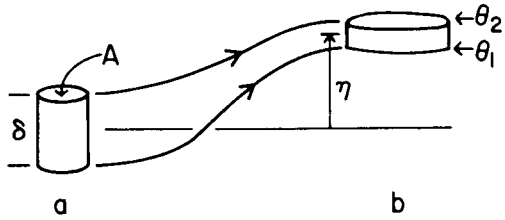

FIG. 16. Synoptic scale vorticity dynamics in a stratified fluid. As an air parcel moves from a region of weaker stability (a) into a region of stronger stability (b), its vertical dimension (δ) decreases while its horizontal area (A) increases. The Coriolis force, acting during the horizontal divergence, produces anticyclonic vorticity.

is conserved, as is the volume $A\delta$ (if the fluid is incompressible). Thus if the distance δ between θ-surfaces decreases from point a to b, the horizontal area A of the fluid column must increase as it moves toward b and the absolute vorticity $\zeta + f$ must decrease. Quantitatively

$$\frac{dA}{A} = -\frac{1}{\delta}\, d\delta \tag{3.9}$$

but the relative stretching of the column $d\delta/\delta$ is due to the different vertical displacement η of the top and the bottom of the column so

$$\frac{d\delta}{\delta} \approx \frac{\partial \eta}{\partial z} \tag{3.10}$$

The conservation of absolute circulation can now be written

$$0 = \frac{D}{Dt}\left[(\zeta + f)A\right] \approx \frac{D}{Dt}\left[(\zeta + f)A_a\left(1 + \frac{dA}{A_a}\right)\right]$$

If $\zeta \ll f$, $f = \text{const}$, $dA/A \ll 1$ and using (3.9), (3.10)

$$0 = \frac{D}{Dt}\left[\zeta - f\frac{\partial \eta}{\partial z}\right] = \frac{D}{Dt}\left[q\right] \tag{3.11}$$

The quantity in square brackets in (3.11) is the "potential vorticity"

$$q \equiv \zeta - f\frac{\partial \eta}{\partial z} \tag{3.12}$$

It can be rewritten using the steam function defined in (3.6)

$$q = \nabla_H^2 \psi - f\,\frac{\partial \eta}{\partial z} \tag{3.13}$$

Finally, using the geostrophic assumption in the form (3.7) and assuming

$N^2 = \text{const}$ gives

$$q = \nabla_H^2 \psi + \frac{f^2}{N^2} \psi_{zz} \tag{3.14}$$

We shall call (3.14) the "geostrophic form of the potential vorticity." In its more basic form (3.11), q will be conserved regardless of whether the flow is geostrophic or not.

Using the geostrophic form (3.14) introduces a paradox which should be mentioned before going further. If the flow were exactly geostrophic, it could not undergo the horizontal divergence shown in Fig. 16. To see this, use (3.1) to evaluate $\nabla_H \cdot \mathbf{u} = (\partial u/\partial x) + (\partial v/\partial y)$. We know from observation that the large-scale winds are nearly geostrophic, but mathematically it can be shown that if the flow was exactly geostrophic, it could not do any of the interesting things the atmosphere is observed to do. The type of analysis used here and throughout much of dynamic meteorology is called quasi-geostrophic theory (see Holton, 1972). Conceptually, the flow is allowed to be slightly divergent (i.e., ageostrophic), but close enough to geostrophy so that an equation like (3.7) gives a sufficiently accurate description of the relation between the wind field and the density field.

The simplest case of quasi-geostrophic flow over a mountain is the case of $q = 0$ upstream, for example, uniform wind approaching a mountain. If the entire flow field is filled with fluid that has come from upstream, then from (3.11) and (3.14)

$$q = \nabla_H^2 \psi + \frac{f^2}{N^2} \psi_{zz} = 0 \tag{3.15}$$

Equation (3.15) must be solved subject to the boundary conditions at the ground (3.8), and at large z where the solution must be bounded. Because of the many simplifying assumptions (e.g., small perturbations, Boussinesq, quasi-geostrophy, constant N and f, $q = 0$ upstream) (3.15) has a simple form. If a stretched vertical coordinate is used $\hat{z} = (N/f)z$, (3.15) becomes Laplace's equation

$$\nabla^2 \psi = \frac{\partial \psi}{\partial x^2} + \frac{\partial^2 \psi}{\partial y^2} + \frac{\partial^2 \psi}{\partial \hat{z}^2} = 0 \tag{3.16}$$

This allows us to use all of the mathematical and conceptual techniques of potential theory while keeping in mind that the vertical scale of the motion is very much less (by a factor of $f/N \approx 0.01$) than the horizontal scale. It turns out that we can construct interesting mountain flow solutions, either in two or three dimensions, by analogy with the simplest potential flow solutions.

3.2.1. The Flow over an Isolated Mountain. The two simplest solutions to Laplace's equation in three dimensions are $\phi = Ux$ and $\phi = -S/4\pi r$ which correspond physically to uniform flow and a source of strength S at the origin. With this as a guide we choose

$$\psi(x, y, z) = Uy - (S/4\pi r) \tag{3.17}$$

where

$$r = [x^2 + y^2 + (N^2/f^2)z^2]^{1/2}$$

as a solution (3.15). Using (3.7) the corresponding pattern of stream surface (or θ-surface) lifting can be determined

$$\eta(x, y, z) = -\frac{f}{N^2}\psi_z = -\frac{S}{4\pi f}\left(x^2 + y^2 + \frac{N^2}{f^2}z^2\right)^{-3/2} z \tag{3.18}$$

Using this form we can consider a whole family of bell-shaped mountains with circular contours by placing the "source" at a distance z_0 beneath the ground surface. Then for a mountain of shape

$$h(x, y) = \frac{h_m}{(R^2/R_0^2 + 1)^{3/2}} \tag{3.19}$$

where $R = (x^2 + y^2)$ and $R_0 = (N/f)z_0$ is the measure of the mountain width. The θ-surface displacement is

$$\frac{\eta(x, y, z)}{h_m} = \frac{(z/z_0 + 1)}{[R^2/R_0^2 + (z/z_0 + 1)^2]^{3/2}} \tag{3.20}$$

The perturbation wind caused by the mountain blows around the mountain in the anticyclonic (clockwise in the northern hemisphere) direction with strength

$$v_\theta = \frac{-h_m N(R/R_0)}{[R^2/R_0^2 + (z/z_0 + 1)^2]^{3/2}} \tag{3.21}$$

One important aspect of this flow is that the maximum vertical displacement of the isentropic surfaces [Eq. (3.20)] decreases with height, but the lifting becomes much more widely distributed so that the volume under the raised surfaces

$$\int_{-\infty}^{\infty}\int \eta(x, y, z)\, dx\, dy = 2\pi h_m R_0^2 \tag{3.22}$$

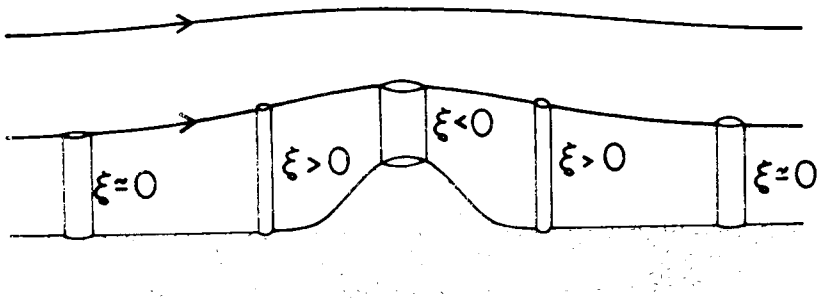

FIG. 17. The vorticity dynamics in the stratified, quasi-geostrophic flow over an isolated mountain. The magnitude of the lifting of θ-surfaces aloft is less than the mountain height, but the lifting is more widespread. As parcels near the ground approach the mountain, they are first stretched producing cyclonic vorticity. Over the mountain, the parcels are shortened producing anticyclonic vorticity. The total amount of cyclonic and anticyclonic vorticities are equal at each level and, as a result, there is no far-field circulation. (After Buzzi and Tibaldi, 1977.)

equals the mountain volume at every level. The lifting of the stream surfaces aloft extends far from the mountain. Thus as a fluid column approaches the mountain it is first stretched due to the lifting of stream surfaces aloft, then shortened due to the mountain elevation (see Fig. 17). This behavior is discussed by Buzzi and Tibaldi (1977).

The velocity field described by (3.17) is the vector addition of uniform flow of strength U and the mountain anticyclone [described by (3.21)] which weakens aloft (see Fig. 18). Near the ground $z \ll z_0$, and far from the mountain $R \gg R_0$, the perturbation velocity falls off like $v_\theta \sim 1/R^2$. This decay is more rapid than in an irrotational vortex and accordingly the circulation around the mountain will decrease as the radius of the

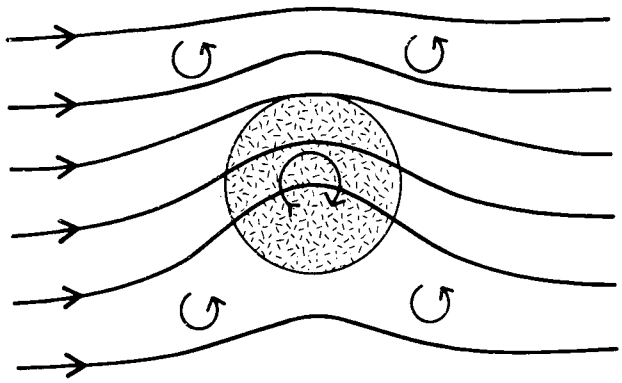

FIG. 18. The streamline pattern in quasi-geostrophic stratified flow over an isolated mountain (see also Fig. 17). The incoming flow is distorted by the mountain anticyclone. The perturbation velocity and pressure field decay away from the mountain.

circuit is increased. This rapid decay is another facet of the weak cyclonic relative vorticity surrounding the core of anticyclonic vorticity directly above the mountain.

Note that this description of a mountain anticyclonic in a rotating unbounded stratified fluid is quite different from the flow over an isolated hill in a homogeneous fluid with a rigid upper lid. In this latter case the vertical displacement η and the relative vorticity ζ would be zero except directly over the mountain, the volume under the raised stream surfaces would decrease aloft, and the strength of the anticyclonic winds would be constant with height and decrease as $1/R$ horizontally away from the hill.

A more general family of mountain shapes can be considered by using a combination of "sources" in or slightly below the $z = 0$ plane. To a large extent the qualitative nature of these more complicated flows can be determined graphically. In any case, far away from the orographic region the behavior will be as described above with the effective source strength [in (3.17), (3.18)] being determined from the total mountain volume according to $S = -N \times$ [mtn. vol.].

As an example, we could consider qualitatively the flow over a long (but finite) narrow ridge. Near the center of the ridge the induced flow is parallel to the ridge as it would be for an infinite ridge, while far away from the ridge the streamlines for the induced flow become circular as in (3.17).

One interesting feature of the flow over a finite ridge is that unlike the circular mountain or infinite ridge solutions, the induced velocity has a component across the height contours of the mountain. Thus, the vertical velocity near the surface which to first order is $U(\partial h/\partial x)$ can be strongly modified by the induced flow. This could have an important effect on the distribution of orographic rainfall along the windward side of a mountain range.

In general, the perturbation stream function and therefore the perturbation pressure will be symmetric with respect to the topography. As a result the net horizontal force on the topography due to the perturbation pressure field (e.g., drag) vanishes identically. This result will, of course, be altered if we introduce a viscous Ekman layer, the β-effect, or if the Rossby number was large enough to allow the generation of mountain waves. Such forces, if they were present, would be proportional to the square of the mountain height [i.e., $O(h_m^2)$].

There is, however, an $O(h_m)$ force on the mountain due to the background geostrophic pressure gradient. Looking downstream, the isolated mountain finds itself in a pressure field increasing linearly to the right. Thus, according to Archimedes Law, the mountain feels a net pressure

force to the left given by

$$F = -\frac{\partial P}{\partial y} \cdot V$$

$$F = \rho U f V$$

where V is the volume of the mountain. This "lift" force acts perpendicularly to the mean flow, regardless of the shape of the mountain. This is true even for a long ridge because the large pressure difference at the ends of the ridge will be just what is needed to make the net for perpendicular to the mean flow direction, not the ridge. In the Boussinesq model described above, the air passing over the mountain does not respond to the lift force reaction (i.e., the force applied to the air by the mountain). Instead the force is passed upward from layer to layer without decreasing. This is so because the volume under each uplifted θ-surface and the cross-stream pressure gradient are both independent of height. The influence of compressibility on this result is discussed by Smith (1979b).

3.2.2. The Flow over an Infinite Ridge. To construct a solution for infinite ridge we can superpose a linear distribution of isolated mountains or simply use the well-known two-dimensional source solution to potential flow theory, $\phi = (S/2\pi)\ln r$. This latter method leads to a stream function of the form

$$\psi(x, z) = -Uy + (S/2\pi) \ln r \tag{3.23}$$

where $r = [x^2 + (N^2/f^2)\, z^2]^{1/2}$. This is a solution for flow over a ridge of shape

$$h(x) = h_m a^2/(x^2 + a^2) \tag{3.24}$$

where a is a measure of the width of the ridge. The vertical displacement is

$$\eta(x, z) = \frac{h_m a^2 (z/z_0 + 1)}{x^2 + a^2 (z/z_0 + 1)^2} \tag{3.25}$$

The induced velocity lies parallel to the ridge

$$v(x, z) = -\frac{h_m N x a}{x^2 + a^2 (z/z_0 + 1)^2} \tag{3.26}$$

As an example, the amplitude factor $h_m N$ might be 10^3 m$\times$ 0.01 sec^{-1} = 10 m/sec.

This flow is in many respects similar to the three-dimensional flow over a mountain with circular contours, discussed earlier. As before, the

general sense of the induced circulation is anticyclonic and its structure and strength is independent of the direction or strength of the incoming wind. The lifting of the θ-surfaces aloft η is again much more widespread than the orographic height $h(x)$. This means that as a fluid particle approaches the mountain it is first vertically stretched, producing positive relative vorticity, and simultaneously slowed to maintain constant mass flux between streamlines. From its vorticity, or from the fact that the slowed particle now feels a decreased Coriolis force, it is clear that the particle will curve to the left. When the particle is directly over the mountain, the θ-surfaces are closer together, the fluid moves faster and has negative relative vorticity, and the particle paths curve strongly to the right. Downstream of the mountain there is again stretching, slowing, and curvature to the left. When averaged over the mountain and the surroundings, the relative vorticity (or the circulation) is zero as the vortex stretching adjacent to the mountain exactly cancels the vortex shrinking over the mountain. Associated with this is the fact that the time necessary for a particle to traverse the whole flow field is the same as it would be without the mountain, thus the next impulse given to the fluid by the Coriolis force is zero. The force to the right acting on the fast-moving fluid over the mountain is exactly balanced by the force to the left acting on the slower fluid adjacent to the mountain. The result of this balance is that *the infinite ridge causes no permanent turning of the flow*. This can be seen from (3.26), as the induced velocity associated with the mountain anticyclone decays far from the mountain as $v \sim x^{-1}$.

Having discussed the stratified, unbounded Boussinesq solution in some detail we are in a position to evaluate critically the models of quasi-geostrophic flow over a ridge which have appeared in the literature. These are shown in Fig. 19.

(a) The flow of a homogeneous fluid with a rigid lid (see, for example, Batchelor, 1967, p. 573). There is a "permanent" turning of the flow

$$\Delta\theta = \tan^{-1}\frac{f}{HU} \cdot (\text{cross-sectional area}) \tag{3.27}$$

caused by vortex line shortening over the ridge. This is a useful model to illustrate the nature of vorticity, but it has no application to the strongly stratified atmosphere.

(b) The flow of a stratified, unbounded fluid described qualitatively in the standard meteorology textbooks (see Haltiner and Martin, 1957, p. 357; Hess, 1959, p. 252; Holton, 1972, p. 70). The lifting of θ-surfaces occurs only above the mountain and the lifting decreases with height, presumably due to the stratification. This model is not a solution to the

governing equations of quasi-geostrophic stratified flow and should be discarded. This housecleaning will not be easy, however, as the textbook model has influenced a generation of meteorologists.

(c) The flow of an unbounded stratified fluid (Queney, 1947) discussed in detail above. There is a local baroclinic disturbance but no permanent turning.

(d) The flow of a stratified fluid with a rigid lid (Robinson, 1960; Jacobs, 1964; Hogg, 1973; Janowitz, 1975; Merkine, 1975; Merkine and Kalnay-Rivas, 1976; Mason and Sykes, 1978). This flow is characterized by both a local baroclinic distance and a barotropic permanent turning given by (3.27). The use of a rigid lid is sometimes defended by suggesting that the great stability in the stratosphere will prevent vertical motion above the troposphere, but this argument is incorrect (Smith, 1979b).

(e) The flow of a compressible, unbounded stratified fluid (Smith, 1979b). In addition to the local baroclinic disturbance there is a barotropic permanent turning [given by (3.27) with H replaced by the density scale height] associated with the production of vorticity by volume changes as the air parcels lift over the ridge.

3.2. The Effect of Inertia on the Flow over Mesoscale Mountains

The foregoing discussion was designed to show the relationship between the different quasi-geostrophic solutions to flow over a mountain. These solutions are applicable only to very large orographic features with their smallest horizontal dimension exceeding 1000 km or so. On this scale it is exceedingly difficult to find a meteorological situation that approximates a uniform steady wind approaching a mountain range. For this and several other reasons, it is appropriate to study slightly smaller mountains, with widths of a few hundred kilometers, which quite frequently produce identifiable steady state flow patterns lasting many hours or even a few days. To do this we must not assume quasi-geostrophy but allow inertial effects to be important.

One attempt to do this is to determine the first effect of inertia. Merkine (1975) used the semi-geostrophic approximation (a slightly less restrictive version of the quasi-geostrophic approximation) to examine the rotating stratified flow over an infinite ridge with a rigid top lid. Merkine and Kálnay-Rivas (1976) examine a similar problem but for an isolated mountain. Buzzi and Tibaldi (1977) use an expansion in powers of the Rossby number to solve for flow over an isolated mountain in an unbounded fluid. These results show interesting differences with the quasi-geostrophic case, which increase as the Rossby number $\mathrm{Ro} = U/fL$ ap-

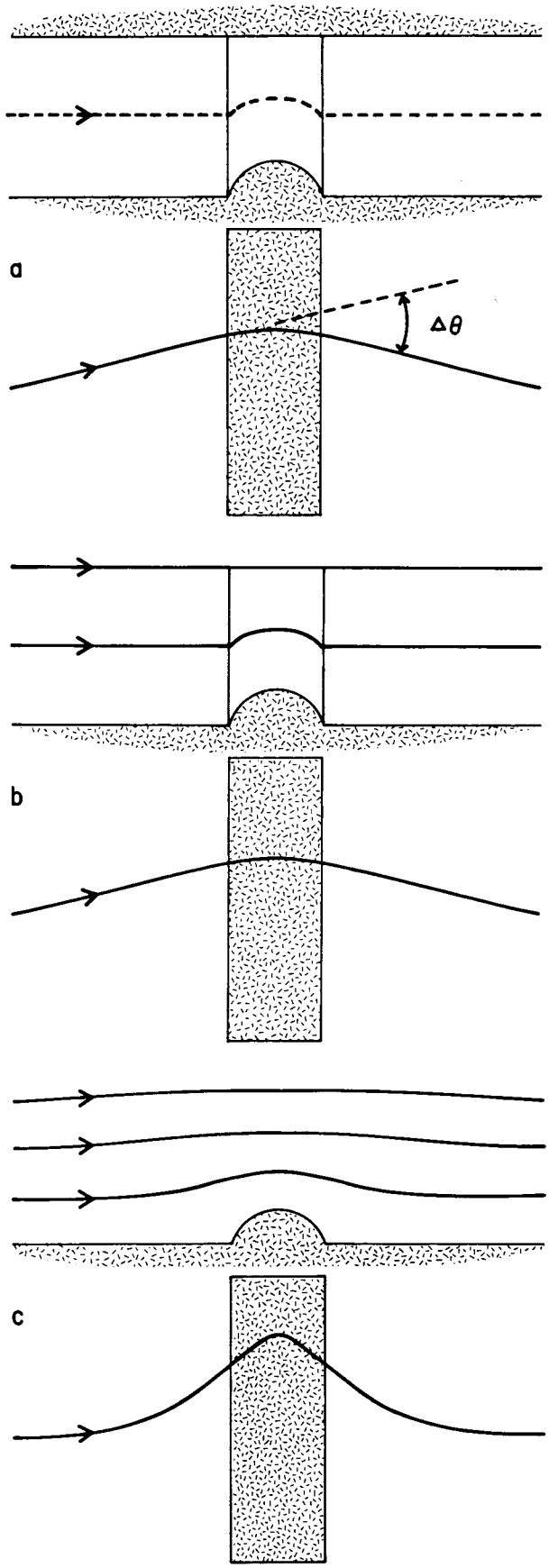
a
Δθ
b
c

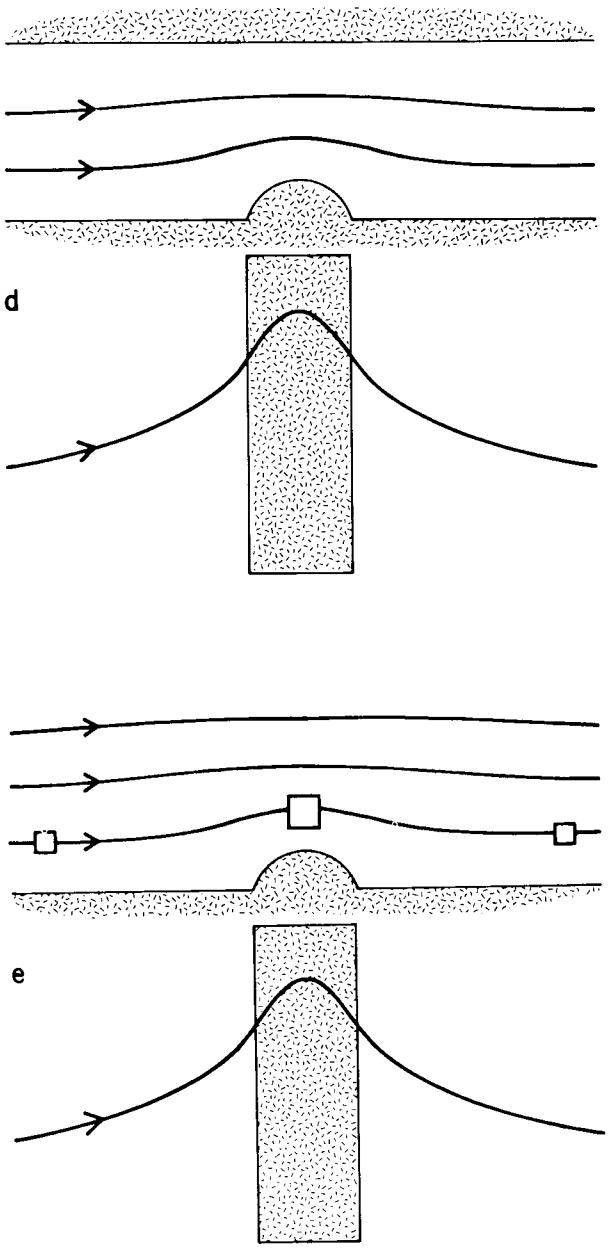

FIG. 19. Five models of quasi-geostrophic flow over a ridge. (a) Homogeneous flow with a rigid lid. The flow is columnar, and relative vorticity is present only over the ridge. There is a "permanent" turning of the flow. (b) "Textbook" description of stratified unbounded flow. According to this model, the flow is similar to (a) with the vertical displacements decaying aloft due to the stratification. This is not a solution to the governing equations. (c) Stratified unbounded flow as given by (3.25) and (3.26). There is no "permanent" turning of the flow. (d) stratified flow with a rigid lid. In addition to the baroclinic disturbance near the mountain, there is a barotropic "permanent" turning caused by the rigid lid. (e) Compressible stratified unbounded flow. In addition to the baroclinic disturbance near the mountain, there is a "permanent" turning associated with an extra production of anticyclonic vorticity caused by volume expansion as the parcels rise over the ridge.

proaches unity. The flow, however, remains symmetric about the y axis (i.e., windward vs. leeward side) and the disturbance decays rapidly with height just as in the quasi-geostrophic case. It is clear then that the mathematical techniques used in these studies (i.e., semi-geostrophic approximation or an expansion in Rossby number) are not sufficiently powerful to describe the propagation of inertia-gravity waves. We suspect physically that these waves will become more and more important as the Rossby number increases toward. and then exceeds unity.

The much earlier work of Queney (1947, 1948) on the flow over a small-amplitude, infinitely long ridge is extremely valuable for clarifying the role of inertia in these difficult mesoscale (Ro $\sim$ 1) flows. Queney considered the two-dimensional rotating stratified flow over a mountain in an unbounded fluid. Using Fourier analysis he represents his solution as an integral over the contributions from the different horizontal wave numbers. For example, the vertical displacement of a fluid particle $\eta(x, z)$ is given by

$$\eta(x, z) = e^{sz} \int_0^\infty \hat{h}(k) \exp\{i[kx + k_z(k)z]\}\, dk \tag{3.28}$$

where $\hat{h}(k)$ is the Fourier transform of the mountain shape $h(x)$

$$\hat{h}(k) = \frac{1}{\pi} \int_0^\infty h(x) e^{ikx}\, dx \tag{3.29}$$

and the vertical wave number $k_z(k)$ is a function of the horizontal wave number k and the background wind, static stability and rotation rate according to

$$k_z(k) = k \left(\frac{k_s^2 - k^2}{k^2 - k_f^2} \right)^{1/2} \tag{3.30}$$

where

$$k_s = N/U \qquad \text{and} \qquad k_f = f/U$$

Equation (3.30) is derived from the equations of motion, the thermodynamic equation, etc. The factor e^{sz} in (3.28), with $S = -(1/2\bar{\rho})/(\partial\bar{\rho}/\partial z)$, describes the tendency for the disturbance amplitude to increase aloft due to the smaller density there.

The solution (3.28) will depend on the nature of the function $k_z(k)$ in the range of k where $\hat{h}(k)$ has appreciable values. For rather wide mountains (say, $L > 50$ km) $\hat{h}(k)$ will be appreciable only for $k \ll k_s \sim 10^{-3}$ and so for the purposes of evaluating (3.28) we can simplify (3.30) to

$$k_z(k) = k k_s (k^2 - k_f^2)^{-1/2} \tag{3.31}$$

This is equivalent to making the hydrostatic approximation.

To simplify the evaluation of (3.28) Queney chooses the familiar bell-shaped ridge

$$h(x) = \frac{h_m a^2}{x^2 + a^2} \tag{3.32}$$

which has a particularly simple Fourier transform

$$\hat{h}(k) = h_m a e^{-ka} \tag{3.33}$$

We are now in a position to investigate two interesting limiting situtions.

In the case of a mountain range that can be crossed in a few hours by a fluid particle, we can neglect the Coriolis force reducing (3.31) to

$$k_z(k) = k_s \tag{3.34}$$

Then using (3.33) and (3.44) in (3.28) gives

$$\eta(x, z) = h_m a e^{sz} e^{ik_s z} \int_0^\infty e^{ikx - ka}\, dk$$

$$= h_m a e^{sz} \frac{e^{ik_s z}}{a - ix}$$

and taking the real part

$$\eta(x, z) = h_m a e^{sz} \frac{a \cos k_s z - x \sin k_s z}{a^2 + x^2} \tag{3.35}$$

This describes a field of vertically propagating hydrostatic internal gravity waves excited by the mountain (Fig. 3). The disturbance is asymmetric about the ridge and does not decay with height. There is a considerable wave drag $[D/l = (\pi/4)\rho U N h^2]$.

The other extreme case is when the mountain is so broad that $\hat{h}(k)$ is appreciable only for $k \ll k_f$. We can then reduce (3.31) to

$$k_z(k) = i \frac{k k_s}{k_f} = i \frac{N}{f} k \tag{3.36}$$

This is equivalent to the quasi-geostrophic assumption. In fact (3.36) could be derived immediately from (3.15). Now (3.28) becomes

$$\eta(x, z) = h_m a e^{sz} \int_0^\infty e^{-ka} \exp\left[i\left(kx + i \frac{N}{f} zk \right) \right] dk$$

which gives

$$\eta(x, z) = -h_m a e^{sz} \frac{1}{[a + (N/f)z] + ix}$$

and taking the real part gives

$$\eta(x, z) = \frac{h_m e^{sz} a^2[(N/f)(z/a) + 1]}{x^2 + a^2[(N/f)(z/a) + 1]^2} \tag{3.37}$$

which is identical to the earlier *a priori* quasi-geostrophic solution (3.25) if s is set equal to 1 consistent with the Boussinesq approximation (see Fig. 17). Of course, the method of sources and sinks used to obtain (3.25) is powerful since it can be used to determine the quasi-geostrophic flow over isolated mountains. In the present context, however, Queney's two-dimensional formulation (3.28) is more useful as it allows us to investigate the flow over mesoscale mountains where the flow is not quasi-geostrophic. By using asymptotic methods to evaluate (3.28) [with (3.31) and (3.33)], Queney was able to plot solutions for intermediate cases $ak_f \approx 1$ where both inertia and Coriolis force are important. In particular, he computed the flow over a mountain with a half-width $a = 100$ which corresponds roughly to the scale of the Alps (Fig. 20).

Note that the pattern of vertical displacement is distinctly wavelike and, judging from the pressure difference across the mountain, the waves are transporting considerable momentum. Just as in the nonrotating case, the phase lines tilt upstream with height but unlike the nonrotating hydrostatic case, the wave energy disperses considerably aloft. The long waves trail behind somewhat because of the influence of the Coriolis force on their group velocity.

The influence of the Coriolis force is more evident in the horizontal projection of the streamlines and isobars. These do not coincide near the mountain as the flow is quite ageostrophic there. Far from the mountain the flow becomes nearly geostrophic and Queney computes the velocity induced along the mountain to be

$$v(x, z = 0) \simeq -h_m a N/x \tag{3.38}$$

This is identical to the asymptotic behavior (3.26) which was derived under the assumption that the flow field was quasi-geostrophic everywhere, even over the mountain. Thus, the fact that a mountain is narrow enough to generate waves and wave drag has no influence on the far-field flow, which behaves as if the flow is quasi-geostrophic everywhere. This result follows immediately from the linearity of the small-amplitude equations as there is no interaction between the small-scale gravity waves and the large-scale Fourier components which are quasi-geostrophic and which dominate the far-field motion.

This result is not of great use because in reality there can be a rather strong coupling between the gravity waves and the larger quasi-geostrophic scales of motion. Of the most obvious form for this interaction

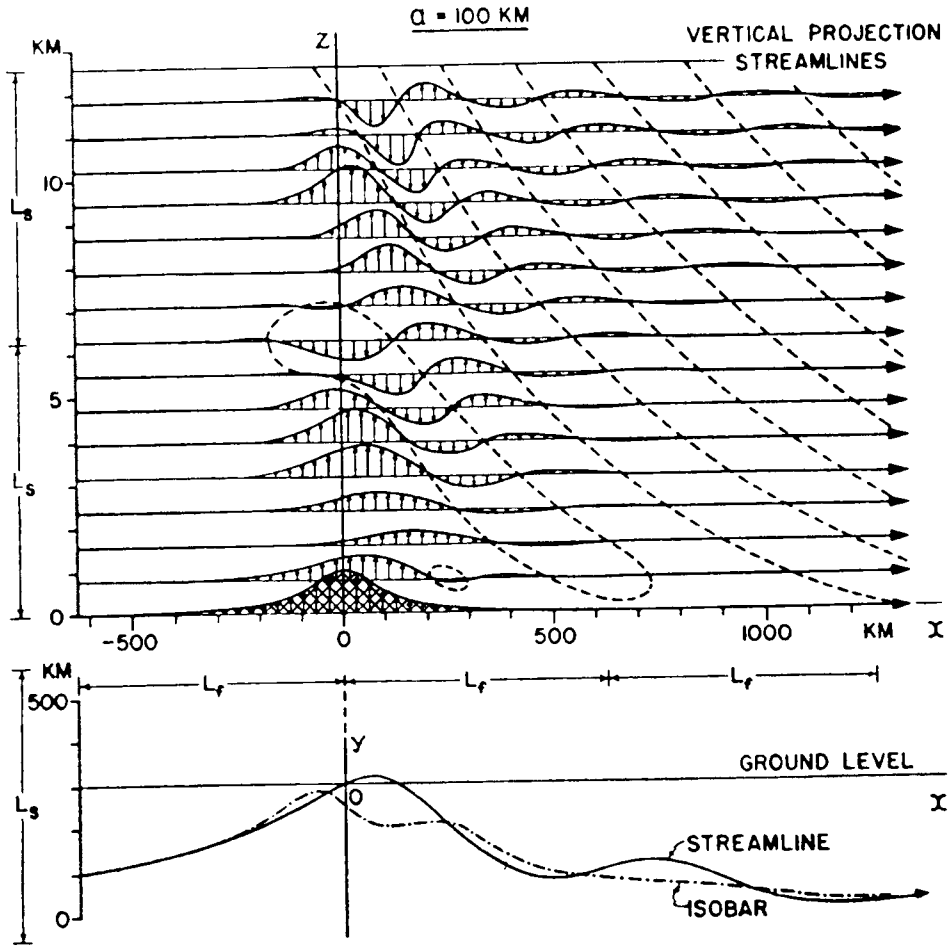

FIG. 20. The stratified rotating hydrostatic flow over a ridge with the parameter $af/U = 1$. In this case the flow is strongly influenced by the Coriolis force but no dominated to the extent that the flow is quasi-geostrophic. This flow is an intermediate type between Fig. 3 and Fig. 19c. The influence of the Coriolis force is evident in the lateral deflection of the streamlines (bottom of figure) and in the dispersive nature of the longer waves trailing behind the mountain. (From Queney, 1948.)

is the breaking of waves and the deposition of their momentum into the flow (see, for example, Bretherton, 1969). To estimate the magnitude of this effect we must be able to predict the magnitude of the drag on the mountain, know where the waves will break, and understand how the mean flow will respond to the loss of momentum. If the wave drag is due to shorter wavelength components which are not affected by the Earth's rotation, then the ideas discussed in the preceding section can be used to estimate the wave drag and the location of breaking. The response of the mean flow to the momentum loss is appropriate for discussion here, but will be postponed until we investigate the possibility that the gravity

waves may be long enough to be influenced by the Coriolis force (i.e., inertial-gravity waves) as, for example, in Queney's intermediate-scale solution.

Queney himself does not appear to have computed the mountain drag associated with his flow field solution. Blumen (1965), using linear theory, attempted to compute the flux of momentum in the disturbance over an isolated bell-shaped mountain [Eq. (3.19)]. Blumen evaluated the expressions

$$\rho \int\int_{-\infty}^{\infty} u'w'\,dx\,dy \qquad \text{and} \qquad \rho \int\int v'w'\,dx\,dy$$

but, as discussed by Jones (1967) and Bretherton (1969), the correct form for the momentum flux is

$$F_x = \int\int_{-\infty}^{\infty} \rho u'w'\,dx\,dy + f\int\int_{-\infty}^{\infty} \rho\eta v'\,dx\,dy \tag{3.39a}$$

$$F_y = \int\int_{-\infty}^{\infty} \rho v'w'\,dx\,dy - f\int\int_{-\infty}^{\infty} \rho\eta u'\,dx\,dy \tag{3.39b}$$

The second term in (3.39) accounts for the excess Coriolis force acting between the undisturbed and the lifted stream surfaces and is necessary so that (3.39) can be unambiguously interpreted as the mountain drag. Using the equations of motion and integrating (3.39) by parts

$$F_x = \int\int_{-\infty}^{\infty} p' \frac{\partial \eta}{\partial x}\,dx\,dy$$

$$F_y = \int\int_{-\infty}^{\infty} p' \frac{\partial \eta}{\partial y}\,dx\,dy \tag{3.40}$$

Near the ground where $\eta(x,y) = h(x,y)$, (3.40) is the pressure force on the mountain, while at any other level (3.40) is the horizontal force acting on each material layer by the layer above. Blumen's formulation leads to the incorrect conclusion that the long, nearly geostrophic, nonpropagating wave components are responsible for a lateral drag force F_y acting on the mountain. In fact the pressure field for these components is symmetric with respect to η or h and from (3.40), the drag forces are zero. As an example, the flow described by (3.20), (3.21) has a nonzero

$\overline{v'w'}$ but F_y is zero as we know from the fact that the perturbation pressure field is distributed symmetrically around the mountain. The wave drag [Eq. (3.40)] on a mesoscale ridge with uniform incoming wind and stability has been computed by Smith (1979a) and is shown in Fig. 21. The effect of rotation is characterized by af/U and as this parameter increases (i.e., progressively wider ridges) the wave drag decreases.

There has been some further theoretical work to understand the influence of a background shear $\partial \bar{U}/\partial z$ on the vertical propagation of inertial-gravity waves. Jones (1967) has shown that the momentum flux as defined by (3.39) or (3.40) will be independent of height in the absence of dissipation.

Eliassen and Palm (1960) and Eliassen (1968) have investigated the relationship between the vertical fluxes of momentum and energy. With $U = U(z)$, the interesting possibility arises that the singularity $k = k_f = f/U(z)$ in (3.30) will occur only at a particular level (i.e., the critical level) for each wave component. Preliminary studies of the structure of this type of critical level has been carried out by Jones (1967) and Eliassen (1968).

Observationally there is no question that large mountain ranges can experience significant drag due to the development of high surface pressure on the windward side and low pressure on the lee side. This phe-

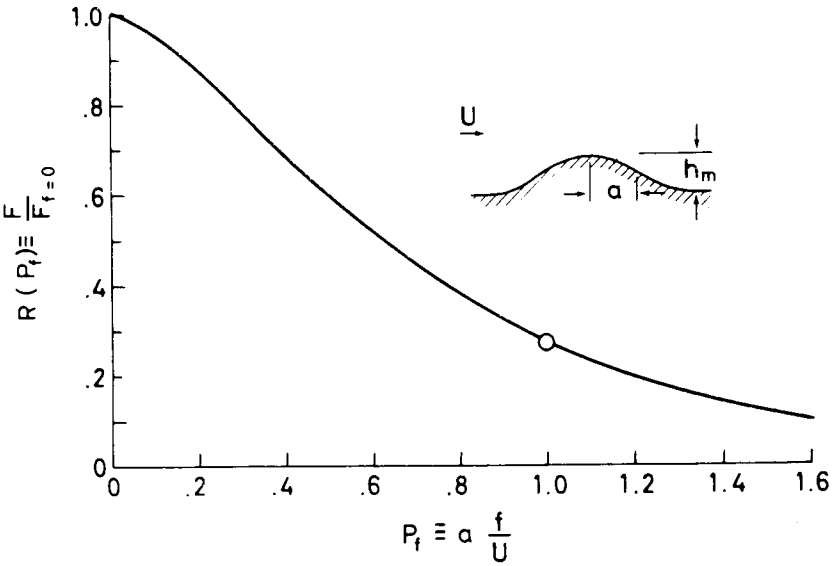

FIG. 21. The influence of the Coriolis force on mountain wave drag. As the parameter $P_f \equiv af/U$ increases, gravity waves are suppressed and the drag F drops below its $f = 0$ value. Note, however, that even for broad mountains with low Rossby numbers, there is still some wave drag. The point at $af/U = 1$ corresponds to the flow shown in Fig. 20. (From Smith, 1979a.)

nomenon is usually referred to as a "föhn nose" in reference to its association with the föhn wind and the characteristic "nose" shape to the surface isobaric patterns.

Qualitative descriptions of the föhn nose can be found in Defant (1951) and Brinkmann (1970). It is difficult to determine precisely the pattern of surface pressure due to the wide spacing of surface microbarographs and the problem of reducing the measured pressure to a standard level, but approximate pressure differences across the mountain of 4 to 6 mbar are not uncommon in the Rockies, Scandinavian Mountains, and the Alps. The drag force associated with this Δp is considerable and must act on the atmosphere somewhere. The response of the synoptic-scale flow to this loss of momentum represents a new facet to the dynamics which is not present in the linear theory of Queney.

Theoretically little is known about the response of the atmosphere to a localized drag. The work of Eliassen (1951), however, is a valuable conceptual guide. Eliassen used the ω-equation (see Holton, 1972) to compute the response of a geostrophically balanced wind to a localized retarding force. He found that a secondary circulation (see Fig. 22) would be produced in the transverse plane as the flow attempts to restore itself to geostrophic balance. Qualitatively this transverse circulation has a strong component down the pressure gradient in the retarded region and a more widely distributed return flow. In this way the external force is balanced locally by the excess downstream Coriolis force there. The

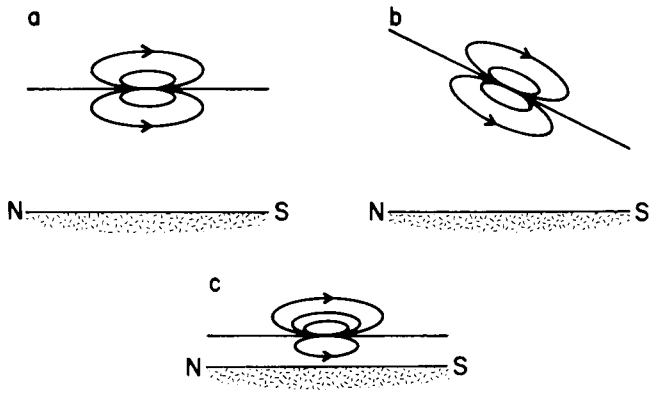

FIG. 22. The cross-stream circulation caused by a local retarding force acting on a stratified geostrophically balanced stream. Such a force could be applied to a stream by the breaking of mountain waves. Locally the retarded fluid is pushed to the left by the pressure gradient force. The surrounding fluid is decelerated by the upstream Coriolis force acting on the return branches of the circulation: (a) barotropic mean flow; (b) mean flow with vertical shear and sloping isentropes; (c) force applied near the ground. (After Eliassen 1951.)

weak return circulation has an excess Coriolis force acting upstream, and this serves to spread the localized imposed force over a much broader region of the flow.

The secondary circulation is altered slightly by the presence of a nearby boundary or preexisting baroclinicity in the airstream. It is difficult to apply these ideas to the mountain flow problem for several reasons. For one thing it is difficult to predict where the mountain wave momentum will be deposited. Another problem is that Eliassen's theory is restricted to two dimensions; that is, the external force acts everywhere along a line parallel to the mean flow.

Observationally, Woolridge (1972), has noted that the equations of synoptic-scale motion involving acceleration, Coriolis force, and pressure gradient force do not balance in the upper troposphere and lower stratosphere over the mountainous terrain of Arizona and New Mexico. The extra force needed to balance the momentum equation is usually a retarding force and is interpreted by Woolridge to be the deposition of mountain wave drag. He defends his interpretation by noting the simultaneous appearance of wave clouds in the satellite photographs of the region.

3.3. Theories of Lee Cyclogenesis

Mountains have been observed to influence the weather in many ways. The literature describing these observations has developed and remains quite separated from the theoretical ideas discussed earlier. The difficulty in connecting the observations and the theories is partly due to the complexity of the problem and partly to the limited training and experience of the investigators. The following discussion will also, unfortunately, fall short in this respect. There is a great need for detailed case studies of the weather in mountainous areas using closely spaced and frequent radiosonde releases, and with interpretation in terms of the fundamental concepts of fluid dynamics.

The phenomenon of lee cyclogenesis has received far more attention than any other aspect of the synoptic-scale mountain flow problem, and for good reason. It is now known that a successful one-day or possibly a two-day weather forecast can be achieved by simply predicting the motion (using perhaps extrapolation or a barotropic numerical model) of the existing cyclonic storms. To go further it is necessary to predict the development of new cyclones, and from the statistical studies of Klein (1957), or Reitan (1974), and Radinovic (1965b), and others, it has become clear that the lee sides of the major mountain ranges are strongly pre-

ferred sites of cyclogenesis. We note immediately that the usual explanation of cyclogenesis in terms of baroclinic instability (see Holton, 1972) makes no mention of orography. On the other hand, the simple prototype problems of the flow around mountains discussed earlier show no evidence of a developing lee-side cyclone. To explain the observed distribution of cyclogenesis will require new and more complicated ideas.

The structure of cyclones developing in the lee of the Rocky Mountains has been analyzed by Newton (1956), Petterson (1956), Hess and Wagner (1948), Carlson (1961), Hage (1961), and Chung *et al.* (1976). Manabe and Terpstra (1974) and Egger (1974) have shown that numerical models can also be used to simulate lee cyclogenesis behind the Rockies and other large mountain ranges. The results of Chung *et al.* are the most comprehensive but do not differ greatly from the earlier studies. They find that it is important to distinguish between the weak depressions which form and then remain just to the lee (25% of cyclogenetic cases) and the stronger cyclones which form in the lee and then move away (75% of the cases). This is similar to the discussion of Speranza (1975) in which he emphasizes the difference between lee-side baric depressions and the actual production of cyclonic vorticity. The local baric depression could be associated with mesoscale mountain wave drag, whereas true cyclonic vorticity, because of its conservation property, could move away downstream as a migratory cyclone. The development of the true migratory cyclone can be described (following Chung *et al.*) as follows. An intense "parent" cyclone approaches the Rocky Mountain cordillera from the northwest. As it draws near, it turns slightly to the left and fills (i.e., weakens). Many hours later a cyclone is seen to form rapidly just downstream of the mountain range and initially move away to the southeast. At the same time the upper level trough which was associated with the parent cyclone has passed over the mountain and the eastern limb of the trough lies over the mountain lee side, the new lee cyclone is seen to develop (Fig. 23).

There are two "classical" explanations for this behavior. The first would be called *upper level* or *jet stream* control of cyclogenesis. According to classical theory, surface cyclogenesis (not just lee cyclogenesis) is associated with divergent flow in the upper troposphere. The upper level divergence is necessary both to cause the pressure to drop at the surface and to allow rising motion in middle levels which in turn produces cyclonic vorticity near the surface by low-level convergence. The region of upper level divergence is usually associated with positive vorticity advection, for example, a jet stream blowing out of a trough. According to the vorticity equation this positive vorticity advection aloft must be balanced by local divergence if the trough is only slowly moving.

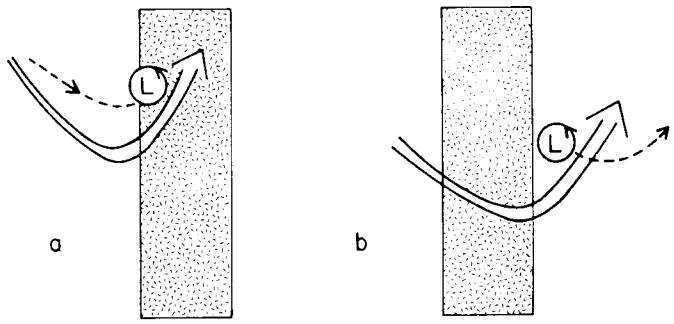

FIG. 23. An observational model of lee cyclogenesis, triggered by an approaching "parent" cyclone. The parent cyclone approaches from the west and weakens as it encounters the high ground. Shortly thereafter a new cyclone forms and moves off toward the east. A number of theories have been proposed to explain these occurrences including simple conservation of potential vorticity and upper level "jet stream" control.

The argument of Newton (1956), Speranza (1975), and Chung *et al.* (1976) is just to say that lee cyclogenesis will occur where and when the low-level vortex stretching caused by divergence aloft is added to that caused by downward flow at the surface on the mountain lee side. This is precisely where the eastern limb of the upper level trough intersects the mountain lee side.

One weakness of this type of argument is that it is difficult to tell whether the upper level divergence *caused* the surface cyclogenesis or whether there relationship is just a diagnostic association.

A simpler explanation of the phenomena involves the conservation of potential vorticity. The potential vorticity of the parent cyclone is conserved as it crosses the ridge, but the relative vorticity is temporarily eliminated by vortex shortening while these air parcels are over the mountain. Upon leaving the mountain the parcels are stretched to their original length and the cyclone reappears. If the upstream flow is partially blocked, the lee cyclone can even be stronger than the parent.

This theory also explains the curvature of parent cyclone path to the left as it approaches the mountain and the initial motion of the new lee cyclone to the right. The vorticity is moving with the fluid and therefore is advected by the mountain anticyclone described earlier. Of course the acid test of this theory is to determine if the lee cyclone is composed of the same fluid particles as the parent cyclone. Unfortunately this trajectory analysis has not been done.

There has also been considerable interest in the influence of the Alps on the formation of cyclones in the Gulf of Genoa (Radinović, 1965a,b; Speranza, 1975; Egger, 1972; Buzzi and Tibaldi, 1977; Trevisan, 1976). There seems to be a consensus that the nature of Alpine lee cyclogenesis

is different than the Rocky Mountain variety previously discussed. Whether this is due to the smaller horizontal dimension of the Alps, different orientation, more complicated geometry, nearby warm sea, or their different synoptic setting is not clear. The work of Radinović (1965a) and Egger (1972) indicates that lee cyclogenesis is associated with southward flow of cold air from central Europe and that the mechanism involves the blocking of cold low-level air by the mountains. The details as described by Radinović are rather complicated.

None of these arguments are so compelling that the matter can be considered settled. The theoreticians have been going off in different directions proposing a wide variety of mechanisms for lee cyclogenesis. Some of these suggestions will be mentioned in the following:

(a) Buzzi and Tibaldi (1977) note that the introduction of Ekman layer friction can alter the symmetric quasi-geostrophic flow discussed earlier to an asymmetric flow with a significant (but fixed) lee-side cyclone. The reason for this is apparently quite simple. The anticyclonic vorticity above the mountain tends to decay due to friction, but this represents an increase in potential vorticity. When the fluid columns leave the mountain, their increased potential vorticity is realized in the appearance of cyclonic relative vorticity. An extreme example of this is when the fluid particles have spent so long over the mountain that their relative vorticity has completely decayed. When dismounting the orography these particles will develop a full measure of cyclonic vorticity. In this sense, elevated regions with friction acting are generally *sources* of potential vorticity. This same mechanism operates in the laboratory study of slightly viscous flow of a rotating homogeneous fluid over an obstacle.

This mechanism also seems to be acting in numerical weather prediction models. Whenever the mountain anticyclone is weaker than that required by constant potential vorticity, cyclogenesis will occur in the area where the air leaves the mountain. The weak anticyclone could be caused by friction in the model or by an incorrect analysis of the input data.

(b) Another possibility is that the formation of a lee cyclone is a transient phenomena associated with rapid changes in the strength of the incoming flow. If initially there is little or no wind, the isentropic surfaces will not be parallel to the mountain surface but will be nearly horizontal. In this case there is no mountain anticyclone. A sudden increase in wind speed could cause the air near the mountain to be blown away downstream and replaced by upstream air. If the motion is adiabatic, the θ-surfaces which intersect the ground must continue to do so; whereas in the vicinity of the mountain, the θ-surfaces lie parallel to the surface

(Fig. 24). The intersection of the θ-surfaces with the ground comprises a warm-core cyclone caused by vortex stretching which moves off downwind. Such a "starting vortex" is commonly observed to be left behind in Taylor column experiments in homogeneous fluids when the obstacle is impulsively started from rest.

This transient mechanism is particularly appealing as it agrees with the observation of Radinović (1965a) that cyclones form to the south of the Alps soon after the onset of strong flow from the north. A difficulty with the theory is that it is hard to know when the θ-surfaces will intersect the mountain and when they will go over. A test of this theory would be to see if the lee cyclone is composed of air parcels that were originally over the mountain.

(c) Merkine (1975), on the basis of a theoretical analysis of baroclinic flow over a ridge, has suggested that the effect of the ridge is to increase the baroclinicity of the atmosphere. This could lead to enhanced cyclogenesis through the classical mechanism of slantwise convection.

(d) If the growth of a cyclone is viewed as a self-sustaining process which need only be triggered by low-level convergence then the lee side

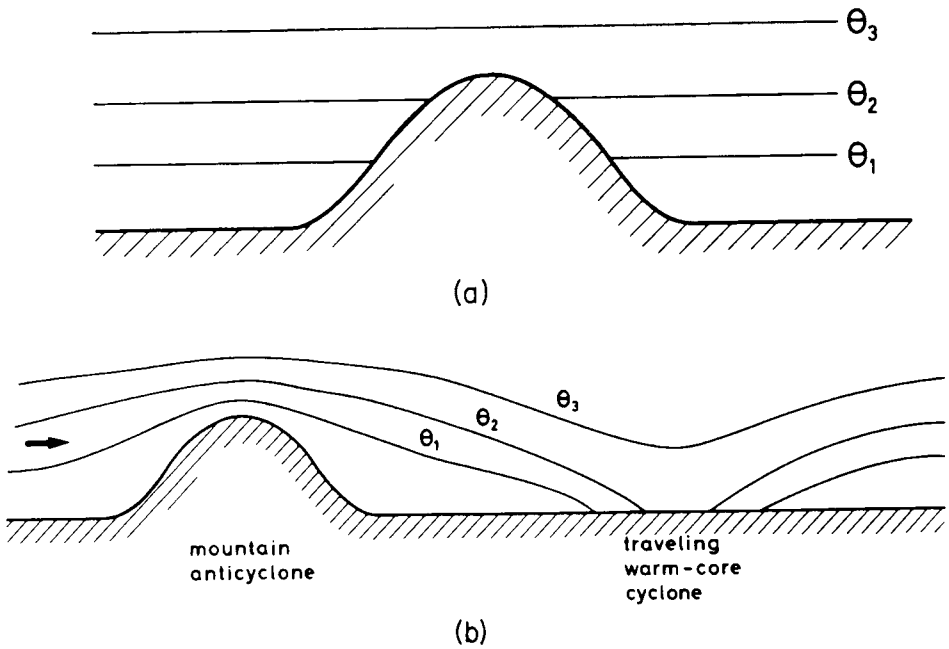

FIG. 24. The generation of a surface-intensified cyclone associated with the onset of a strong wind. (a) Initially there is no flow and the isentropic surfaces lie flat, intersecting the mountain. (b) With the onset of a strong wind, the air over the mountain is blown away and at the same time vertically stretched to form a traveling warm-core cyclone. The isentropes that initially intersected the ground continue to do so. Near the mountain, the uplifted θ-surfaces indicate the presence of a mountain anticyclone.

of a mountain would be a natural location for growth initiation. In a barotropic inviscid atmosphere, however, the lee-side convergence acts only to restore the vortex lines to their original length, not to create new cyclonic vorticity. This triggering mechanism seems to be implicit in several observational descriptions of lee cyclogenesis but apparently has not been investigated theoretically.

(e) It is known theoretically from the work of Queney (1948) and Johnson (1977) among others that if the Coriolis force is taken to be a function of latitude, the generation of Rossby waves will introduce an asymmetry in the flow. In fact the first trough of the wave system will occur just downstream of the mountain. There is a certain resemblance between this flow and a lee cyclone except that this Rossby wave is a standing wave and the trough will not move away downstream.

The effect of a nonconstant f (i.e., the β-effect) is not expected to be important unless the mountain dimension L approaches the Earth radius. The restoring force for Rossby waves is not just β, however, but the gradient in the background potential vorticity. Locally the horizontal gradients in wind speed and temperature (or thickness) can cause a restoring force much larger than that due to the variation of f. It follows that the influence of Rossby waves could be important for much smaller mountains. This may have had an influence on the numerical simulation of lee cyclogenesis by Trevisan (1976).

(f) One simple way to explain lee cyclogenesis is to hypothesize that the mountain blocks the low-level flow. The flow aloft must then descend in a föhn-type wind producing warming and vortex stretching in the lee (Defant, 1951). This is related to, but is not the same as, the effect of blocking as described by Radinović (1965a) and Speranza (1975).

(g) Another possibility is that the mountain drag may act in some way to create the lee cyclone. For example, near one flank of the mountain the variable drag could produce a torque on the atmosphere which in turn will produce vorticity.

This list of mechanisms is not meant to be inclusive but is merely intended to illustrate the kinds of possibilities that may have to be considered. These proposals are certainly less precise than the mathematical problems considered earlier in the section. The use of numerical models appears to be one promising method for closing the gap between the simple, but precise, analytical ideas and the reality of atmospheric flow. Several authors (Egger, 1972, 1974; Manabe and Terpstra, 1974; Trevisan, 1976) have reported success in numerically simulating lee cyclogenesis. This represents a great step forward, but as of yet it is not known exactly how these solutions can be used to understand the flow physi-

cally. All of these models incorrectly model the dynamics of inertial gravity waves and so cannot be compared with the analytical solutions of Queney. Eliassen and Rekustad (1971) have taken more care to treat these waves by using greater resolution in the vertical and a radiation condition aloft. Their model, however, is restricted to two dimensions, has dangerously close inflow and outflow boundaries, and has been evaluated only for very special upstream conditions. Clearly more work is needed in this area.

4. Orographic Control of Precipitation

One of the most striking ways in which topography influences the weather is in its strong local control of the rainfall distribution. The most obvious examples are the rainfall maxima on the upwind side and the corresponding dry, rain-shadow regions in the lee of major mountain barriers at latitudes with consistent prevailing winds. The clearest case of this is the wet–dry contrast across the Andes in South America which reverse its orientation when passing south from the tropical easterlies to the midlatitude westerlies.

On a much smaller scale, but equally striking, is the now well-confirmed observation that rainfall can often be a factor of 2 greater at the tops of small (50 to 100 m) hills than in the surrounding valleys. This has an especially large impact on the plant life of the region and also on the scientist trying to construct regionally averaged rainfall data. Of course we expect these two examples of orographic control of rain to be physically somewhat different, as between these two extreme scales there lie several natural "cloud physics" length scales—especially the distance of the downwind drift during (a) the lifetime of a cumulus cloud, (b) the formation of raindrops from cloud droplets, and (c) the fall of hydrometeors to the ground, as well as the natural scales N/U and f/U which affect the dynamics of airflow over the hills. One of the challenges of this section will be to investigate the effect of mountain size on the nature of orographic rain. Some aspects of this problem have been reviewed by Bergeron (1949).

4.1. Observations of Rainfall Distribution

4.1.1. Distribution of Annual Rainfall with Respect to Elevation. A tremendous amount of information has been collected concerning the distribution of precipitation in mountainous areas. These data are for the

most part concentrated in the hydrological, geographical, agricultural, and water resources literature—mostly in unpublished reports of government agencies. As a first attempt to organize these data it has become standard practice to correlate statistically the annual average precipitation (mm/yr) against station elevation (meters above sea level). In most cases it has been found that *precipitation tends to increase with height.* This is also consistent with Longley's (1975) observation that precipitation decreases with depth down in isolated valleys. To easily represent this trend, the linear regression slope is

$$\frac{dP(\text{mm/year})}{dz} \equiv a \tag{4.1}$$

computed where the coefficient a describes the rate of increase of annual precipitation with height. An alternative description (Ryden, 1972) is the relative increase of precipitation with height

$$R \equiv \frac{d \log P}{dz} = \frac{1}{P}\frac{dP}{dz} \tag{4.2}$$

Some typical examples of values for a and R are shown in Table II where the height increment is taken to be 100 m, and R is expressed in percent.

The linear regression equations (4.1) or (4.2) are somewhat misleading as in almost every case there is considerable scatter about the linear regression representation. This is to be expected as the precipitation should depend on many other factors, for example, the yearly pattern of weather type, ground temperature, the size and shape of the surrounding

TABLE II. TYPICAL EXAMPLES OF VALUES FOR a AND R

	$a\left(\frac{\text{mm}}{\text{yr}}\Big/ 100\text{ m}\right)$	R(%/100 m)
United Kingdom		
Bleasdale and Chan (1972)	250	25%
Pennines (UK)		
Chuan and Lockwood (1974)		
East Pennines	200	40
West Pennines	190	25
Western Canada, Mormot Creek		
Storr and Ferguson (1972)	60	10
Northern Sweden		
Ryden (1972)		
Kamajokk (1967)	18	7
Kamajokk (1968)	7	6
Malmagen	22	9

mountains, and the vertical profile of temperature, humidity, wind, speed and direction, and possibly the aerosol distribution. Furthermore, there are exceptions to the trend shown in Table II. On very high mountains the rainfall may increase up to a certain height and then decrease. From the wide variation of a between different regions (a factor of 40) it is clear that a is not in any sense a fundamental constant. The variation in R is somewhat less, indicating that regions with greater annual rainfall have greater variation of rainfall with height, but R is still clearly not a fundamental quantity. For the scientist trying to understand the nature of orographic rain, the data in Table II are of little use. It cannot be interpreted to mean that in a single rainfall event the precipitation increases with height, which might, for example, be explained by the evaporation of raindrops before hitting the ground. This method also fails to describe the upslope rain–rain shadow contrast which we know is important for broad mountains. If the region being considered has a consistent prevailing wind, this latter effect is well represented by the areal distributions of annual precipitation.

4.1.2. Rainfall distribution with Respect to Wind Direction and Weather Type. In order to gain more information about the orographic control of precipitation, while retaining the statistical approach, it is necessary to classify the data according to *weather type, wind direction,* or both. Some examples of this kind of analysis will be given here.

Wilson and Atwater (1972) studied the distribution of rainfall in the state of Connecticut, a region of low (<300 m) hills. They restricted their study to rainstorms of the large-scale stratiform type and classified the cases according to wind direction. They conclude that the major part for the spatial variation of rainfall can be explained by the influence of topography. Generally there was greater precipitation in the hills, but with the maximum shifted toward the upwind slopes.

Bergeron (1968, 1973) studied the rainfall distribution in the region of low hills (<60 m) near Uppsala, Sweden. For the most part Bergeron used monthly averaged data with each month classified according to weather convective showers or continuous stratus rain was predominant. With convective showers (typically summertime) the rainfall distribution is characterized by swaths of rainfall corresponding to convective clouds passing over the area. Topography appears to have little effect. In the fall months, with primarily stratus rain, Bergeron found a remarkably strong dependence of rainfall in height. For example, between Lake Ekoln and Lunsen Hill, 60 m higher and only 5 km away, the rainfall nearly doubled. Bergeron (1968) presents a conceptual model for this effect which will be described later.

On a larger scale, Nordø and Hjortnæs (1966) and Andersen (1972) considered the precipitation distribution over the broad mountains (width ~ 250 km, height ~ 1500 m) of southern and central Norway. Nordø and Hjortnæs statistically relate the rainfall distribution to the component of geostrophic wind directed against the mountain during the same period. Andersen, on the other hand, uses monthly mean precipitation, with each month being classified as to prevailing wind direction and weather type. In spite of the differing technique the results of both studies are broadly similar. The rainfall is strongly controlled by topography with the maximum occurring near or slightly upwind of the steepest surface slope. At the divide the rainfall is a small fraction of the upslope maximum and the lee side is remarkably dry. There are some important exceptions to this simple picture, for example, the strong precipitation maximum that sometimes occurs in the wintertime on the southeast coast of Norway. Bergeron (1949) noticed this same anomaly in a case study and has put forward a possible kinematic explanation (see also Smebye, 1978).

Andersen (1972) and Utaaker (1963) appear to find that the smaller scale mountains in Norway exhibit a quite different rainfall pattern with the maxima occurring at mountain top or in the lee.

The use of rain gauge data, even from special networks, has so far proved unable to provide a clear picture of the structure of orographically induced cumulonimbus rain. This is not surprising as these cloud elements appear rapidly and apparently randomly over mountains terrain on warm summer days and seem to move away downstream. Biswas and Jayaweera (1976), using satellite observations, concluded that there can be strong topographical control of air mass thunderstorms in the Alaskan region. Kuo and Orville (1973) studied the climatology of convective clouds in the Black Hills using radar. They also found strong topographic control with the maximum cloud development appearing downwind of the mountain peaks. Skaar (1976) indicates that in the summer over Norway the prevalence of convective rain results in a much broader distribution of rainfall although in detail, much more complex.

This sampling of observational results seems to suggest the importance of two factors:

1. The weather type (or season) which can determine the relative importance of stable versus convective rain.
2. The size of the mountain which determines whether the orographic rain will occur on the upwind slope with a rain shadow in the lee (i.e., larger mountains $L > 100$ km), or with the maxima more nearly centered on the mountain (i.e., smaller mountains $L < 20$ km).

There appear to be three rather independent mechanisms of orographic

rain. These are (see Fig. 25):

1. Large-scale upslope precipitation. Orographically forced vertical motion or convection triggered by smooth orographic ascent brings the air to saturation and after some delay, raindrops form and fall to the ground.

2. Enhancement of rainfall over small hills (after Bergeron, 1968). Rainfall from preexisting clouds (either frontal or orographic) is partially evaporated before hitting low ground, but over hills amplification occurs by washout of cloud droplets from low-level pannus clouds.

3. Orographic control of the formation of cumulonimbus clouds in a conditionally unstable airmass. Heating of the mountain slopes by insolation causes upslope winds leading to thermals above the mountain peak which trigger the formation of convective clouds.

In the following sections 4.2, 4.3, and 4.4, we will examine each of the above mechanisms.

4.2. The Mechanism of Upslope Rain

4.2.1. A Prototype Model of Upslope Rain. We will derive a simple model of upslope rain which will serve as a focal point for further discussion. Consider a reference volume $V = 1\ \text{m}^3$ at some height z above the surface in a saturated region of the atmosphere. The rate of condensation (kg/sec) in the volume will be the rate at which the saturation water vapor density $\rho_{w_s} = r_s \rho_{air}$ decreases following the parcels flowing through the volume,

$$\frac{D\rho_{w_s}}{Dt}$$

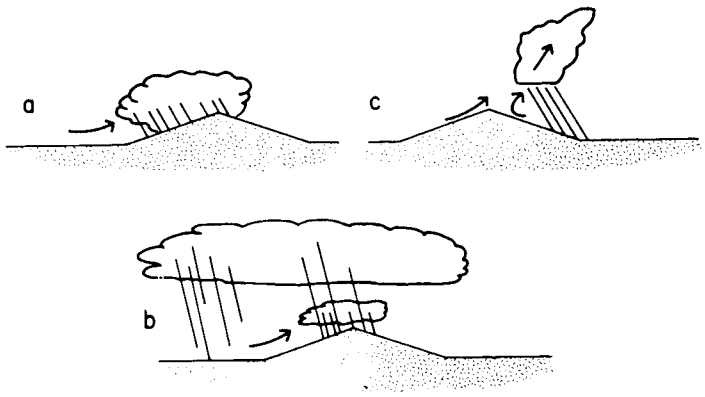

FIG. 25. Three mechanisms of orographic control of precipitation: (a) broad-scale upslope rain, (b) small-scale redistribution of rain by hills, and (c) orographic-convective showers.

If the decrease in ρ_{w_s} is caused by adiabatic lifting, then

$$\frac{D\rho_{w_s}}{Dt} = \left.\frac{d\rho_{w_s}}{dz}\right|_{ad} w \tag{4.3}$$

If precipitation-size particles (raindrops or snowflakes) can form immediately from the cloud droplets, and if these hydrometeors fall directly to the ground with no downwind drift, then the rate of precipitation at the ground (kg/m^2 sec) is just the vertical integral of (4.3).

$$R\left(\frac{\text{kg}}{\text{m}^2/\text{sec}}\right) = \int_0^\infty \text{w} \left.\frac{d\rho_{w_s}}{dz}\right|_{ad} dz \tag{4.4}$$

Equation (4.4) is still rather general in that w in (4.2) could be associated with (a) large-scale frontal uplift, $w \sim$ 10–50 cm/sec; (b) orographic uplift, $w \sim$ 10–50 cm/sec; or (c) convective updraft, $w \sim$ 1–5 m/sec. In all of these cases the precipitation rate will be closely associated with the strength of the updraft. The intensity of orographic uplift can be estimated by assuming the the flow at all levels is parallel to the sloping mountain surface. Then

$$w(z) = U(z)\alpha \tag{4.5}$$

where α is the surface slope and $U(z)$ is the horizontal wind. With this simplification (4.2) becomes

$$R\left(\frac{\text{kg}}{\text{m}^2/\text{sec}}\right) = \alpha\int_0^\infty U(z) \left.\frac{d\rho_{w_s}}{dz}\right|_{ad} dz \tag{4.6}$$

To obtain a representative estimate for the intensity of orographic precipitation we can consider the special case (1) $U(z) = U =$ const and (2) the environmental temperature $T(z)$ lies along a moist adiabat, so that

$$\left.\frac{d\rho_{w_s}}{dz}\right|_{ad} = \frac{d\rho_{w_s}}{dz} \tag{4.7}$$

This is nearly true in many cases of orographic rain (see, for example, Douglas and Glasspole, 1947). With these, (4.6) becomes

$$R\left(\frac{\text{kg}}{\text{m}^2/\text{sec}}\right) = \alpha U \int_0^\infty \frac{d\rho_{w_s}}{dz} dz = \alpha U[\rho_{w_s}]_0^\infty$$

and as $\rho_{w_s} \to 0$ aloft

$$R\left(\frac{\text{kg}}{\text{m}^2/\text{sec}}\right) = \alpha U \rho_{w_s}(0) \quad \text{or} \quad \alpha U r_s(0)\rho_{\text{air}}(0) \tag{4.8}$$

In this special case the general dependence of (4.6) on the temperature and humidity structure reduces to a simple dependence on $r_s(o)$, the mixing ratio at the ground. As an example, choose $\alpha = 1/100$, $U = 10$ m/sec, $r_s(P = 1000$ mbar, $T = 15°C) = 11$ gm/kg $= 0.011$ kg/kg, $\rho_{\text{air}} = 1.2$ kg/m^3. Then R(kg/m sec) $= R$(mm/sec) $\cong 1.3 \times 10^{-3}$, or $R = 4.7$ mm/hr. This value is not atypical of observed rates, but the analysis above is intended only to illustrate the kind of assumptions which are often used.

4.2.2. Efficiency of Release. A number of authors have made estimates of the efficiency of precipitation release during orographic lifting. These estimates require (1) rawinsonde profiles of the incoming wind, humidity, and temperature; (2) a way to estimate the amount of lifting that occurs at each level; (3) rain gauge measurements of precipitation over the upslope area. Sawyer (1956) compared six examples of measured precipitation on the windward slopes in Wales with the amount calculated from an equation like (4.6). He found that when conditions are favorable for heavy orographic rain, the efficiency (i.e., observed rainfall/computed condensed water) is nearly 100%. On the other hand, when only shallow layers of moist air is present, so that less total condensation occurs, the efficiency is reduced to 30–50%, and thus the rainfall is greatly reduced.

Browning *et al.* (1975) have computed the efficiency during four cases of pre-cold-frontal upslope rain in the same area, i.e., Wales. They as-

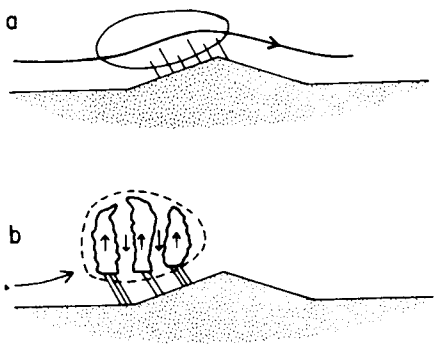

FIG. 26. Two possible mechanisms of upslope precipitation: (a) stable upglide and (b) orographic triggering of closely packed convective showers.

sumed that the lifting was independent of height [as in (4.6)], but included only the condensation occurring below $z = 3$ km, arguing that the liquid water formed above that level would be blown downstream out of the upslope control region. In two cases the efficiency was quite large, close to 70%. These cases were characterized by (a) a strong, moist low-level jet directed against the mountain slope; (b) incident airstream already near saturation; (c) some condensation occurring above the freezing line allowing ice-phase process to aid in the release of precipitation.

The two other cases examined by Browning *et al.* (1975) had much lower efficiencies—approximately 10% and 30%. These cases were characterized by initially unsaturated air requiring some finite ascent before condensation begins, and in one case, little or no condensation above the freezing line.

A number of papers have been written concerning the efficiency of orographic rain on the western side of the California mountain ranges (Myers, 1962; Elliot and Shaffer, 1962; Elliot and Hovind, 1964; Colton, 1976). Myers computed an efficiency of 70% for the large Sierra Nevada Range using a modified form of (4.6). Instead of taking α to be constant with height, he assumes that α drops off linearly from the ground to a presumed "nodal surface" at about $z = 5$ km. This somewhat reduces the computed condensation and increases the efficiency. Elliot and Hovind (1964) used a similar nodal surface assumption in the study of rainfall on the smaller San Gabriel and the still smaller Santa Ynez mountains. They classified each case according to the conditional stability of the incoming air (Table III). They conclude (looking also at Myer's data) that efficiency tends to increase with mountain size. The increased efficiency for unstable flows over the Santa Ynez could either be caused by an improved release mechanism or by an increase in condensation over that given by (4.6) due to the strong vertical motions in local convective elements.

TABLE III

Mountains	Number of cases	Efficiency
San Gabriel		
Stable	31	26%
Unstable	8	27
Total	39	26
Santa Ynez		
Stable	21	17%
Unstable	22	26
Total	43	22

Colton (1976) compared computed and observed rainfall rates on the Sierra Nevada (130 km wide) and the Smith River Basin (70 km) using the assumption of full release. The use of a flow model with w going to zero at about $z = 5$ km, gives remarkably good results, suggesting nearly complete release. As in the other studies, however, it is difficult to sort out the efficiency of raindrop formation (a cloud microphysical process) from errors in the assumed w-field.

We have seen that the precipitation efficiency depends both on the assumed field of lifting and on the microphysical processes leading to the formation of hydrometeors. In later sections we will discuss the former problem both with regard to the mean flow and to the possibility of small-scale convection triggered by the orographic lifting. Some insight into the cloud physics problem associated with orographic precipitation is provided by Young (1974a,b). Using a specified flow field and upstream sounding, Young computed the distribution of precipitation over the Front Range in Colorado. His model included a wide variety of microphysical processes and the downwind drift of hydrometeors. The parameterization of artificial seeding by silver iodide was also allowed for. The efficiency found by Young is

natural conditions	0.04%
with optimum seeding	20.00%

The natural efficiency found by Young (.04%) is so much smaller than the observations discussed previously, that some attempt must be made to explain it. Either Young's model is incorrect, or the mechanism of Front Range orographic rainfall is entirely different than that of California and Wales. The primary differences between these mountain flows are:

(a) Unlike the mountains of Wales and California, the Front Range is set well inland and even its base is 1500 m above sea level. In the case studied by Young, the bottom of the moist layer is at about 3400 m with $T = 0°C$. Thus the amount of available water is much less than in the case of a coastal range. We have already seen the suggestion (from Sawyer and Browning *et al.*) that a decreased moisture content can lead to a decreased efficiency.

(b) Another important difference is that the Front Range is only 40 km wide—significantly narrower than the mountains of California or Wales considered previously. One result of this is that the distribution of precipitation computed by Young is nearly symmetric with respect to the ridge crest instead of having a maximum on the windward slope. Possibly, by considering narrower mountains such as the Front Range we have stepped into a new regime where the time for hydrometeor formation and

fallout is the same or longer than the time for the air to pass over the mountain. The condensed water aloft is never realized as precipitation at the ground. The narrower mountains can cause precipitation only by the introduction of seeding, either natural or artificial. Young finds that the efficiency can be significantly increased by artificial seeding and this agrees with results of the Climax experiment (Mielke *et al.*, 1971), which found significant increases in wintertime precipitation by artificial seeding.

The other possible way to get small-scale orographic precipitation is that described by Bergeron (1960a, 1968), namely natural seeding from above by a larger scale cloud system. This possibility will be discussed in a later section.

Even if we accept the idea that large-scale orographic lifting a deep warm moist air current can cause some release, it is still surprising, in light of the difficulties in forming precipitation-size particles, to find release efficiencies of 70% to 100% such as reported by Sawyer (1956), Myers (1962), and Browning *et al.* (1975). Is it possible to convert such a high fraction of the condensed water into precipitation? If not, the simple method of computing the vertical motion field (4.3) must be considerably in error. Either the mean streamlines aloft are lifted by an amount greater than the mountain height or the orographic lifting triggers deep convection.

4.2.3. The Controversy concerning Stable versus Unstable Upslope Rain. In a lecture before the Royal Meteorological Society, L. C. W. Bonacina (1945) surveyed the regions of intense orographic rain around the world and the possible mechanisms. He concluded that orographic rain does not occur every time an airstream impinges on a mountain, but rather that the airstream must have been conditioned by the prevailing synoptic situation. In particular he emphasized the importance of convective instability for the generation of intense orographic rain.

Two years later Douglas and Glasspoole (1947) refuted Bonacina's contention by examining several cases of warm-sector orographic rainfall in the British Isles. They noted that the upstream surroundings showed slight conditional stability rather than instability. Further, they showed that simple orographic lifting could (assuming 100% release) account for the observed rainfall amounts. They concluded that, at least in their cases, the orographic uplift was a stable well-ordered process without convection. The interested reader should also notice the controversial discussion that follows Douglas and Glasspoole's paper. To a certain extent Douglas and Glasspoole's arguments seem to have carried the day

as many subsequent authors have flatly assumed stable lifting in their models. Recently, however, a much more detailed study of warm-sector orographic rain in this same geographical area has been reported by Browning *et al.* (1974). From frequent rawinsonde releases, a network of continuously recording rain gauges, and radar observations of the precipitation-bearing clouds they were able to construct a remarkably complete picture of precipitation mechanism. The distribution of precipitation rate (mm/hr) in space and time is shown in Fig. 27. It is clear that while there is continuous rain over the mountain, the rain is really due to a coalescence and intensification of the rain from moving convective cells (called MPA's—mesoscale precipitation areas, by the authors). This structure is also shown in Fig. 28. These MPA's form upstream in a middle-level layer of potentially unstable air—presumably triggered by far-reaching orographic lifting. They move downstream at a speed characteristic of the wind speed at midlevels. Note on Fig. 28 that the vertical extent of the MPA's is about 2000 m, and this is probably a fair estimate for the ascent distance of air parcels within these convective elements. This represents a great increase in lifting over the stable ascent hypothesis as the mountain in this case is only 300 meters high.

Browning *et al.* also found small-scale convection occurring in a 2-km thick, potentially unstable layer near the ground. Again the lifting in these clouds probably far exceeded the height of the mountain, leading to considerable condensation. If it were not for these low-level clouds, the precipitation reaching the ground would have been considerably reduced and distributed more widely downstream. These low-level clouds are responsible for the apparent coalescence and intensification of rainfall over the mountain. The low-level clouds probably have insufficient time to form precipitation by themselves before the lee slope descent begins. Thus they would produce no rain. In the presence of precipitation from above, however, their condensed water can be efficiently washed out, greatly increasing the rainfall at the ground. This redistribution of rain by low-level clouds will be discussed again later.

The contrast between stable and unstable rain has also been considered in the frequent orographic rain on the west coast of Norway. In two papers Spinnangr and Johansen (1954, 1955) attempted to use conventional synoptic and radiosonde data to describe, and to distinguish between, cases of stable and convective orographic rain. Their 1955 paper describes the approach of Maritime Polar (MP) air toward the mountains. They show that the rainfall begins when the sounding just upstream has become slightly unstable with respect to saturated lifting. They argue that the cold MP air has been destabilized by its passage over the warm Gulf Stream and the orographic lifting then triggers the shower activity.

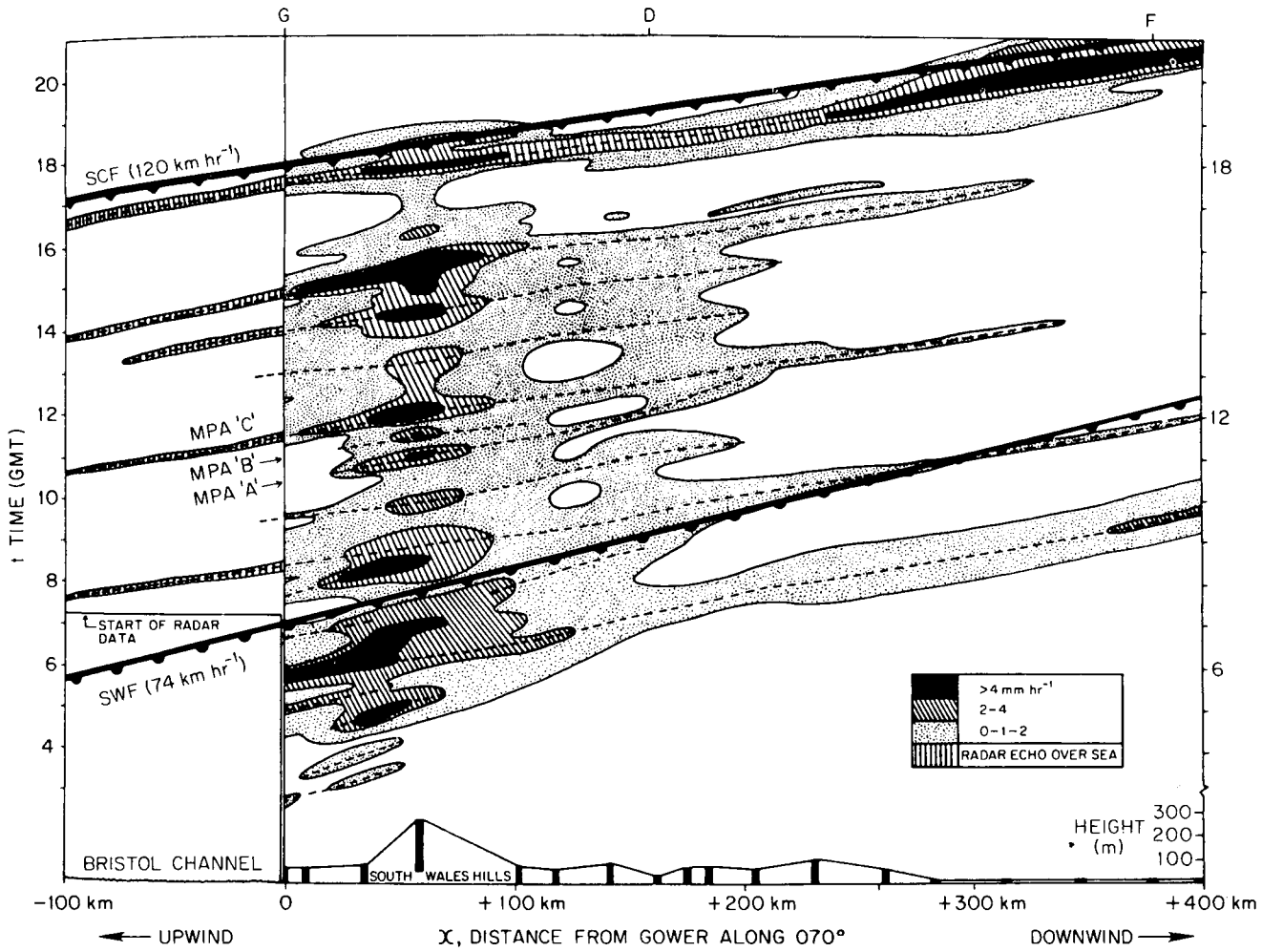

FIG. 27. A *xt* diagram showing the rainfall rates (mm hr^{-1}) and the movement of "mesoscale precipitation areas" (MPA) over the hills of South Wales. The rainfall begins ahead of the cold front and continues in the warm sector. The rainfall rate over the hills is continuous, but variable, and closely associated with the passage of convective clouds (MPA's) aloft. (After Browning *et al.*, 1974.)

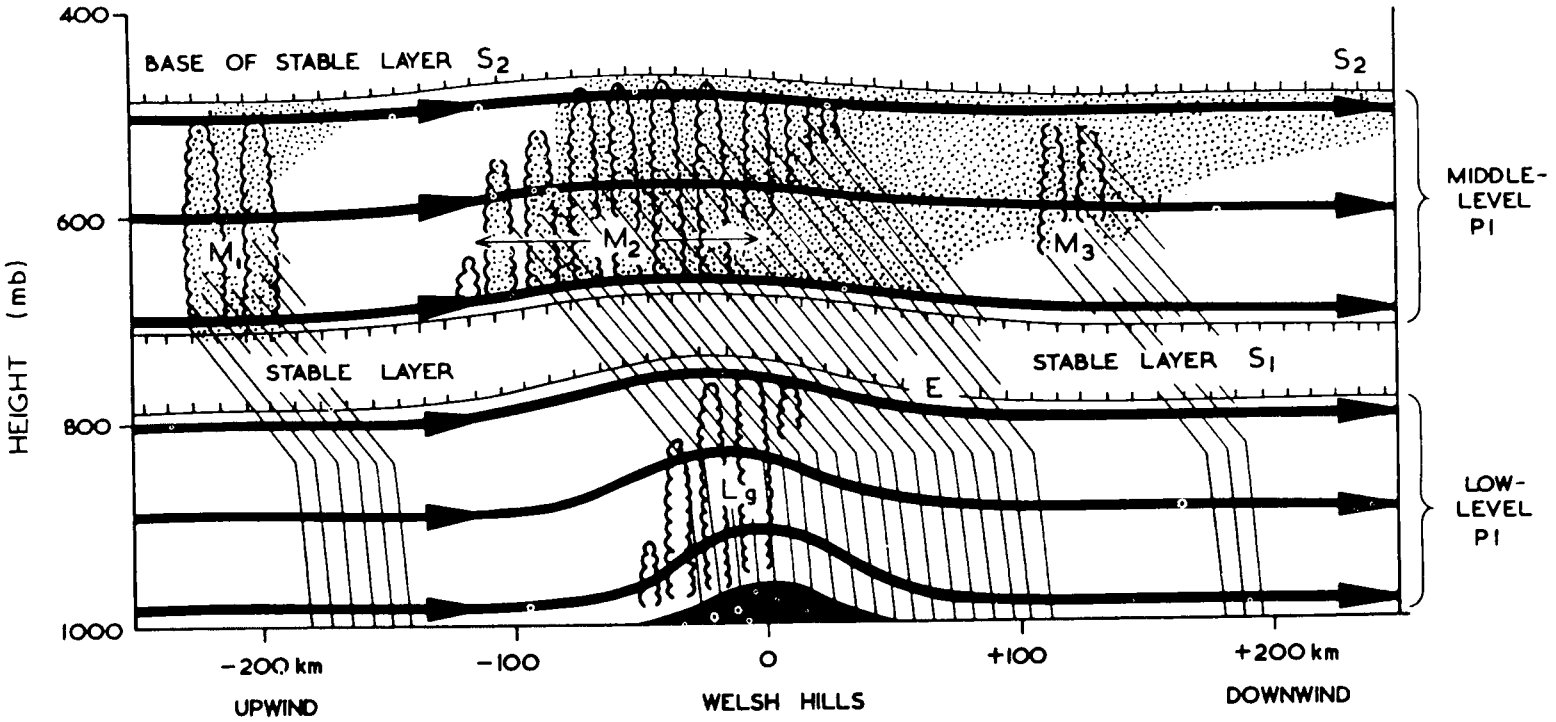

FIG. 28. A schematic cross section of the rain clouds in a warm sector over hills of South Wales. The moving, orographically triggered, convective clouds aloft produce precipitation which is locally enhanced by the low-level convective clouds over the hills (see Fig. 27). The slope of the hydrometer trajectories changes abruptly at the freezing line as snow changes to rain. (After Browning *et al.*, 1974.)

Occasional showers out at sea give additional evidence of the unstable state of the atmosphere. In spite of this, the heavy orographic rain inland was described as *continuous rain* by local observers—*not rain showers.* The showers had apparently "been packed together and had amalgamated into continuous rain." This is similar to the observations of Browning *et al.* (1975) discussed earlier. The intense rainfall concentrated just inland from the coast where the topographic slope is the greatest, with little rain reaching the divide 100 km inland. This rapid decrease of rain downstream is attributed by the authors to the short lifetime of convective clouds.

In the second paper Spinnangr and Johansen (1954) consider cases of southwest flow of warmer Maritime Tropical (MT) air toward the west coast of Norway. This air was contained in the warm sector of a developed cyclone just as in the case studies of Douglas and Glasspoole and Browning *et al.* discussed earlier. They argue that the northward flow of this tropical air should generate a stable air column. The soundings taken well upstream (in England) are noticeably, but not strongly stable against saturated lifting. The observed intense orographic rainfall was distributed spatially in a similar way to their 1955 study of instability showers. The observations of rain type was also similar with a predominance of *continuous rain* (although of temporally variable intensity) and reports of *rain showers* near the beginning and end of the rain period. Spinnangr and Johansen also show, using arguments similar to those of Douglas and Glasspoole, that the observed intense rainfall can be explained by stable upglide if 100% release is assumed.

Upon re-reading these two studies by Spinnangr and Johansen (1954, 1955), one is struck by the great similarity between them and with the studies of Browning *et al.* (1975) and Douglas and Glasspoole (1947). Certainly the reports of rain type cannot be used to distinguish reliably between the two types of orographic rain as even the rain showers tend to coalesce as shown in Browning *et al.* and Spinnangr and Johansen (1955). The spatial distribution of precipitation may also be similar. Even the observation of slight conditional stability in the approaching air, as in Douglas and Glasspoole, and Spinnangr and Johansen (1954), does not rule out instability showers because (as will be shown later) the orographic lifting aloft upstream of the mountain acts strongly to destabilize the column. It seems possible then that even the events which were presumed to be cases of stable rain [i.e., Douglas and Glasspoole (1947) and Spinnangr and Johansen (1954)] may have been in fact instability showers such as described in the more detailed observations of Browning *et al.* (1975). This interpretation also offers an explanation of the rainfall intensity found in these cases without requiring the assumption that all of the condensate reaches the ground as rain.

Two recent technological developments are providing new insights into the orographic rain problem. The first is the use of cloud seeding to enhance orographic precipitation (Chappell *et al.*, 1971; Mielke *et al.*, 1971; Grant and Elliot, 1974). The success of this seeding is itself an indication the *natural* efficiency of precipitation release must be significantly less than 100%.

More direct evidence comes from visible and infrared imagery of orographic clouds from satellite (Reynolds *et al.*, 1978; Reynolds and Morris, 1978). As a frontal system approaches, the precipitating orographic cloud is often obscured by a high-level layer of cirrus. Later in the storm, the cirrus moves off downwind and the orographic cloud is revealed. The top of the orographic cloud appears very irregular indicating vigorous convection within the cloud layer (see Fig. 29).

4.2.4. The Interaction of Frontal and Upslope Rain. It often happens that *frontal rain* appears to be intensified and prolonged in mountainous areas. To a certain extent this could be explained as a sequential ap-

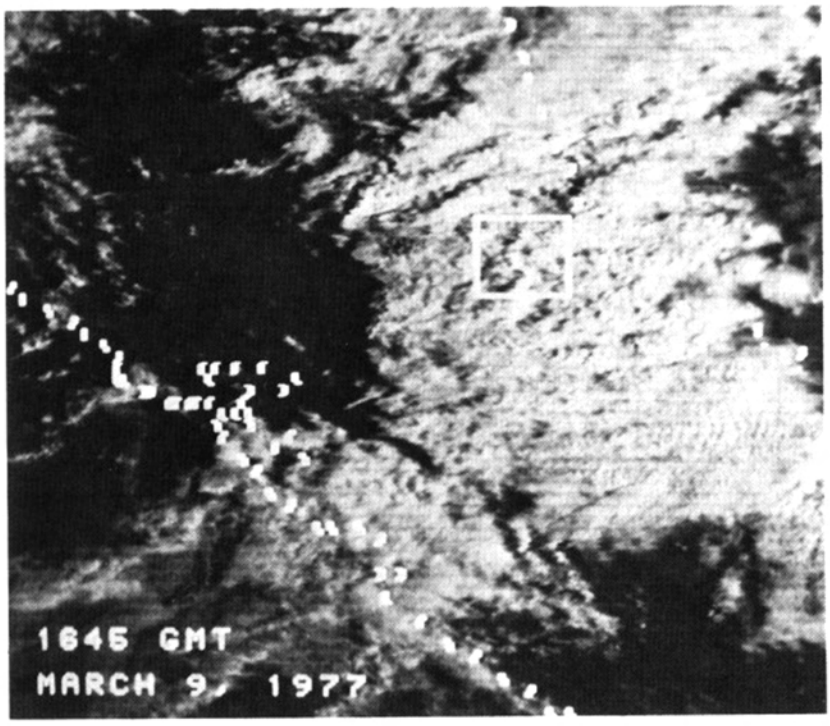

FIG. 29. Satellite photograph of a broad-scale orographic cloud over the Sierra Nevada range east of San Francisco, California. The rectangle has dimensions 68 km north–south and 42 km east–west. The irregular top of the cloud layer indicates the presence of vigorous small-scale convection. (From Reynolds and Morris, 1978.)

pearance of prefrontal "pure" orographic rain followed by the frontal passage. As an example, the warm-sector orographic rain discussed by Douglas and Glasspoole (1947) and Browning *et al.* (1974), ended with the passage of the cold front. They found, however, that the frontal rain itself was not much increased by the orography. Browning *et al.* (1975) also discussed the interaction between a cold front and the Welsh hills.

A somewhat different view is expressed by Petterssen (1940, pp. 298–302) and Bergeron (1949) who describe the orographic influence on frontal characteristics. The most detailed case study of mountain–front interaction is that of Hobbs *et al.* (1975). Using aircraft measurements, frequent soundings, and a network of automatic rain gauges, they were able to piece together a fairly complete picture of the passage of an occluded front over the Cascade Mountains in Washington state. They find a definite influence of the mountain on the front. The timing of the precipitation is strongly influenced by the front, but the location of the rainfall is almost entirely on the windward slopes. This is shown in Fig. 30.

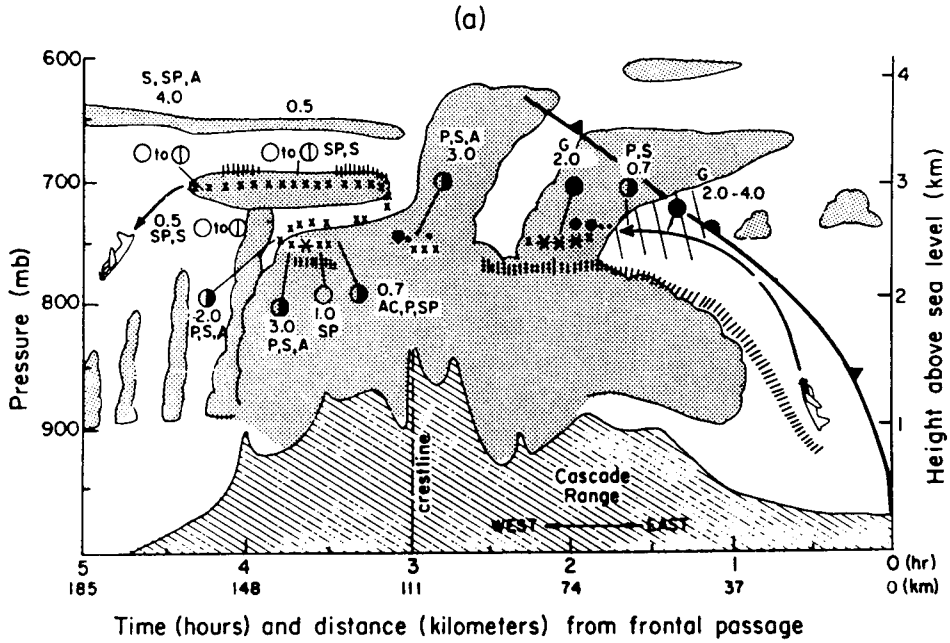

FIG. 30. The passage of an occluded front over the Cascade Range in Washington state: (a) the distribution of clouds 1 hr after the front crossed the mountain crestline; (b) the precipitation rate (10^{-1} mm/hr) plotted as a function of the distance from the crestline (km) and the elapsed time from local frontal passage (hr). Frontal precipitation occurs even before the front reaches the mountain (region A on the figure). The mountain greatly increases the frontal precipitation (region D), but this seems to "dry out" the front as frontal precipitation stops as the mountain is left behind (region F). In the upslope region, rain continues for many hours after the passage of the front (region E). (From Hobbs *et al.*, 1975.)

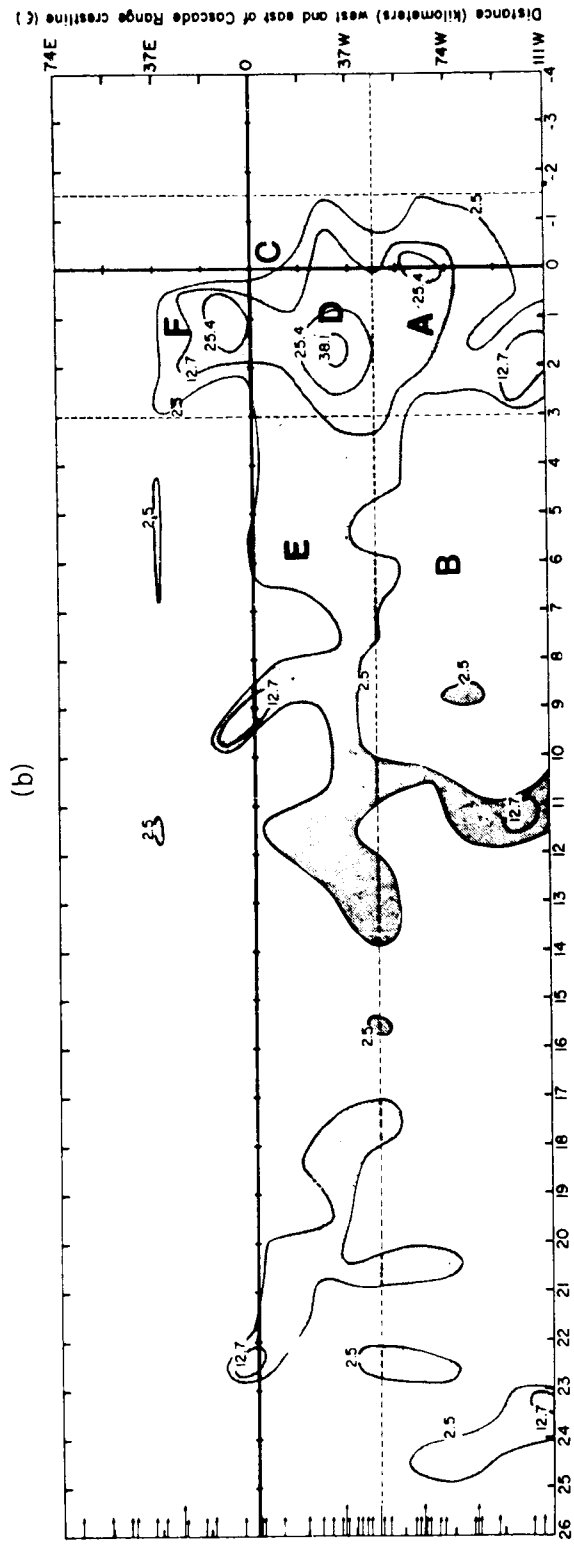

FIG. 30. (Continued.)

The relationship between orographic precipitation and synoptic situation in the central Rockies has been studied by Williams and Peck (1962).

4.2.5. The Dynamics of Airflow in Connection with the Problem of Upslope Rain. The general dynamical problem of airflow over mountains has been discussed in the other sections. Still there are some special aspects to the problem which are associated with upslope rain and they deserve attention here. First, there is the question of the dynamical influence of the latent heat of condensation. Second, the results of the earlier sections should be re-examined to understand their implications for the generation of orographic precipitation. For example, if conditional instability is important in orographic rain, we should see what destabilizing influence the mountain may have.

It has become quite common to assume that the vertical velocities above a mountain are confined to the region directly over the mountain and that the slope of the streamlines is either constant with height [as in Eq. (4.5)] or decreases to zero at some midtroposphere level (see Fig. 31). Dynamically such models are clearly incorrect as are the attempts to derive them from the governing equations. Myers (1962) defended such a solution using arguments taken from hydraulics—the study of discrete fluid layers. Such arguments are not applicable to the continuously stratified atmosphere, however, as in this latter case there is no maximum long-wave speed. Atkinson and Smithson (1974) use a correct set of governing equations (without moisture) to derive such a flow field, but their solution violates the important upper radiation condition and is therefore incorrect. On the other hand, the use of such a simplified model as in Fig. 31 probably does not introduce very much error in the computation of total condensation *if* the air is passing smoothly and stably over the mountain. This is especially true in cases when most of the moisture

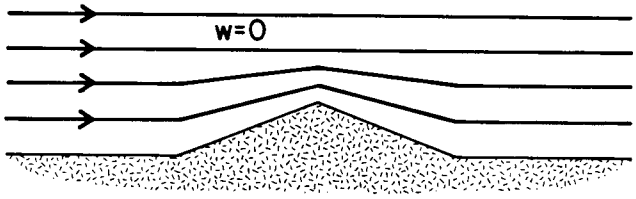

FIG. 31. The simple model of airflow used by several authors in their models of orographic rain. The lifting of the air is confined to the region directly over the mountain, and the slope of the streamlines decreases upward to zero at an undisturbed level. Such an airflow pattern probably would not occur, but it is not known whether the use of such a model would introduce appreciable error.

is in the lowest layers as these layers must follow the ground regardless of what model is used (unless there is blocking).

The primary point here is that all actual solutions to flow over an isolated mountain or ridge show that the lifting aloft begins well upstream of the mountain. This is true for hills and mountains of all scales regardless of whether the flow is dominated by inertia, buoyancy, or rotation, but it is probably most marked for mountains from 10 to 200 km wide, generating gravity waves which tilt strongly upstream. For example, the flow over a 1-km high mountain could well experience 500 m of lifting aloft, say, at 600 mbar, before the ground surface begins to rise. In a model of stable upslope rain, this effect would move the *condensation maximum* some distance out ahead of the point of steepest surface slope. Of course the delays associated with the formation of hydrometeors and their fall to the ground could well push the *rainfall maximum* back to or even beyond the steepest mountain slopes, depending on the horizontal scale of the mountain.

The lifting of middle-level air ahead of the mountain has a stronger implication if we consider the destabilization of the air by the mountain. Consider the case where the incident airstream is slightly undersaturated (relative humidity slightly less than 100%) and slightly conditional stable (θ_w increases slowly with height). As the air approaches the mountain there is lifting aloft, but not at the surface. The lifting by itself is important, of course, as it brings the air closer to saturation, but, the fact that the column is vertically stretched, may be just as important in the generation of showers. The lifting aloft is at first along a dry adiabat (see Fig. 32) and acts strongly to destabilize the column. Then, when saturation is reached, the column is conditionally unstable even if it was conditionally stable way upstream. Such a destabilization cannot be described by the simple models with an undisturbed nodal level as only column shortening occurs in such a model.

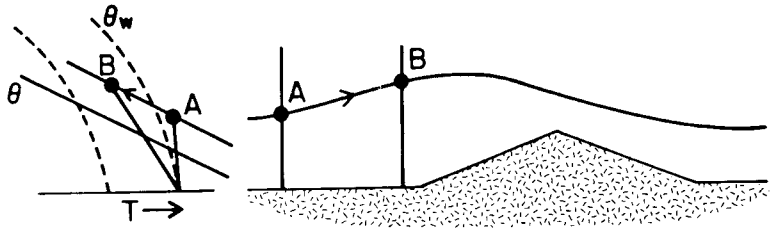

FIG. 32. The destabilization of a nearly saturated, nearly conditionally unstable air mass due to lifting aloft upstream of the mountain. The air parcels aloft rise dry adiabatically thus decreasing the stability of the air column against moist convection.

There have been a number of studies in which the governing equations for fluid motion have been used to determine the airflow pattern over a mountain for use in a orographic rain model. As a first step, Sawyer (1956) discussed the application of the adiabatic linear theory solutions to the orographic rain problem. He also estimated the amount of "spill-over" of rainfall into the downslope area due to the delays in droplet coalescence and fallout. A more complete model of this sort has been presented by Gocho and Nakajima (1971). There must be some question as to the validity of their flow solutions, however, as their streamline patterns do not agree with those of other investigators. Their computation of spillover shows that most precipitation falls downstream of the crest, but this follows naturally from their model as the trajectory slope (droplet fall speed/speed) was approximately 5 m sec^{-1}/20 m sec^{-1} = 1/4 and the mountain width was only 10 km. Actually, the small-scale orographic rain pictured by Gocho and Nakajima would be unlikely without vigorous seeding from above (Bergeron, 1960a). A more recent treatment is Gocho (1978).

To form a consistent model of orographic rain, the latent heat released by condensation should be included in the dynamics. Within the methodology of linear theory this added heat can be accounted for by the use of the saturated adiabatic lapse rate, in the definition of static stability, at the levels that are saturated. This method was used by Sarker (1966) in his model of flow over the Western Ghats in India—an area noted for its torrential monsoonal rains (Ramage, 1971, p. 111). In Sarker's case the observed lapse rate was equal to the saturated adiabatic lapse rate Γ_s over a deep layer. Thus when Γ is replaced by Γ_s in the expression for the Scorer parameter

$$l^2(z) = \frac{-g[(\partial T/\partial z) - \Gamma]}{TU^2} - \frac{1}{U^2}\frac{\partial^2 U}{\partial z^2}$$

the buoyancy term (i.e., the first term) vanishes. Sarker concludes that the restoring force due to the curvature in the mean velocity profile, a term which is usually quite small, must dominate. This leads to a rather peculiar flow field solution, partly because the profile curvature must be evaluated from a sounding near the mountain which is strongly altered by the mountain. Some alterations in the model are described in Sarker (1967).

One problem with the use of linear theory is that in a nearly saturated atmosphere, even slight lifting will bring the air to saturation and thus change the effective stability of the fluid. This problem has been avoided in the nonlinear models of Raymond (1972) and Fraser *et al.* (1973). Fraser *et al.* introduced nonlinear corrections at the interface between

saturated and unsaturated layers. Raymond used a more straightforward model with a local heating function prescribed as a function of the vertical velocity. A few iterations are necessary before a consistent solution is found. Raymond finds that the heating makes only minor changes in the flow field—a result which suggests that the adiabatic flow-field solutions might be applicable, at least qualitatively, to the orographic rain problem. This view is strongly contested by the observations of Hill (1978) who measured precipitation-induced vertical motion in winter orography storms in the Wasatch Range, Utah. In particular, Hill's observations suggest that the role of heat release in condensation and cooling during evaporation is to generate small-scale convective motion. These motions locally control the rainfall intensity.

A fully numerical, finite difference solution to the two-dimensional, orographic rain problem has been presented by Colton (1976). The computed rainfall distribution over the Sierras and the Smith River Basin in California agrees well with observations, but it is difficult to understand completely why this is so. One would think that his assumptions of 100% release of condensate with no delay and a reflective upper boundary condition at 11 km would degrade his results. Such an incorrect upper boundary condition requires the flow (except for the action of friction) to be of a standing wave form with a level of no disturbance and with lifting confined to the region directly over the mountain. Colton appears to find no evidence of convective instability, but his coarse grid and frequent numerical smoothing of the flow field probably rule out such a possibility *a priori*.

The remaining dynamical problem concerning orographic rain is the question of whether an incoming airstream will pass over the mountain, or whether due to the mountain's disturbing influence, it will slow, turn aside, and either flow completely around the mountain or pass over at a more convenient spot. Such a turning would surely influence the horizontal distribution of precipitation. Two examples from the Scandinavian mountains will serve to illustrate the point.

When a large-scale westerly flow crosses the west coast of Norway, there is usually a local disturbance to the pattern of reduced sea level pressure (see Spinnangr and Johansen, 1954). This pressure perturbation has the form of a high at, or upstream of, the ridge crest and a trough in the lee. This description roughly coincides with the theoretical solution for the flow over a mesoscale mountain (see Section 3). The pressure perturbation does not seem to be so strong as to suggest a complete blocking of the flow, but at the same time the surface winds just upstream are observed to be northward, parallel to the mountainous coastline. The occurrence of upslope rain indicates that there is lifting aloft, so that the

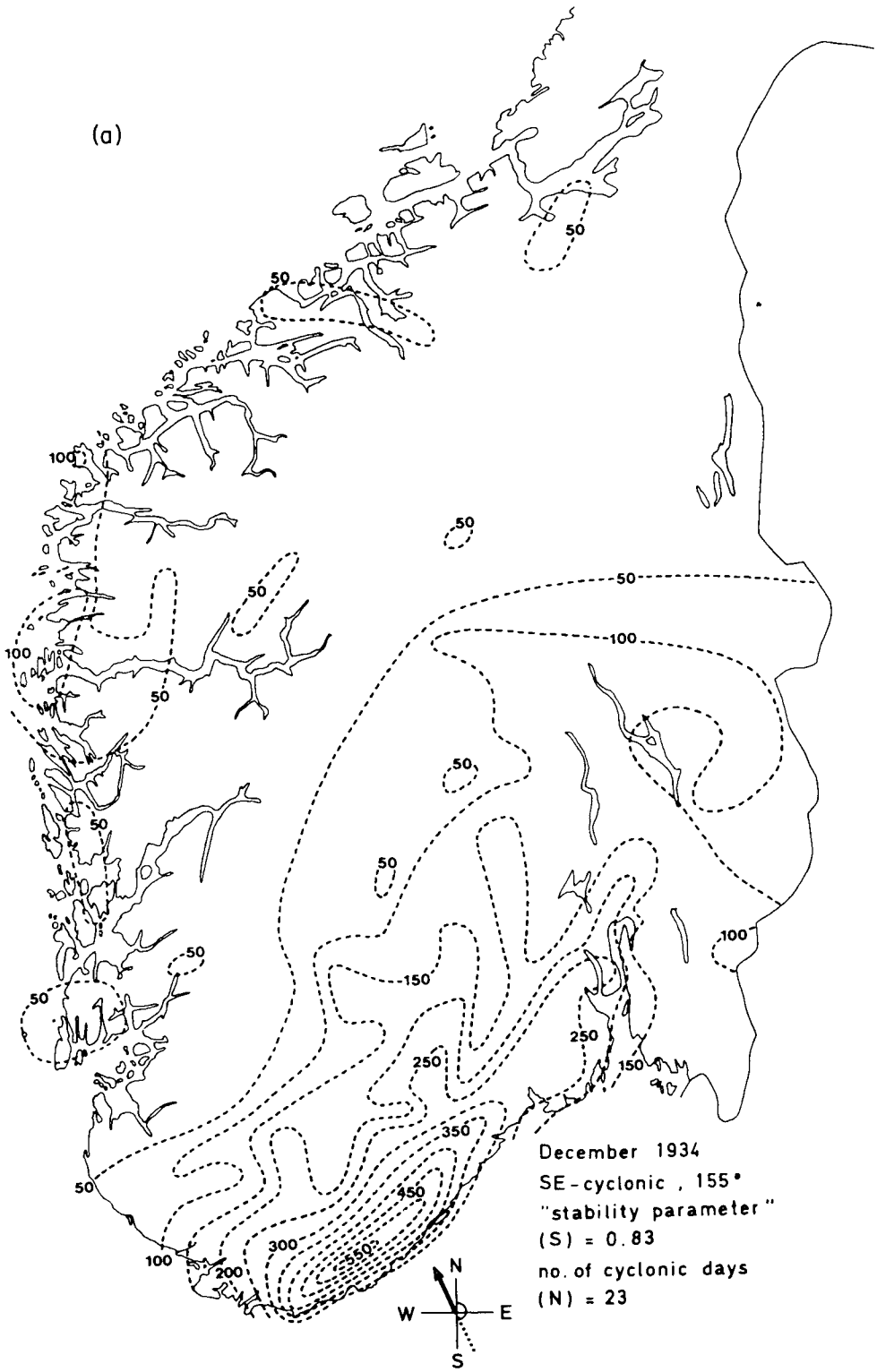
(a)
50
100
150
200
250
300
350
400
450
500
December 1934
SE-cyclonic , 155°
"stability parameter"
(S) = 0.83
no. of cyclonic days
(N) = 23
N
W
E
S

FIG. 33. (a)

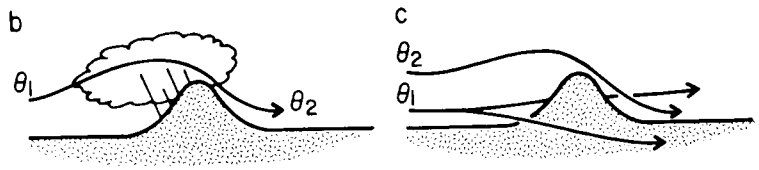

FIG. 33. Examples of the horizontal redistribution of precipitation by the blocking influence of the mountain. (a) The maxima of SE Norway occurring with SE winds. (After Andersen, 1972.) Two possible models of the foehn wind; (b) with flow over the mountain and upslope rain, and (c) with blocking and descent from aloft.

blocked air must be confined to a shallow layer (perhaps only the lower part of boundary layer) near the ground.

When the wind approaches southern Norway from the east or southeast, the surface winds may also turn to the left and run down the coast. In this case, however, there appears to be an alteration to the horizontal distribution of precipitation with a maxima occurring in southeast Norway (see Fig. 33a). This maxima appears in case studies described by Bergeron (1949) and Smebye (1978) and in monthly averaged rainfall patterns described by Anderson (1972). According to the linear theory of flow over mesoscale mountains, this local intensification could be explained by the increased wind at the left end of a mountain range by the mountain anticyclone (see Section 3).

The horizontal deformation of the wind field is also important in the warm, dry *föhn wind* that blows down the lee slopes of mountains such as the Alps (Defant, 1951; Yoshino, 1975), and the Rockies (Brinkman, 1971). There seems to be two possible explanations for the appearance of the dry, warm air. The first, shown in Fig. 33b, is connected to the theory of orographic rain. If the incoming air is nearly saturated and if it goes directly over the mountain, it will rise along a saturated adiabatic to the top. If the condensed moisture has rained out, the air will be warmed adiabatically as it descends—ending up warmer and with lower relative humidity. There are many "ifs" in this "textbook" explanation and sometimes it is difficult to explain the extreme dryness of a föhn in this way. The consideration of *unstable* upslope rain may be of some help in this regard.

The other possibility (Fig. 33) is that the low-level air has been blocked upstream by the mountain or has been diverted to the sides. Then the potentially warm, dry air from aloft must descend generating a föhn effect. This mechanism can produce drier air than the classical explanation as the air need not be saturated at mountain top level.

The general relationship between the three-dimensional perturbation of the flow by orography and the distribution of orographic precipitation

is little understood. There seems to be a need for more synoptic studies of this problem.

4.3. The Redistribution of Rainfall by Small Hills

Recent studies of the small-scale distribution of precipitation using dense networks of precipitation gauges have revealed an important effect due to small hills. Examples include Bergeron (1960b) for the hills around Uppsala, Sweden; Skaar (1976) for the Sognefjord district of western Norway; Wilson and Atwater (1972) for the state of Connecticut; Changnon *et al.* (1975) for southern Illinois. In general these studies reveal a strong positive correlation between altitude and precipitation, although in the case of a sudden rise to a plateau (Wilson and Atwater, 1972) the precipitation decreases further in on the plateau in the downwind direction. The correlation is most marked in the case of stable frontal rain from nimbostratus clouds, but Browning *et al.* (1974) found a similar correlation in unstable rain.

This type of orographic control is clearly different than the larger scale processes considered earlier. First, this control by small-scale hills results in a rainfall maximum near the hill top instead of in the upslope region. Second, the small size of the hills means that by themselves they could not produce precipitation. As the air passes over the mountain, there is insufficient time for raindrops or snowflakes to form from cloud droplets.

The simplest explanation for this would be called "differential evaporation." The raindrops falling from cloud base to the ground experience evaporation in the drier air beneath the cloud. This is sometimes visible as *virgae* (i.e., fall-streaks) which occasionally terminate before reaching the ground. Mason (1971, p. 313) estimates that drizzle drops falling from 1750 m through the air with 90% relative humidity would decrease in radius from 250 μm to 100 μm. The rainfall (mm/hr), being proportional to the radius cubed, would decrease even more strongly. Thus even if a hill does not disturb the flow, it will experience a higher precipitation rate than the surrounding valleys as *it reaches up to intercept the droplets before they evaporate*. The full implications of this model have apparently never been computed, but Bergeron (1968, p. 5) suggests that by itself the "differential evaporation" cannot account for the strong increase of precipitation with height.

Bergeron (1968) suggested that there may actually be an enhancement of precipitation over hills by *washout of cloud droplets which have formed as the low-level flow lifts over the hill.* Thus over the valleys the drops evaporate as they fall, but over the hills the drops expand as they

fall through low-level pannus or skud clouds. The large-scale rain cloud aloft—perhaps a frontal stratus cloud or an orographic upslope cloud mass—plays a crucial role as (1) a moistener of low-level air bringing the boundary layer near to saturation and (2) a seeder cloud providing a mechanism for release of the low-level condensate. This is shown in Fig. 25b.

Recently Storebø (1976) and Bader and Roach (1977) have estimated the efficiency of the washout of low-level cloud droplets by raindrops falling from above. These estimates are still rather crude, but they provide a feeling for the magnitude of the effect. In a sample calculation Bader and Roach considered the lifting of 1500-m thick layer of saturated air onto a 500-m hill. The rainfall rate from above is prescribed and the growth of the raindrops as they fall is computed using a radius-dependent collection efficiency. They find that the local precipitation rate can be doubled or tripled by low-level washout. There is, however, one difference between Bergeron's conceptual model and Bader and Roach's computation. Bergeron makes the consistent (although perhaps incorrect) assumption that the seeder cloud aloft is unaffected by the hill. Bader and Roach, on the other hand, use an *ad hoc* upper boundary condition in which the rainfall from above is specified as constant along a surface which parallels the irregular terrain. This means that the incoming rainfall aloft varies along a level surface which could only occur if the upper cloud is influenced by the hill.

4.4. Orographic—Convective Precipitation

The final mechanism of orographic control of rainfall to be discussed is the local generation of cumulonimbus in a conditionally unstable air mass. The classical description of this process is similar to that given by Henz (1972) in his study of thunderstorms in the Rockies. Beginning in the morning the mountain slopes are heated by the sun. The air near the surface is heated by conduction and small-scale convection and begins to rise buoyantly—first directly up the slopes and later, in a more organized way, up the valleys (Defant, 1951). At the mountain tops the warm air breaks away from the surface to form rising thermals. When these thermals reach the lifting condensation level, visible cumulus clouds are formed, which can grow into cumulonimbus if the air mass existing in the area is conditionally unstable. These developing clouds will generally be carried with the local gradient wind; thus any showers that occur will be located downwind of the mountain which triggered that particular cloud. It is of course true that thermals, cumulus clouds, and convective

rain can occur on warm days over flat land without the disturbing influence of mountains, but it is clear that such development tends to occur sooner over mountains.

The transient nature and small scale of this type of orographic rainfall means that the conventional rain gauge networks and radiosonde soundings are of little use. The most useful methods for the study of this phenomenon are:

(a) *Aircraft measurements*. Silverman (1960) and Braham and Draginis (1960) have reported aircraft flights near the mountains of southwest North America. Braham and Draginis were able to confirm the supposed link between the thermally driven upslope winds and the observed cumuli.

(b) *Satellite photography*. The infrared motion pictures, which are now being produced from geostationary satellite photography, show clearly the diurnal cycle of cumulus activity in mountainous regions. In the summertime over the Rockies, for example, the cumulus appear over mountain peaks almost every morning. Biswas and Jayaweera (1976) have combined satellite and synoptic observations in the study of thunderstorms in Alaska.

(c) *Radar*. The spatial and temporal distribution of precipitation-size particles can be determined from the intensity of radar return. Ackerman (1960) and Kuo and Orville (1973) have used this method in the study of orographic convection in Arizona and South Dakota, respectively. Harrold *et al.* (1974) discusses the general problem of using radar to estimate rainfall in hilly terrain.

(d) *Surface wind measurements*. The onset of orographic convection is closely connected to the dynamics of slope and valley winds at the surface. Defant (1951) reviews the observations of the diurnal cycle of slope and valley winds. Examples of more recent observations include MacHattie (1968) for Alberta, Canada, and Sterten (1963) for the fjords of western Norway.

(e) *Theory and numerical simulation*. The dynamical problem of the rising of fluid along heated boundaries was treated first by Prandtl (see Defant, 1951). A more general treatment of buoyancy driven flow is given by Turner (1973). Fosberg (1967) and Orville (1968) have specifically attacked the orographic convection problem by using finite difference techniques to solve the governing equations in two dimensions. Fosberg concentrates on the formation of slope winds and convective plume above the ridge, while Orville follows the development of the cumulus clouds.

5. Planetary-Scale Mountain Waves

The availability of a hemispheric network of regularly reporting radiosonde stations has made it possible to construct monthly averaged upper air charts. From these time-averaged maps it is clear that in addition to the transient disturbances in the atmosphere, there are planetary-scale waves which remain stationary with respect to the Earth (see, for example, Van Loon *et al.*, 1973; Saltzman, 1968). It has also become clear that these stationary planetary waves are partly responsible for the variation in climate around a latitude circle. Reiter (1963), for example, has compiled a good deal of evidence relating the meridional position of the jet stream to the stormy cyclogenetic belts near the ground. The relationship is particularly evident when the stationary wave shifts its position causing an anomalous pattern of climate around the globe. This mechanism has been invoked by Namias (1966) to explain the drought in the northeastern United States during 1962–1965 and by Wagner (1977) to describe the abnormally cold 1976–1977 winter in the same region. There has also been some success using monthly averaged upper air patterns to predict the following months' weather (Ratcliffe, 1974).

It is obvious that the existence of stationary disturbances must be related in some way to the irregularities on the Earth's surface. It is much more difficult to determine whether it is the geographical distribution of ground elevation, surface roughness, or surface thermal properties which is most important. The first theories of the stationary waves by Charney and Eliassen (1949) and Bolin (1950) suggested that large-scale orography, primarily the Rocky Mountains Cordillera and the Tibetan Plateau, could cause the observed disturbance. Soon after, Smagorinsky (1953) showed that nonuniform heating could also produce such a disturbance. Now, 25 years later, the numerical models of the atmosphere suggest that both orography and heating are influential but their relative importance is still in doubt. Following the theme of this review we will describe only the forcing due to orography.

Models of Topographically Forced Planetary Waves

The theoretical study of planetary-scale waves requires consideration of two new aspects which were not included earlier, namely:

1. The influence of the spherical shape of the Earth. This requires either the use of a spherical coordinate system or, if a local Cartesian coordinate system is used, the waves must belong to a discrete spectrum with an integer number of waves around the globe. Further, in such a

Cartesian coordinate system the Coriolis parameter must be considered a function of latitude to retain the dynamical effect of the Earth's curvature.

2. Unlike the mesoscale disturbances which has a vertical length scale of a few kilometers, synoptic- and planetary-scale motions can have a vertical scale equal to a scale height H or greater. Therefore full consideration must be given to the variation of density. The Boussinesq approximation is no longer suitable. These new factors complicate the analysis. On the other hand, the simple quasi-geostrophic theory, which was questionable for mesoscale flows, should accurately describe this larger scale of motion.

A further complication is that we can no longer consider the effect of the mountain on a uniform steady current. The description of the stationary planetary wave given, for example, by Van Loon *et al.* (1973), is a time-averaged picture. Occurring at the same time are energetic smaller scale eddies and storms. The incorporation of these smaller scale motions in the planetary wave model is discussed by Saltzman (1968). For the most part in this review we will ignore this problem and concentrate on the direct topographic forcing of planetary waves. By neglecting the forcing due to nonuniform heating, nonuniform friction, and smaller scale storms, it is impossible for us to compute quantitatively valid results. Instead we will review what is known about the natural resonances and the response characteristics of the midlatitude westerlies. In any case, it seems a bit premature to discuss the quantitative results of the different published studies as there is still little agreement concerning the basic nature of the physical system (for example, whether it is appropriate to consider the atmosphere as vertically bounded).

A natural starting point for this discussion is the perturbation equations of quasi-geostrophic flow as given by Charney and Drazin (1961)

$$\frac{D}{Dt}(\zeta + f) = -f\nabla_H \cdot \mathbf{V} \tag{5.1}$$

$$\bar{\rho}\nabla_H \cdot \mathbf{V} + \frac{\partial(\bar{\rho}w)}{\partial z} = 0 \tag{5.2}$$

$$\frac{D(\partial\psi/\partial z)}{Dt} + \frac{gw}{f}\frac{\partial \ln \bar{\theta}}{\partial z} = 0 \tag{5.3}$$

$$\mathbf{V}_H = \mathbf{k} \times \nabla_H\psi, \qquad \zeta = \nabla_H^2\psi \tag{5.4}$$

The first equation states that the rate of change of vorticity is due to the Coriolis torque caused by divergent motion. The influence of vortex

twisting and baroclinic generation of vorticity are not important for these large-scale, nearly horizontal flows. The second equation is a reduced form of the continuity equation where the terms $\partial\rho/\partial t + V_H \cdot \nabla\rho$, which can be important for higher frequency motions, have been eliminated. The third equation, along with the definition

$$\psi \equiv p'/\bar{\rho}f \tag{5.5}$$

is the hydrostatic form of the thermodynamic equation. It states that temperature changes are caused by vertical motion in the presence of a variable background $\bar{\theta}(z)$ in accordance with the conservation of potential temperature. Equation (5.4) is the statement of geostrophic balance.

This set of equations is not exact. Equation (5.2) is the anelastic form of the continuity equation and (5.3) is exact only in the limit of γ, the ratio of specific heats, going to one. The nature of these assumptions has been clarified recently by White (1977).

5.1. *A Vertically Integrated Model of Topographically Forced Planetary Waves*

If there is no need to understand the vertical structure of the disturbance, then a reduced set of vertically integrated equations can be used. Substituting (5.2) into (5.1) gives

$$\frac{D}{Dt}(\zeta + f) = \frac{f}{\bar{\rho}}\frac{\partial \bar{\rho} w}{\partial z} \tag{5.6}$$

which relates vorticity changes to the vertical motion field; either vortex stretching

$$f(\partial w/\partial z)$$

or to the expansion of the particles as they rise

$$\frac{fw}{\bar{\rho}}\frac{\partial \bar{\rho}}{\partial z}$$

Multiplying by $\bar{\rho}$ and integrating vertically

$$\int_0^\infty \bar{\rho}\frac{D}{Dt}(\zeta + f)dz = f[\rho w]_0^\infty \tag{5.7}$$

If either the vertical velocity or the background density (or both) approaches zero as $z \to \infty$, then there is no contribution from the upper limit of the integral. Taking w at the ground to be $U_0(\partial h/\partial x)$ gives

$$\int_0^\infty \rho\frac{D}{Dt}(\zeta + f)dz = -f\rho_0 U_0\frac{\partial h}{\partial x} \tag{5.8}$$

To help interpret the left-hand side of (5.8), define a mass-velocity weighted average vorticity according to

$$\overline{\zeta + f} = \frac{\int_0^\infty \rho(z)U(z)(\zeta + f)\, dz}{\int_0^\infty \rho(z)U(z)\, dz} \tag{5.9}$$

where $\rho(z)$ and $U(z)$ are background density and wind speed. Then, in the steady state, (5.8) becomes

$$\frac{\partial}{\partial x}\overline{(\zeta + f)} = \frac{-f\rho_0 U_0 \dfrac{\partial h}{\partial x}}{\int_0^\infty \rho(z)U(z)\, dz} \tag{5.10}$$

In the simple case of $U(z) = \text{const} = U_0$, the denominator on the right-hand side of (5.10) is

$$U_0 \int_0^\infty \rho(z)\, dz \approx U_0 \rho_0 H$$

where H is the density scale height and (5.10) is

$$\frac{\partial}{\partial x}(\overline{\zeta + f}) = -\frac{f}{H}\frac{\partial h}{\partial x} \tag{5.11}$$

The mathematical form of (5.11) is similar to the equation describing columnar motion of a homogeneous fluid with a rigid lid at $z = H$. This analogy helps to visualize the solution to (5.11) [or (5.10)] but is also dangerous. The actual flow field may vary strongly with height and the vertical motion probably does not vanish at $z = H$. As an example, the integrated equation (5.10) or (5.11) continue to be valid even when the disturbance takes the form of a vertical propagating planetary wave with strongly tilted phase lines. Thus, while the integrated equations are easier to solve than the full equations, the results are sometimes difficult to interpret.

A vertically averaged perturbation velocity, vorticity, and stream function can be defined in a similar way to (5.9) so

$$\nabla^2\bar{\psi} = \bar{\zeta} \qquad \bar{v} = \bar{\psi}_x$$
$$\bar{u} = -\bar{\psi}_x \tag{5.12}$$

Then with the β-plane approximation $f = f_0 + \beta y$, $\beta y \ll f_0$, (5.11) becomes

$$\nabla^2 \bar{\psi} + \frac{\beta}{U} \bar{\psi} = -\frac{f}{H} h \tag{5.13}$$

Charney and Eliassen (1949) and Bolin (1950) used an equation of this type in their pioneering studies of the influence of orography on the midlatitude westerlies. Charney and Eliassen assumed that the perturbation would vanish at certain bounding latitudes determined by the meridional extent of the mountains. If the mountains are chosen of the form

$$h(x, y) = h_m \cos ly \cos kx \tag{5.14}$$

where h_m is the amplitude of the topography, then π/l must be chosen as the distance between the bounding latitudes, and k must be chosen according to

$$n(2\pi/k) = n\lambda = L \tag{5.15}$$

so that an integer (n) number of wavelengths (λ) fit exactly into the circumference of a latitude circle $L = 2\pi a \cos \phi$, where a and ϕ are the Earth's radius and latitude. The solution to (5.13) with (5.14) is

$$\bar{\psi}(x, y) = \left[\frac{f h_m / H}{k^2 + l^2 - \beta/U} \right] \cos ly \cos kx \quad \text{for} \quad -\frac{\pi}{2} < ly < \frac{\pi}{2} \tag{5.16}$$

Here $\beta = (2\Omega/a) \cos \phi$ and U is chosen to represent the strength of the mean westerly current in midlatitudes. Mountains with a sufficiently small longitudinal and meridional scale have $k^2 + l^2 > \beta/U$. The bracketed coefficient in (5.16) is positive in this case and the streamlines will be displaced northward over the regions of high ground—southward over lower ground. When the mountain's horizontal scale is so large that $\beta/U > (k^2 + l^2)$, the response is reversed with southward displacement over the high ground (see Fig. 34).

In both cases the absolute vorticity $\zeta + f$ is decreased over the high ground. In the so called "long" waves, $k^2 + l^2 > \beta/U$, the decrease in absolute vorticity is brought about by the generation of negative relative vorticity. In the "ultralong" waves, $\beta/U > k^2 + l^2$, the decrease in absolute vorticity is associated with the movement of air parcels southward to a region of smaller planetary vorticity. Near $\beta/U = k^2 + l^2$ these two tendencies nearly cancel and the amplitude given in (5.16) becomes exceedingly large. This singularity associated with the fact that there is a free solution to (5.13), that is, a solution with the forcing $h = 0$. Physically this is a standing Rossby wave with its westward directed

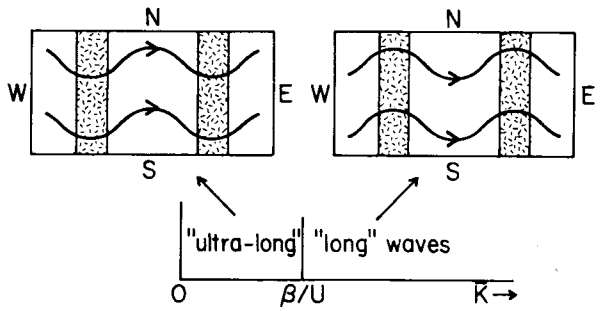

FIG. 34. The orographic perturbations to a westerly wind according to the vertically integrated model. For $\bar{k}^2 = k^2 + l^2 > \beta/U$, the pressure disturbance and meridional streamline displacement are in phase with the orographic height (so-called long-wave behavior). For longer waves ($\bar{k}^2 < \beta/U$) there is southward displacement and low pressure over the mountain regions (so-called ultralong wave behavior).

phase speed exactly balanced by the eastward advection by the basic current.

The actual topography of the Earth around a particular latitude circle can be represented as a sum of Fourier components each similar to (5.14). According to linear theory the atmospheric response is a superposition of disturbances like (5.16), some acting like "long waves" and some like "ultralong waves." It is unlikely that there will be any forcing at the singular wave number

$$k^2 + l^2 = \beta/U \tag{5.17}$$

as the possible wave numbers are strongly restricted by (5.15). Nonetheless, the flow may be dominated by the components which most closely satisfy (5.17). This near resonance would presumably also be important for other types of forcing, for example, heating.

Charney and Eliassen (1949) used the orographic distribution of 45°N to compute the steady-state perturbation to the January westerlies. Considering the simplicity of their model, the results (Fig. 35) are remarkably close to the observed pattern.

Bolin (1950), using the same integrated equations (5.13), considered the perturbation to the westerlies by a large isolated mountain on an infinite β-plane. He did not demand that disturbance vanish at "bounding latitudes" nor that the solution join itself smoothly after once around the Earth. He found that the mountain generates a standing Rossby wave in its lee. Bolin found good agreement between his theory and the upper air trough and ridge system observed to the east of the Rockies in winter.

To understand more about these topographically generated disturbances and to understand the success of the vertically integrated models

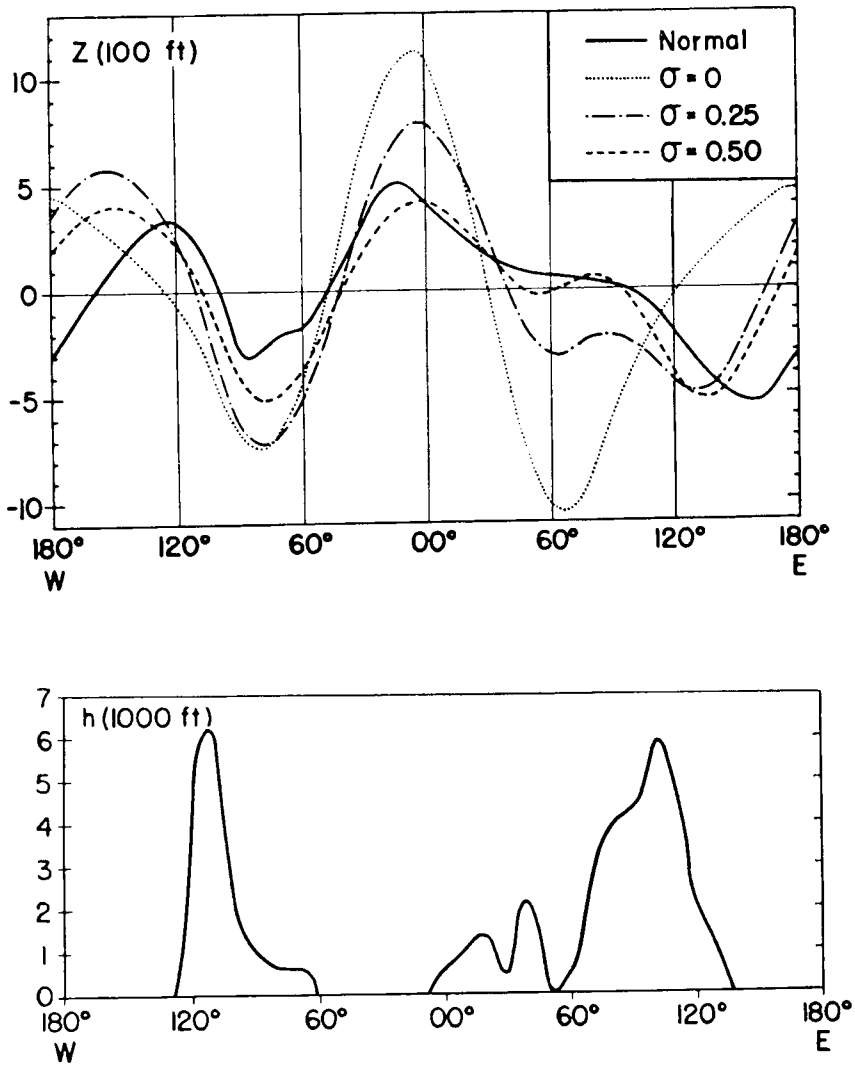

FIG. 35. The topographic profile (bottom) and the observed (solid line) and computed (dotted line) 500-mb heights at 45°N (top). (After Charney & Eliassen, 1949.) Mean zonal wind is chosen as 17° longitude/day and the north-south distance between bounding latitudes is 33°.

we must investigate the full structure of these motions using the complete set of governing equations.

5.2. *The Vertical Structure of Planetary Waves on a β-Plane between Bounding Latitudes*

In this section we will investigate the vertical structure of topographic disturbances following the treatments of Charney and Drazin (1961) and

Hirota (1971). We will retain the assumption that the disturbance is contained between two bounding latitudes on a β-plane and cannot propagate meridionally. After describing this type of solution we can show the connection to Queney's (1948) work by making the Boussinesq approximation and the connection to the work of Saltzman (1965, 1968) and Sankar-Rao (1965a,b) by imposing a reflective top lid on the system.

The quasi-geostrophic perturbations on a zonal flow can be described using Eq. (5.1)–(5.4) given earlier. Combining (5.1) and (5.2) and assuming steady state ($\partial/\partial t = 0$) flow on a β-plane gives

$$U\frac{\partial}{\partial x}\nabla_H^2\psi + \beta\frac{\partial\psi}{\partial x} = f_0\left(\frac{\partial}{\partial z} - \frac{1}{H}\right)w \tag{5.18}$$

Equation (5.3) can be rewritten as

$$U\frac{\partial}{\partial x}\left(\frac{\partial\psi}{\partial z}\right) + \frac{N^2}{f_0}w = 0 \tag{5.19}$$

At the ground

$$w = U_0\frac{\partial h}{\partial x} \tag{5.20}$$

so the lower boundary condition can be written in terms of ψ as

$$\frac{\partial\psi}{\partial z} + \frac{N^2}{f_0}h = 0 \qquad \text{at} \quad z = 0 \tag{5.21}$$

To construct a simple prototype problem we will treat $U(z)$ and $N(z)$ as constants. Then eliminating w between (5.18) and (5.19) gives

$$\psi_{zz} - \frac{1}{H}\psi_z + \frac{N^2}{f_0^2}\left(\nabla_H^2 + \frac{\beta}{U}\right)\psi = 0 \tag{5.22}$$

The troublesome second term in (5.22) can be eliminated by introducing the new dependent variable

$$\phi = (\bar{\rho}/\rho_0)^{1/2}\psi \tag{5.23}$$

so that (5.22) becomes

$$\phi_{zz} + n^2\phi = 0 \tag{5.24}$$

with

$$n^2 = \frac{N^2}{f^2}\left(\nabla_H^2 + \frac{\beta}{U}\right) - \frac{1}{4H^2} \tag{5.25}$$

The transformation (5.23) can be motivated physically as the magnitude of ϕ^2 is directly proportional to the kinetic energy density of the disturbance.

Because of (5.23) the lower boundary condition becomes slightly more complicated

$$\phi_z + \frac{1}{2H}\phi = -\frac{N^2}{f_0}h \qquad \text{at} \quad z = 0 \tag{5.26}$$

If

$$h(x, y) = h_m \cos lx \cos kx \tag{5.27}$$

where k and l are constrained by (5.15). The solution to (5.24), (5.25), and (5.26) can be written as

$$\phi(x, y, z) = \mathrm{Re}\{\hat{\phi}(z) \cos ly e^{ikx}\} \tag{5.28}$$

If

$$n^2 = \frac{N^2}{f_0^2}\left[\frac{\beta}{U} - (k^2 + l^2)\right] - \frac{1}{4H^2} \tag{5.29}$$

is positive, for example with weak westerly winds and very broad orography, $\hat{\phi}(z)$ is given by

$$\hat{\phi}(z) = \frac{-(N^2/f_0)h_m}{in + (1/2H)} e^{+inz} \tag{5.30}$$

where a positive sign has been chosen in the exponent to satisfy the radiation condition aloft. The substituting (5.30) and (5.28) and using (5.23) gives

$$\begin{aligned}\psi(x, y, z) = [\rho_0/\tilde{\rho}(z)]^{1/2}&\left[\frac{-(N^2/f)h_m}{(N^2/f_0^2)[\beta/U - (k^2 + l^2)]}\right] \cdot \cos ly \\ &\cdot \left\{\frac{1}{2H}\cos(kx + nz) + n \sin(kz + nz)\right\}\end{aligned} \tag{5.31}$$

Equation (5.31) describes a vertically propagating planetary wave with phase lines tilting westward with height. The phase of the disturbance relative to the orographic highs and lows is determined by the relative importance of the two terms in the curly brackets. The first term represents a pattern of high and low pressure which at the ground is exactly opposite to the orography. This is similar to the "ultralong" behavior discussed earlier. There is no vertical energy flux associated with this term as the pressure and the vertical velocity are 90° out of phase. This term vanishes in the Boussinesq limit.

The second term in (5.31) represents a pattern of high and low pressure which, at the ground, is shifted one-quarter of a wavelength westward relative to the orography. The high pressure regions, for example, with streamline displacement to the north, occur on the westward (i.e., upwind) slopes of the mountains. From this we can see that the vertical velocity will be in phase with the pressure and there will be an upward flux of wave energy.

If the mountains have a smaller horizontal scale or if the winds are easterly, n^2, given by (5.29), will be negative and the solution to (5.24) and (5.26) with (5.8) is

$$\hat{\phi}(z) = \frac{-(N^2/f_0)h_m}{-|n| + (1/2H)} \exp(-|n|z) \tag{5.32}$$

where the negative sign in the exponent has been chosen to keep the solution bounded. Putting (5.32) into (5.28) and using (5.23)

$$\psi(x, y, z) = [\rho_0/\rho(z)]^{1/2} \left[\frac{-(N^2/f)h_m}{-|n| + (1/2H)}\right] \cdot \cos ly \cdot \cos kx \exp(-|n|z) \tag{5.33}$$

This describes a perturbation which decays exponentially with height. The phase is constant with height and is determined by the relative magnitudes of the two terms in the denominator of the square brackets. For smaller scale mountains, $L \sim 1000$ km or so, the $|n|$ term will dominate. In this case the square bracket is positive and the high and low pressure regions are in phase with the highs and lows of the orography. This is similar to the "long wave" dynamics discussed earlier. This would always be the case if we made the Boussinesq approximation in (5.33) by taking $H \to \infty$.

For broader mountains (but keeping $n^2 < 0$) the solution changes sign. The high pressure areas lie over the orographic lows and vice versa. The situation is similar to the "ultralong waves" discussed earlier. When $k^2 + l^2 - \beta/U = 0$ the denominator of (5.33) vanishes and the solution is infinite. This singularity clearly has the same physical origin as the singularity in the vertically integrated equations, namely, the existence of a free standing Rossby wave characterized by a balance of relative and planetary vorticity. This free wave has $\psi(w,y,z)$ independent of height, while $\phi(x,y,z)$ decreases as $\sim e^{-z/2H}$ and so has a finite total kinetic energy. To summarize this complicated variety of cases we can fix β, H, U, f, N in our minds and consider the wave number $|\bar{k}| = (k^2 + l^2)^{1/2}$ as a variable (see Fig. 36).

In 1948, Queney discussed the effect of a nonzero β on the flow over

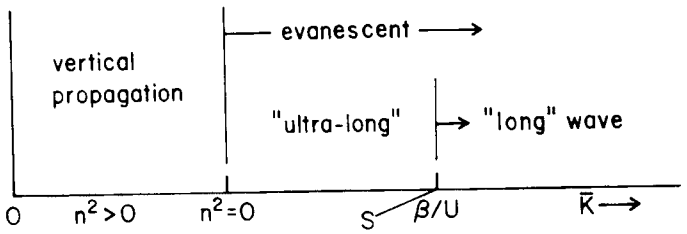

FIG. 36. The influence of wave number $\bar{k}^2 = k^2 + l^2$ on the phase and vertical structure of the orographic disturbance. Short waves ($\bar{k}^2 > \beta/U$) are in phase with the orography (i.e., "long-wave" behavior) and are evanescent. Longer waves ($\bar{k}^2 < \beta/U$) are out of phase ("ultralong wave" behavior) and evanescent. Still longer waves ($n^2 > 0$) are vertically propagating with westward tilting phase lines. At $\bar{k}^2 = \beta/U$ there is a singularity (S) in the response.

an isolated mountain. He obtained a simple solution by using the Boussinesq approximation (see also Johnson, 1977, in this regard). To understand this solution we must see how this approximation changes the above result. Looking back to (5.6) see that changes in absolute vorticity can be caused either by a term

$$f_0(\partial w/\partial z)$$

which would be interpreted as the vertical stretching of a vortex line, or by a term

$$-f_0(w/H)$$

which is best described as the effect of volume expansion as the fluid particles move upward to a region of lower density. In the Boussinesq approximation the volume expansion is neglected. The effect of this assumption is easily seen by taking the scale height H to be very large in the above analysis. The most striking simplification is that the boundary between propagating and evanescent behavior now coincides with the Rossby wave singularity. The range of scales where the solution is evanescent, with "ultralong" behavior, is gone (see Fig. 37). Unfortunately, the vertical length scales associated with planetary motions are the same order as the scale height H and the Boussinesq approximation is not valid. Vorticity generation by volume expansion can play an important role.

A number of authors have attempted to model stationary planetary waves using a system of equations similar to that used in the preceding, but with the use of a *reflective upper boundary condition*. Examples include Saltzman (1965) and Sankar-Rao (1965), while Saltzman (1968) has reviewed several others. To understand these models we must investigate the influence of reflective condition aloft as opposed to the

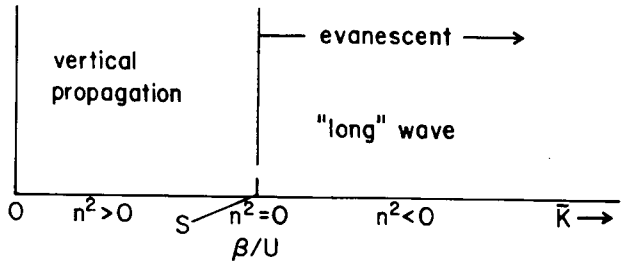

FIG. 37. The influence of wave number on the phase and vertical structure of the orographic disturbance in a Boussinesq fluid. Unlike a compressible fluid (Fig. 36) the evanescent "long" waves go directly over to vertically propagating waves as the wavelength increases.

radiation condition used in Eq. (5.30). Out of a number of possibilities the arbitrary choice of $v = 0$ at the top, or equivalently $u = \phi = \psi = 0$, has been made by Saltzman, Sankar-Rao, and others. This is quite a strong condition as it requires the horizontal flow, not just the vertical motion, to vanish at the top of the domain of interest. Applying this condition at $z = D$ gives instead of (5.30) and (5.32)

$$\hat{\phi}(z) = \left[\frac{-(N^2/f_0)h_m}{-n\cos nD + (1/2H)\sin nD}\right]\sin n(D - z) \tag{5.34}$$

for the case n^2 ($|\bar{k}|$, N, U, H, β, f) > 0 and

$$\hat{\phi}(z) = \frac{-(N^2/f)h_m}{-|n|(e^{|n|D} + e^{-|n|D}) + (1/2H)(e^{|n|D} - e^{-|n|D})} \tag{5.35}$$

for the case $n^2 < 0$. The nature of the flow for a given wave number and the location of the singularities of (5.34) and (5.35) in wave number space depend on the height D at which the upper boundary condition is applied. The singularities in (5.34) and (5.35), respectively, occur at

$$\tan nD = 2nH \tag{5.36}$$

and

$$\tanh nD = 2nH \tag{5.37}$$

Qualitatively it is particularly important to know whether D is greater or less than $2H$. For the sake of illustration it will suffice to describe just one case, and the $D < 2H$ case seems to bear the closest relationship to the solutions of Saltzman (1965), Sankar-Rao (1965), and others. In this case there are no solutions to (5.37) so all the singularities occur with $n^2 > 0$.

Referring to Fig. 38, note that there is no longer a singularity at $k^2 + l^2 = \beta/U$. This is explained by the fact that the upper boundary

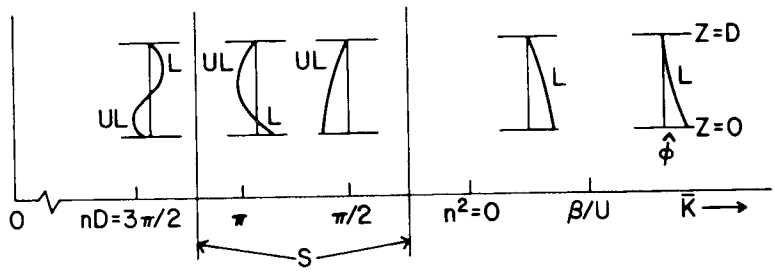

FIG. 38. The influence of wave number on the nature of the orographic disturbance in a model with a particular reflective upper boundary condition ($\psi = 0$ at $z = D < 2H$). The small diagrams represent the variation of $\hat{\phi}(z)$ according to (5.34) and 5.35). The solutions could be described as standing waves in the vertical with no phase line tilt. Positive $\hat{\phi}$ implies "long-wave" behavior (L), while negative $\hat{\phi}$ means "ultralong wave" behavior (UL). The response characteristics of this unbounded model are fundamentally different than the unbounded model (Fig. 36). The Rossby wave singularity is gone, while other singularities (S) arise due to reflection at the upper boundary.

condition $\phi_{z=D} = 0$ has eliminated the free barotropic Rossby wave. The first singularity occurs at a much longer wavelength where the form of $\hat{\phi}(z)$ demanded by (5.24) has become oscillatory. Near this value the amplitude of the solution becomes very large and upon crossing over the singularity (to smaller wave numbers) the sign of the solution changes from "long wave" behavior to "ultralong wave" behavior. At smaller wave numbers the horizontal motion acquires a node at a certain height. Above the node the high pressure regions lie directly over the topographic lows (i.e., "ultralong behavior"), while near the ground the pressure and $h(x,y)$ are in phase. At still smaller wave numbers another singularity will be encountered.

Clearly the use of a reflective upper boundary condition has significantly altered the physical characteristics of the system. It is still true that each singularity can be associated with a standing free Rossby wave. These free waves, however, are not the naturally trapped barotropic wave with $k^2 + l^2 = \beta/U$, but baroclinic waves trapped by the reflective upper boundary. The description just given agrees remarkably well with the more detailed computations of Saltzman and Sankar-Rao. Such a comparison is not completely straightforward, however, as those computations were carried out using pressure coordinates. The difficulty with this is that pressure coordinates become strongly stretched at high altitudes, while the vertical scale of the disturbance (e.g., the vertical wavelength) remains about the same. Thus in pressure coordinates the disturbance appears to oscillate rapidly at high levels. For this reason it is advantageous to use Cartesian or log pressure coordinates (see Holton, 1975) which do not have this unwanted stretching. To avoid this problem

Saltzman and Sankar-Rao use the somewhat unphysical device of choosing an $N^2(z)$ which becomes vanishingly small at high altitudes. This causes the vertical scale of the disturbance to increase with height and thus to remain well behaved when described in pressure coordinates.

We have seen that a reflective upper condition can radically change the response characteristics of the atmosphere. As an ad hoc hypothesis such a condition should probably be avoided. There are, however, valid reasons for interest in such a system. First, the numerical models of the atmosphere invariably use a reflective condition aloft (usually $\omega = dP/dt = 0$). If we wish to understand the results from these models we must know about the influence of a reflective lid. Second, and more to the point, there are conditions that will naturally cause the reflection of planetary waves. If the wind speed increases with height, then, as discussed by Charney and Drazin (1961), waves which can propagate at low levels [$n^2 > 0$ in (5.25)] become evanescent ($n^2 < 0$) aloft. In this situation the wave energy will be totally reflected and resonant response such as described by (5.34) and (5.35) becomes possible.

The validity of $\psi = 0$ as an upper boundary condition cannot be defended by arguing that the disturbance is absent high in the atmosphere. This could occur either because the disturbance is dissipated or reflected at lower levels. In the former case a radiation condition is appropriate, while in the latter a reflective condition at the correct altitude is appropriate.

Since the study of Charney and Drazin (1961) there have been a number of theoretical studies concerning the eventual fate of vertically propagating planetary waves. Dickinson (1968a) treated the problem in spherical coordinates with the background westerly wind field assumed to be in solid body rotation. He found that Charney and Drazin's estimate of the critical wind speed [i.e., the speed beyond which the waves become evanescent, see Eqs. (5.29)], may be too low. In 1969 Dickinson considered the decay of vertically propagating waves by preferential cooling at the warm regions by radiation to space.

Geisler and Dickinson (1975) use a realistic vertical profile of background wind to determine the possible free waves of the system. They found an "external" wave, which closely corresponds to the natural free Rossby wave discussed previously, and four "internal" modes which are associated with reflection from levels of high wind speed.

Another interesting possibility arises if the background wind $U(z)$ decreases to zero at some level and then becomes easterly. Clearly from (5.29) the wave cannot propagate above this critical level so it must either be absorbed or reflected. From the analogy with small-scale mountain waves (Booker and Bretherton, 1967) we note from (5.29) that as $U(z)$

$\rightarrow 0$, the vertical wave number n approaches infinity, making the disturbance susceptible to viscous and radiative dissipation or to small-scale instability. A further insight into this problem is given by Dickinson (1970) and Beland (1976) who investigated the time development of a Rossby wave critical level. The interested reader should also consult Holton's (1975) recent review of stratosphere and mesosphere dynamics.

5.3. *Models of Stationary Planetary Waves Allowing Meridional Propagation and Lateral Variation in the Background Wind*

Throughout the previous section we have retained two strong assumptions about the meridional structure of the mean flow and the perturbations. First, we assumed that the mean flow was independent of latitude (i.e., y). Second, we eliminated the possibility of meridional propagation by requiring that the disturbance vanish at the walls of a fictitious zonal channel. Both these assumptions are incorrect and they are clearly the severest *ad hoc* hypothesis remaining in the model.

A more general three-dimensional approach has been tried by Dickinson (1968b), Matsuno (1970), Simmons (1974),and Schoeberl and Geller (1976), and some of the results of these theories have been compared with observation by McNulty (1976). A brief description of Matsuno's model will serve to explain some of these new results and concepts.

Matsuno (1970) derived the steady, linearized quasi-geostrophic potential vorticity equation in spherical coordinates and log pressure coordinates

$$\bar{\omega}\frac{\partial}{\partial\lambda}\left[\frac{\sin^2\theta}{\cos\theta}\frac{\partial}{\partial\theta}\left(\frac{\cos\theta}{\sin^2\theta}\frac{\partial\phi'}{\partial\theta}\right)+\frac{1}{\cos^2\theta}\frac{\partial^2\phi'}{\partial\lambda^2}+4\Omega^2a^2\sin^2\theta\frac{\partial}{p\partial z}\left(\frac{p}{N^2}\frac{\partial\phi'}{\partial z}\right)\right]+\frac{\partial\bar{q}}{\partial\theta}\frac{1}{\cos\theta}\frac{\partial\phi'}{\partial\lambda}=0 \tag{5.38}$$

where

a	radius of the Earth
Ω	rotation rate of the Earth
N	Brunt-Väisälä frequency
$\bar{\omega}$	angular speed of the basic flow
ϕ'	perturbation height field
z	$-H\ln(p/p_0)$ vertical coordinate
λ	longitude
θ	latitude

The physical meaning of each term in (5.38) is easy to establish. The

square bracket is the perturbation potential vorticity and is composed of the perturbation relative vorticity (the first two terms) and the Coriolis torque caused by horizontal divergence. The last term in (5.38) is the meridional advection of potential vorticity which is proportional to the local gradient in background potential vorticity $\partial\bar{q}/\partial\theta$. Matsuno gives

$$\frac{\partial\bar{q}}{\partial\theta} = \Bigg[\underset{\text{(a)}}{2(\Omega + \bar{\omega})} - \underset{\text{(b)}}{\frac{\partial^2\bar{\omega}}{\partial\theta^2}} + \underset{\text{(b)}}{3\tan\theta\frac{\partial\bar{\omega}}{\partial\theta}} - \underset{\text{(c)}}{4\Omega^2a^2\sin^2\theta\frac{1}{p}\frac{\partial}{\partial z}\left(\frac{p}{N^2}\frac{\partial\bar{\omega}}{\partial z}\right)}\Bigg]\cos\theta \tag{5.39}$$

This can be compared with the same quantity expressed in local Cartesian coordinates on a β-plane (Simmons, 1974)

$$\frac{\partial\bar{q}}{\partial y} = \underset{\text{(a)}}{\beta} - \underset{\text{(b)}}{\frac{\partial^2\bar{U}}{\partial y^2}} - \underset{\text{(c)}}{\frac{f_0^2}{\rho_0}\frac{\partial}{\partial z}\left(\frac{\rho_0}{N^2}\frac{\partial\bar{U}}{\partial z}\right)} \tag{5.40}$$

The terms marked (a) in (5.39) and (5.40) represent the gradient in planetary vorticity; those marked (b), the gradient in background relative vorticity; and those marked (c), the gradient in background static stability written in terms of the vertical shear.

The last term in (5.38), together with (5.39) or (5.40), is of crucial importance as it represents the restoring force for Rossby wave motion. In our previous models with $\bar{U}(y,z) = \text{const}$ this restoring force was due soley to β, the gradient in planetary vorticity, and indeed this is the classical view of Rossby wave dynamics. Matsuno uses the observed Northern Hemisphere wintertime distribution of zonal winds (shown in Fig. 39) to compute $\partial\bar{q}/\partial\theta$ from (5.39). The most striking result of this computation is that *the contribution of the basic wind to $\partial\bar{q}/\partial\theta$ is comparable to or larger than β.* This suggests that the propagation of Rossby waves is not necessarily associated with the variation of f with latitude. It is also interesting to note that the pattern of $\partial\bar{q}/\partial\theta$ is quite nonuniform with maxima just to the south of the tropospheric jet stream and the high-latitude polar night jet. It is not surprising that it never goes negative in this seasonally averaged picture as a negative value would lead to baroclinic instability which would tend to restore the stability of the system.

Matsuno avoided the question of what drives the stationary waves by using the observed pattern at 500 mbar as his lower boundary condition. Then, Fourier transforming in x and using (5.38) and (5.39), he computed the flow field aloft and the pattern of wave energy flux in the y,z-plane.

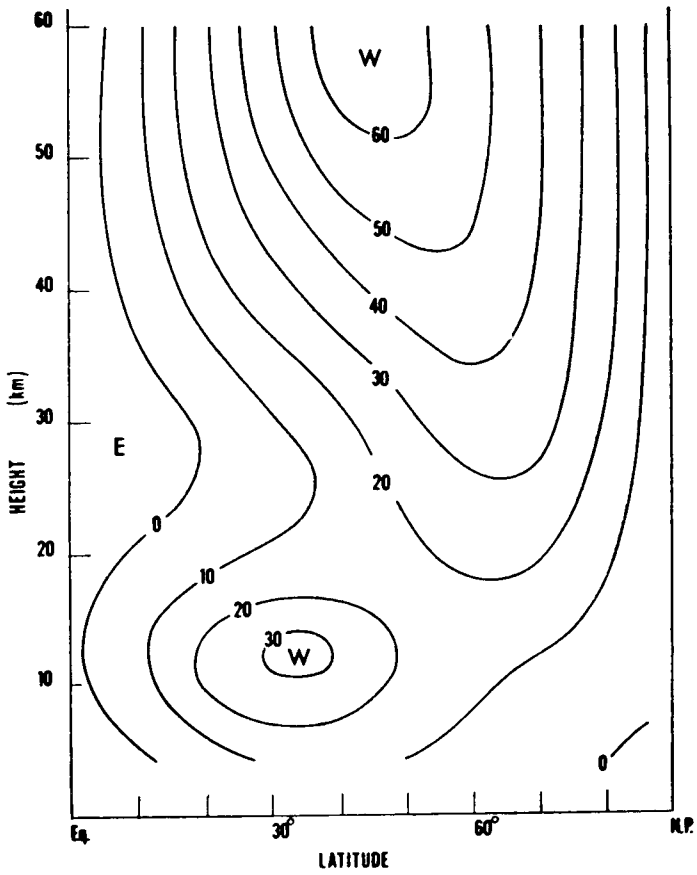

FIG. 39. The basic state zonal wind distribution (m sec^{-1}) in the winter Northern Hemisphere used by Matsuno (1970) in his model of stationary planetary waves. Note the jet stream near the tropopause at 30–40° and the strong polar night jet.

Generally the flow of energy was found to be upward and southward, but in detail strongly controlled by the nonuniform field of $\partial\bar{q}/\partial\theta$. In particular the wave energy was drawn into regions of high mean wind (Fig. 40). At high latitudes the wave energy is channeled upward along the axis of the polar night jet until the mean velocity becomes so large that the wave is reflected. Thus the distribution of $\partial\bar{q}/\partial\theta$ forms a partial resonant cavity, and Matsuno finds the strongest response for a zonal wave number between 1 and 2.

These results of Matsuno together with those of Dickinson and Simmons have provided a more complete and possibly a more correct view of the response characteristics of the atmospheric system. Matsuno's description of the "resonant cavity" may provide some qualitative justification for approach of Saltzman (1965) and Sankar-Rao (1965) who used zonal walls and a reflective upper boundary condition. At the same time it points out the arbitrariness of such ad hoc assumptions. The

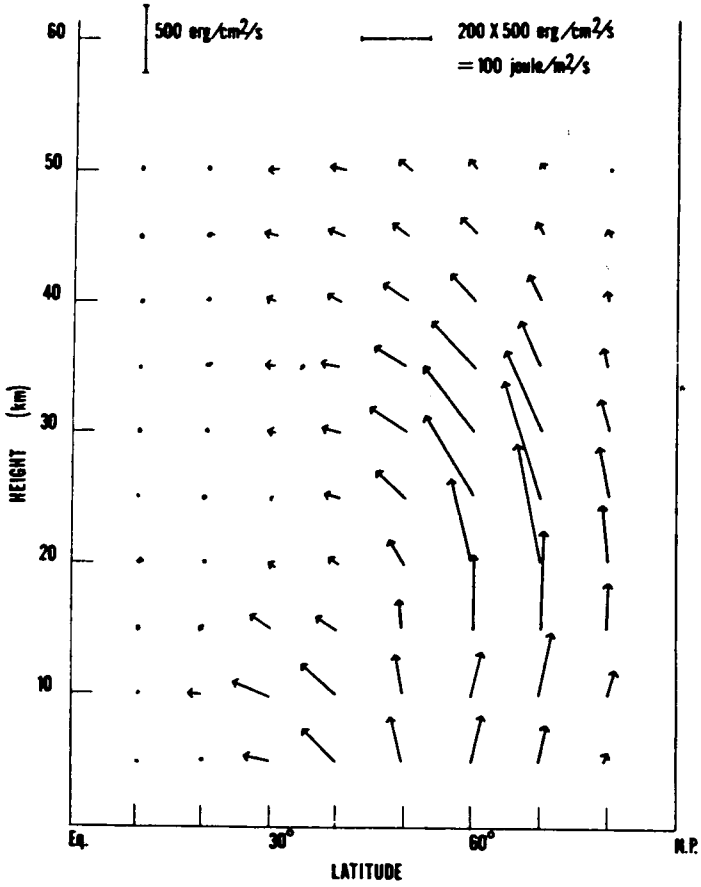

FIG. 40. The computed distribution of energy flow in the meridional plane associated with the longest (i.e., one wavelength around the globe) stationary wave. Due to the nonuniform distribution of U and $\bar{d}q/d\theta$, the wave energy flux is guided into regions of high wind speed—particularly the polar night jet. (After Matsuno, 1970.)

precise nature of the resonant activity, if indeed one exists, cannot be specified *a priori,* but will depend, perhaps sensitively, on the structure of the atmosphere at the time being considered.

Many questions still remain concerning the effects of nonlinearity and the relative importance of forcing by topography, heating, and migratory storms. Andrews and McIntyre (1976) and Holton (1976) have investigated the nonlinear interactions between planetary waves and the mean flow. A more comprehensive treatment, including the vastly complicated forcing and dissipation in the troposphere, requires the use of a numerical model. The past few years have witnessed rapid progress in the numerical simulation of planetary-scale atmospheric motions. The models range from two-layer systems (e.g., Egger, 1978) with specified forcing, to multilayer models with much of the forcing determined parametrically within the model (e.g., Kasahara and Washington, 1971; Kasahara *et al.*,

1973; Manabe and Terpstra, 1974). In these models the primary goal of the investigator is to simulate the atmosphere, not to explain its behavior. The analysis of model output is, however, significantly easier to diagnose than is observational data since the spatial and temporal coverage is complete and the investigator is free to do controlled experiments. The primary difficulty with this approach is that, like the atmosphere itself, the models are so complicated that the connection between the fundamental laws of physics and the model results cannot be clearly traced. Unlike the atmosphere, there are also the uncertainties involving the finite difference representation, the parameterization of subgrid scale processes, and the arbitrary choice of a restricted vertical domain.

Probably the most valuable simulation with regard to the influence of mountains on the atmosphere is the work of Manabe and Terpstra (1974). This study is notable both for the comprehensiveness of the model and for the detail in which the results are compared with observations. The global climate under perpetual January conditions was computed both with and without mountains. In this way the influence of the mountains can be clearly identified. It would take too long to give a detailed description of Manabe and Terpstra's model and results. We will mention only three interesting points.

(a) *The structure of the stationary disturbance.* Both in the simulations with (M) and without (NM) mountains the distribution of time mean meridional winds is qualitatively similar to the observed winds (Fig. 41). In the presence of mountains, however, the disturbance to the zonal flow is much stronger and its dominance over the thermally induced disturbance increases with height. In both models the phase of the disturbance tilts westward with height, although it is not clear whether this is due primarily to vertical propagation or to nonadiabatic effects associated with the northward transfer of sensible heat. Manabe and Terpstra point out that the description of stationary disturbances given by their model is much more realistic than in the linear theory model of Sankar-Rao (1965a). They suggest that Sankar-Rao's model may have been unduly influenced by the phenomenon of resonance. In the highly nonlinear and dissipative atmosphere, they argue, resonances may not be important. On the other hand, they have made no attempt to determine whether *their* solutions were influenced by quasi-resonance. Furthermore, the distribution of zonal winds, which is determined internally in the Manabe and Terpstra model, is much stronger than the observed distribution. Referring back to the work of Charney and Drazin (1961) and Matsuno (1970), we know that this can have an important influence on the structure of the stationary disturbances.

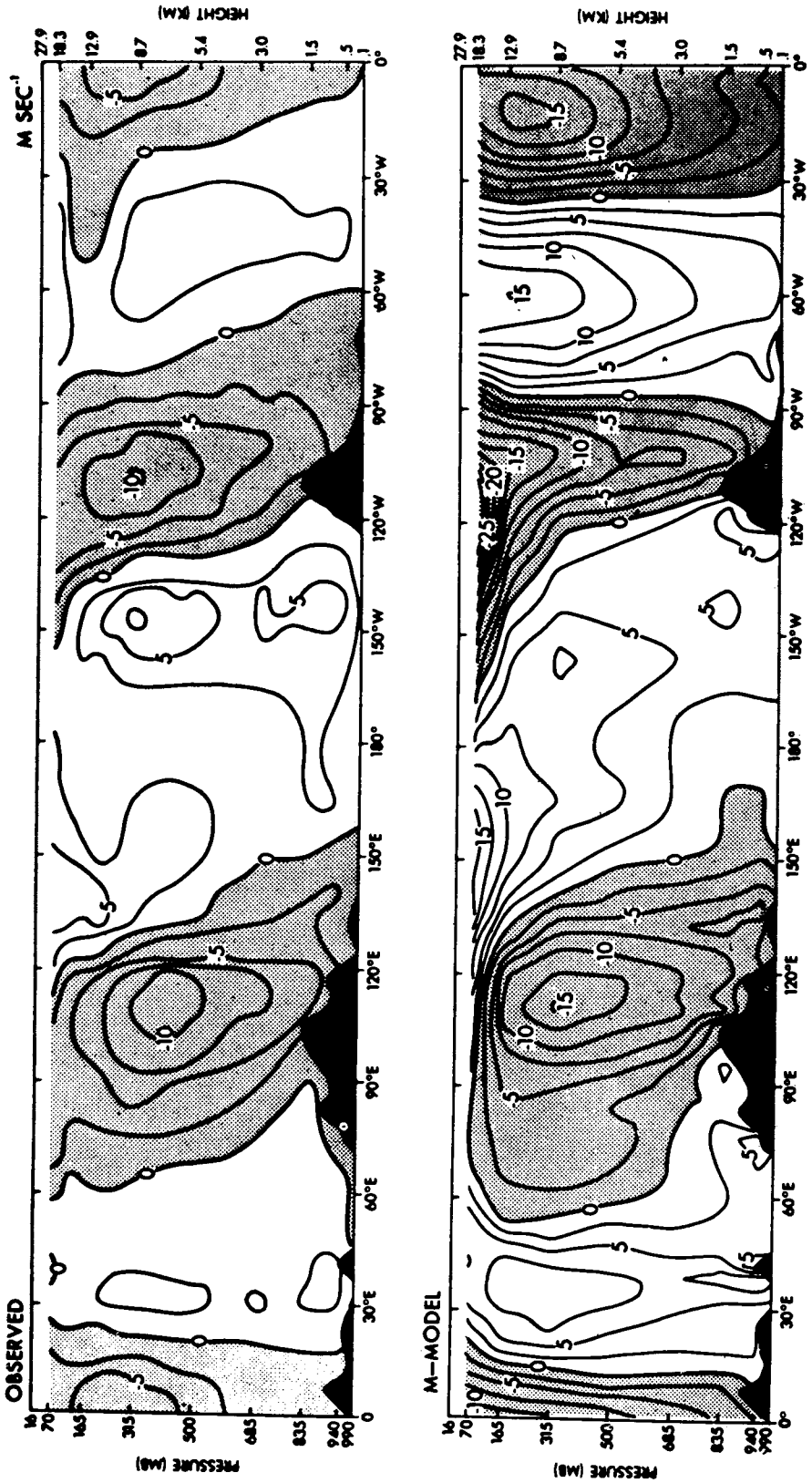
OBSERVED
M-MODEL
M SEC⁻¹
HEIGHT (KM)
PRESSURE (MB)
27.9
18.3
12.9
8.7
5.4
3.0
1.5
.5
0
70
165
315
500
685
835
940
990
30°E
60°E
90°E
120°E
150°E
180°
150°W
120°W
90°W
60°W
30°W
0°

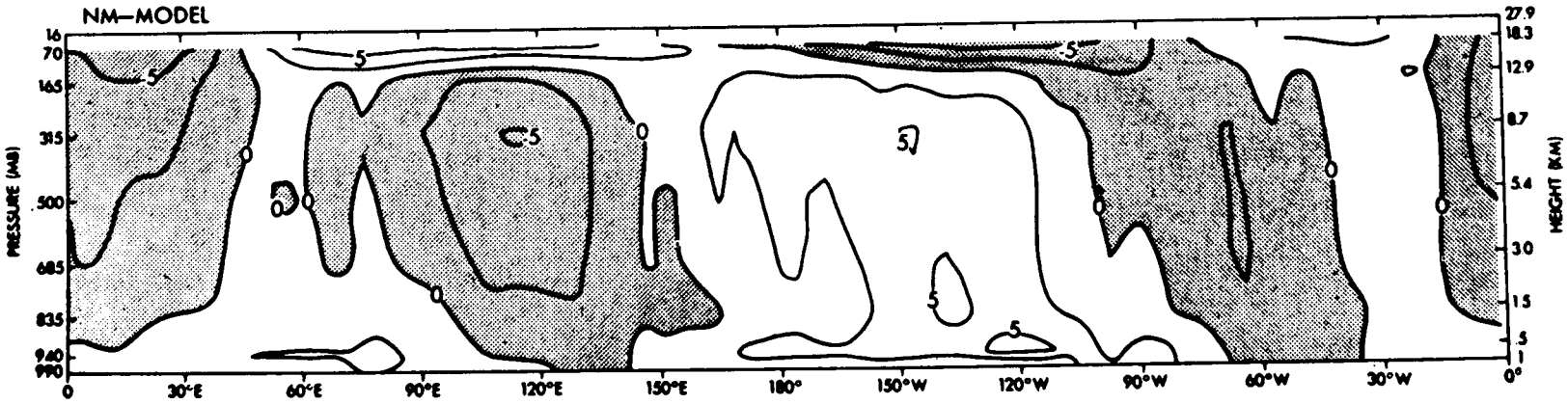

FIG. 41. The longitude–height distribution of the time mean meridional component of wind (m sec^{-1}) along the 45° latitude circle: (top) observed (Oort and Rasmusson, average over five Januaries, 1959–1963); (middle) the computed distribution with mountains (i.e., the M-model); (bottom) the computed distribution without mountains (NM-model). (From Manabe and Terpstra, 1974.)

(b) *The distribution of cyclogenesis*. Manabe and Terpstra's numerical model is quite successful at simulating the increased frequency of cyclogenesis in the lee of the Rocky Mountains and the Tibetan Plateau. As in the atmosphere, the reason for this increase is not clear. One possibility is that the increased baroclinicity in the southeastern side of the first trough of the orographic planetary wave provides a preferred site for frontal instability.

Cyclogenesis in the Alpine region is not simulated in the model as the Alps are too small to be represented in the 250-km grid system.

(c) *Meridional heat transfer and midlatitude storms*. The most dramatic difference between the mountain and no-mountain computer runs is in the nature of the northward transfer of heat and the conversion of available potential energy to kinetic energy in midlatitudes. Without mountains the northward transport of heat is accomplished by *transient* waves, especially wave numbers 5, 6, and 7. These transient waves are also responsible for much of the conversion of available potential energy into the kinetic energy of the winds.

With orography in the model the situation is quite different. The heat transport is dominated by the meridional motions associated with the stationary planetary wave, primarily with wave number 2. To a certain extent this heat transfer is caused by orographically induced north–south motion with air parcels gaining heat at low latitudes and losing heat at high latitudes. At the same time, however, these standing waves are responsible for the major part of the conversion of potential energy to kinetic energy. Thus the standing waves are in part driven by the meridional temperature gradient.

Apparently then the Earth's orography is large enough to change completely the nature of the midlatitude dynamics. Without mountains the midlatitudes would have many more energetic transient storms associated with baroclinic instability of an intensified north–south temperature gradient. With mountains the meridional heat flux is partially accomplished by the stationary disturbances. The temperature gradient is weaker and the transient storms less frequent and intense. The stationary waves are now an interesting mix, being forced partly by orography and partly by baroclinic instability.

Further insight into this problem is afforded by the much simpler two-level model of Smith and Davies (1977). Without mountains, the midlatitude flow is characterized by the recurring buildup of a strong meridional temperature gradient and breakdown into transient baroclinic waves. With mountains present in the model, large-amplitude standing waves occur and the amplitudes of the transient disturbance are decreased.

ACKNOWLEDGMENTS

My introduction to mountain flow dynamics came through the lectures of F. P. Bretherton and R. R. Long at The Johns Hopkins University and A. Eliassen at the 1974 Summer Institute at the National Center for Atmospheric Research. Conversations with W. Blumen, D. K. Lilly, J. Klemp, B. Gjevik, and M. Lystad among others, have also been informative and stimulating. Most of this review was written while the author was a visiting lecturer and scientist at the Institute of Geophysics at the University of Oslo under Fulbright–Hays and NATO fellowship support. During this time, frequent discussions with Professor A. Eliassen provided much needed encouragement and advice. The review was completed at Yale University with support from National Science Foundation grant ATM-7722175. The help of S. R.-P. Smith in organizing the references, E. Moritz in drafting the figures, and B. Dabakis in typing the manuscript is gratefully appreciated. Several authors and journals were kind enough to allow their figures to be reproduced in this review. Unfortunately, because of the breadth of this review and the limited time available for its completion, many excellent research papers have been omitted from the foregoing discussion. I apologize to those authors whose work I did not include.

REFERENCES

Section 2. The Flow over Hills and the Generation of Mountain Waves

Abe, M. (1932). The formation of cloud by the obstruction of Mt. Fuji. *Geophys. Mag.*, **6,** 1–10.

Anthes, R. A., and Warner, T. T. (1978). Development of hydrodynamic models suitable for air pollution and other mesometeorological studies. *Mon. Weather Rev.* **106,** 1045–1078.

Atkinson, B. W., and Smithson, P. A. (1974). Meso-scale circulations and rainfall patterns in an occluding depression. *Q. J. R. Meteorol. Soc.* **100,** 3–22.

Baines, P. G. (1977). Upstream influence and Long's model in stratified flows. *J. Fluid Mech.* **82,** 147–159.

Ball, F. K. (1956). The theory of strong katabatic winds. *Aust. J. Phys.* **9,** 373.

Benjamin, T. B. (1970). Upstream influence. *J. Fluid Mech.* **40,** 49–79.

Beran, D. W. (1967). Large amplitude lee waves and chinook winds. *J. Appl. Meteorol.* **6,** 865–877.

Bergan, J. D. (1969). Cold air drainage on a forested mountain slope. *J. Appl. Meteorol.* **8,** 884–895.

Berkshire, F. H., and Warren, F. W. G. (1970). Some aspects of linear lee wave theory for the stratosphere. *Q. J. R. Meteorol. Soc.* **96,** 50–66.

Blumen, W. (1965). A random model of momentum flux by mountain waves. *Geofys. Publ.* **26,** 1–33.

Blumen, W., and McGregor, C. D. (1976). Wave drag by three-dimensional mountain lee waves in nonplanar shear flow. *Tellus* **28,** 287–298.

Booker, J. R., and Bretherton, F. P. (1967). The critical layer for internal gravity waves in a shear flow. *J. Fluid Mech.* **27,** 513–539.

Breeding, R. J. (1971). A nonlinear investigation of critical levels for internal atmospheric gravity waves. *J. Fluid Mech.* **50,** 545–563.

Bretherton, F. P. (1966). The propagation of groups of internal gravity waves in a shear flow. *Q. J. R. Meteorol. Soc.* **92** (394), 466–480.

Bretherton, F. P. (1969). Momentum transport by gravity waves. Q. J. R. Meteorol. Soc. **95,** 213–243.

Bretherton, F. P., Thorpe, S. A., and Wood, I. R. (1967). Appendix to a paper by P. Hazel. *J. Fluid Mech.* **30,** 781–784.

Brighton, P. W. M. (1978). Strongly stratified flow past three-dimensional obstacles, *Q. J. R. Meteorol. Soc.* **104,** 289–307.

Brinkmann, W. A. R. (1970). The chinook at Calgary (Canada). *Arch. Meteorol. Geophys. Bioklimatol. (B)* **18,** 279–286.

Brinkmann, W. A. R. (1971). What is a foehn? *Weather* **26** (6), 230–239.

Chopra, K. P. (1973). Atmospheric and oceanic flow problems introduced by islands. *Adv. Geophys.* **16,** 297–421.

Clark, T. L., and Peltier, W. R. (1977). On the evolution and stability of finite amplitude mountain waves. *J. Atmos. Sci.* **34,** 1715–1730.

Claus, A. (1964). Large-amplitude motion of a compressible fluid in the atmosphere, *J. Fluid Mech.* **19,** 267–289.

Colson, D. Lindsay, C. V., and Hand, J. M. (1961). Radar echo of a mountain wave on February 15, 1960. *Mon. Weather Rev.* **89,** 17–19.

Conover, J. H. (1964). The identification and significance of orographically induced clouds observed by TIROS satellites. *J. Appl. Meteorol.* **3,** 226–234.

Corby, G. A. (1957). A preliminary study of atmospheric waves using radiosonde data. *Q. J. R. Meteorol. Soc.* **83,** 49–60.

Corby, G. A., and Sawyer, J. S. (1958). The airflow over a ridge: The effects of the upper boundary condition and high-level conditions. *Q. J. R. Meteorol. Soc.* **84,** 25–37.

Corby, G. A., and Wallington, C. E. (1956). Airflow over mountains: The lee-wave amplitude. *Q. J. R. Meteorol. Soc.* **82,** 266–274.

Counihan, J., Hunt, J. C. R., and Jackson, P. S. (1974). Wakes behind two-dimensional surface obstacles in turbulent boundary layers. *J. Fluid Mech.* **64,** 529–563.

Crapper, G. D. (1959). A three-dimensional solution for waves in the lee of mountains. *J. Fluid Mech.* **6,** 51–76.

Crapper, G. D., (1962). Waves in the lee of a mountain with elliptical contours. *Philos. Trans. R. Soc. London (A)* **254,** 601–623.

Critchfield, H. J. (1966). "General Climatology." Prentice-Hall, Englewood Cliffs, New Jersey.

Cruette, D. (1976). Experimental study of mountain lee-waves by means of satellite photographs and aircraft measurements. *Tellus* **28,** 500–523.

Danard, M. (1977). A simple model for mesoscale effects of topography on surface winds. *Mon. Weather Rev.* **105,** 572–581.

Davis, R. E. (1969). The two-dimensional flow of a stratified fluid over an obstacle. *J. Fluid Mech.* **36,** 127–143.

Dawson, P. J., and Marwitz, J. D. (1978). "An Investigation of Winter Winds in Southern Wyoming." (Preprint Vol.: Conference on Climate and Energy, Asheville, N. C.). American Meteorological Society, Boston, Massachusetts.

De, U. S. (1971). Mountain waves over northeast India and neighboring regions. *Ind. J. Met. Geophys.* **22,** 361–364.

Deaven, D. G. (1976). A solution for boundary problems in isentropic coordinate models. *J. Atmos. Sci.* **33,** 1702–1713.

Deaves, D. M. (1976). Wind over hills: A numerical approach. *J. Ind. Aerodyn.* **1,** 371–391.

Defant, F. (1951). Local winds, *in* "Compendium of Meteorology" (T. F. Malone, ed.), pp. 655–672. American Meteorological Society, Boston.

Döös, B. R. (1961). A mountain wave theory including the effect of the vertical variation of wind and stability. *Tellus* **13,** 305–319.

Döös, B. R., (1962). A theoretical analysis of lee wave clouds observed by TIROS I. *Tellus* **14,** (3), 301–309.

Doron, E., and Cohen, A. (1967). Mountain lee waves in the Middle East: Theoretical calculations compared with satellite pictures. *J. Appl. Meteorol.* **6,** 669–673.

Drazin, P. G. (1961). On the steady flow of a fluid of variable density past an obstacle. *Tellus* **13,** 239–251.

Drazin, P. G., and Moore, D. W. (1967). Steady two-dimensional flow of fluid of variable density over an obstacle. *J. Fluid Mech.* **28,** 353–370.

Eliassen, A. (1974). Airflow over mountains. *In* "Subsynoptic Extratropical Weather Systems" (M. Shapiro, ed.), pp. 103–184. "National Center for Atmospheric Research, Boulder, Colorado.

Eliassen, A., and Palm, E. (1954). Energy flux for combined gravitational–sound waves. Institute for Weather and Climate Research, Oslo, Publ. No. 1.

Eliassen, A., and Palm, E. (1960). On the transfer of energy in stationary mountain waves. *Geofys. Publ.* **22,** 1–23.

Foldvik, A. (1962). Two-dimensional mountain waves—A method for the rapid computation of lee wavelengths and vertical velocities. *Q. J. R. Meteorol. Soc.* **88,** 271–285.

Foldvik, A., and Wurtele, M. G. (1967). The computation of the transient gravity wave. *Geophys. J. R. Astron. Soc.* **13,** 167–185.

Fritz, S. 1965. The significance of mountain lee waves as seen from satellite pictures. *J. Appl. Meteorol.* **4,** 31–37.

Fritz, S., and Lindsay, C. V. (1964). Lee wave clouds photographed over the Appalachians by TIROS V and VI. *Soaring* March, pp. 14–17.

Förchtgött, J. (1957). Active turbulent layer downwind of mountain ridges. *Schweiz. Aero-Rev. Bern* **32,** 324–335.

Förchtgött, J., (1969). Evidence for mountain-sized lee eddies. *Weather* **24,** 255–260.

Furukawa, T. (1973). Numerical experiments of the airflow over mountains. 1. Uniform current with constant static stability. *J. Meteorol. Soc. Jpn* **51,** 400.

Geller, M. A., Tanaka, H., and Fritts, D. C. (1975). Production of turbulence in the vicinity of critical levels for internal waves. *J. Atmos. Sci.* **32,** 2125–2135.

Gerbier, N., and Berenger, M. (1961). Experimental studies of lee waves in the French Alps. *Q. J. R. Meteorol. Soc.* **87,** 13–23.

Gjevik, B., and Marthinsen, T. (1977). Three-dimensional lee-wave pattern. *Q. J. R. Meteorol Soc.* **104,** 947–957.

Godske, C. L., Bergeron, T., Bjerknes, J., and Bundgaard, R. C. (1957). "Dynamic Meteorology and Weather Forecasting." American Meteorological Society, Boston.

Granberg, I. G., and Dikiy, L. A. (1972). Steady state solution of a nonlinear problem of airflow over mountains. *Izv. Acad. Sci. USSR* **8,** 151–153.

Grimshaw, R. (1968). A note on the steady fluid over an obstacle. *J. Fluid Mech.* **33,** 293–301.

Grønås, S., and Sivertsen, B. (1970). Studies of local meteorology in a mountain/valley system in North Norway. Norwegian Defense Research Establishment Internal Report K-328, N-2007 Kjeller, Norway.

Gutman, L. N. (1969). "An Introduction to the Nonlinear Theory of Mesoscale Meteorological Processes." Israel Program for Scientific Translations, Jerusalem.

Gutman, L. N., and Khain, A. P. (1975). Mesometeorological processes in the free atmosphere governed by orography. *Atmos. Oceanic Phys.* **11,** 65–70.

Hallet, J., and Lewis, R. E. J. (1967). Mother-of-pearl clouds. *Weather* **22,** 56–65.

Holmes, R. M., and Hage, K. D. (1971). Airborne observations of three chinook-type situations in Southern Alberta. *J. Appl. Meteorol.* **10,** 1138–1153.

Houghton, D. D., and Isaacson, E. (1970). Mountain winds. *In* "Studies in Numerical Analysis" Vol. 2, pp. 21–52. Siam Publ. Philadelphia, Pennsylvania.

Houghton, D. D., and Kasahara, A. (1968). Nonlinear shallow fluid flow over an isolated ridge. *Commun. Pure Appl. Mech. 21,* 1–23.

Huppert, H. E., and Miles, J. W. (1969). Lee waves in a stratified flow. P. 3. Semi-elliptical obstacle. *J. Fluid Mech.* **35,** 481–496.

Jackson, P. S., and Hunt, J. C. R. (1975). Turbulent wind flow over a low hill. *Q. J. R. Meteorol Soc.* **101,** 929.

Janowitz, G. S. (1973). Unbounded stratified flow over a vertical barrier. *J. Fluid Mech.* **58,** 375–388.

Jensen, G., Kristensen, L., Dorph-Petersen, P., and Taagholt, J. (1976). Unmanned geophysical observatories in North Greenland 1972–1975. Danish Meteorological Institute, Copenhagen, Internal Report, pp. 1–93.

Jones, W. L., and Houghton, D. (1971). The coupling of momentum between internal gravity waves and mean flow: A numerical model. *J. Atmos. Sci.* **28,** 604–608.

Khatukayeva, Zh. M., and Gutman, L. N. (1962). The influence of the Coriolis force in the passage of a cold air mass across a mountain ridge. *Bull. (Izv.) Acad. Sci. USSR Geophys. Ser.* **6.**

Klemp, J. B., and Lilly, D. K. (1975). The dynamics of wave-induced downslope winds. *J. Atmos. Sci.* **32,** 320–339.

Klemp, J. B., and Lilly, D. K. (1978). Numerical simulation of hydrostatic mountain waves. *J. Atmos. Sci.* **35,** 78–107.

Kozhevnikov, V. N. (1968). Orographic perturbations in the two-dimensional stationary problem. *Atmos. Oceanic Phys.* **4,** 16–27.

Kozhevnikov, V. N. (1970). A review of the present state of the theory of mesoscale orographic inhomogeneities of the vertical current field. *Tr. (Trans.) Tsent. Aero. Observ.* **98.**

Kozhevnikov, V. N., Bibikova, T. N., and Zhurba, Ye. V. (1977). Orographic atmospheric disturbances over the Northern Urals. *Izv. Atmos. Oceanic Phys.* **13**(5), 318–324.

Kuettner, J. (1958). The rotor in the lee of mountains. *Schweiz. Aero-Rev. Bern* **33,** 208–215.

Larsson, L. (1954). Observations of lee wave clouds in the Jämtland Mountains, Sweden. *Tellus* **6,** 124–138.

Leovy, C. B. (1977). The atmosphere of Mars. *Sci. Am.* **237** (1), 34–43.

Lester, P. F. (1976). Evidence of long lee waves in southern Alberta. *Atmosphere* **14,** 28–36.

Lester, P. F., and Fingerhut, W. A. (1974). Lower turbulent zones associated mountain lee waves. *J. Appl. Meteorol.* **13,** 54–61.

Lettau, H. H. (1966). A case study of katabatic flow on the south polar plateau. Studies in Antarctic Meteorology of the American Geophysics Union, Washington, D. C. Pp. 1–11.

Lied, N. T. (1964). Stationary hydraulic jumps in a katabatic flow near Davis, Antarctica 1961. *Aust. Meteorol. Mag.* **47,** 40–51.

Lilly, D. K. (1978). A severe downslope windstorm and aircraft turbulence event induced by a mountain wave. *J. Atmos. Sci.* **35,** 59–77.

Lilly, D. K., and Kennedy, P. J. (1973). Observations of a stationary mountain wave and its associated momentum flux and energy dissipation. *J. Atmos. Sci.* **30,** 1135–1152.

Lilly, D. K., and Lester, P. F. (1974). Waves and turbulence in the stratosphere, *J. Atmos. Sci.* **31,** 800–812.

Lilly, D. K., and Zipser, E. J. (1972). The front range windstorm of 11 January 1972—A meteorological narrative. *Weatherwise* **25** (2), 56–63.

Lilly, D. K., Waco, D. E., and Adelfang, S. I. (1974). Stratospheric mixing estimated from high-altitude turbulence measurements. *J. Appl. Meteorol.* **13,** 488–493.

Lindsay, C. V. (1962). Mountain waves in the Appalachians. *Mon. Weather Rev.* **90,** 271–276.

Long, R. R. (1953). Some aspects of stratified fluids, I. A theoretical investigation. *Tellus* **5,** 42–58.

Long, R. R. (1954). Some aspects of the flow of stratified fluids, II.Experiments with a two fluid system. *Tellus* **6,**97–115.

Long, R. R. (1955). Some aspects of the flow of stratified fluids, III. Continuous density gradients. *Tellus* **7,** 341–357.

Long, R. R. (1970). Blocking effects in flow over obstacles. *Tellus* **22,** 471–479.

Long, R. R. (1972). Finite amplitude disturbances in the flow of inviscid rotating and stratified fluids over obstacles. *Annu. Rev. Fluid Mech.* **4,** 69–92.

Lopez, M. E., and Howell, W. E. (1967). Katabatic winds in the equatorial Andes. *J. Atmos. Sci.* **24,** 29–35.

Ludlam, F. H. (1952). Orographic cirrus. *Q. J. R. Meteorol. Soc.* **78,** 554–562.

Lyra, G. (1943). Theorie der stationären Leewellenströmung in freier Atmosphäre. *Z. Angew. Math. Mech.* **23,** 1–28.

MacHattie, L. B. (1968). Kananaskis valley winds in summer. *J. Appl. Meteorol.* **7,** 348–352.

McIntyre, M. E. (1972). On Long's hypothesis of no upstream influence in uniformly stratified or rotating flow. *J. Fluid Mech.* **52,** 202–243.

Mahrer, Y., and Pielke, R. A. (1975). A numerical study of the airflow over mountains using the two-dimensional version of the University of Virginia mesoscale model. *J. Atmos. Sci.* **32,** 2144–2155.

Mahrer, Y., and Pielke, R. A. (1977). A numerical study of the airflow over irregular terrain. *Beitr. Phys. Atmos.* **50,** 98–113.

Manley, G. (1945). The Helm wind of Crossfell, 1937–1939. *Q. J. R. Meteorol. Soc.* **71,** 197–219.

Mawson, D. (1915). "Home of the Blizzard" (Vol. 1). Heinemann, London.

Miles, J. W. (1968). Lee waves in a stratified flow. Pt. 1. Thin barrier. *J. Fluid Mech.* **32,**

Miles, J. W. (1969). Waves and wave drag in stratified flows. *Proc. Int. Congr. Appl. Mech., 12th, 1968.* Springer-Verlag, Berlin and New York.

Miles, J. W. (1971). Upstream boundary-layer separation in stratified flow. *J. Fluid Mech.* **48,** 791–795.

Musaelyan, Sh. A. (1964). Barrier Waves in the Atmosphere, Israel Program for Scientific Translations, Jerusalem.

Nansen, F. (1890). "Paa Ski over Grønland. "Kristiania, Oslo.

Nicholls, J. M. (1973). The airflow over mountains: Research 1958–1972. WMO Tech. Note No. 127.

Onishi, G. (1969). A numerical method for three-dimensional mountain waves. *J. Meteorol. Soc. Japan* **47,** 352–359.

Palm, E. (1958a). Airflow over mountains. Indeterminacy of solution-comment. *Q. J. Roy. Met. Soc.* **84,** 464–465.

Palm, E. (1958b). Two-dimensional and three-dimensional mountain waves. Oslo, Geofys. Publ. **20,**

Pearce, R. P., and White, P. W. (1967). Lee-wave characteristics derived from a three-layer model. *Q. J. R. Meteorol Soc.* **93,** 155–165.

Queney, P. (1947). Theory of perturbations in stratified currents with applications to airflow over mountain barriers. Dept. of Meteorology, Univ. of Chicago, Misc. Report No. 23.

Queney, P., Corby, G. A., Gerbier, N., Koschmieder, H., and Zierep, J. (1960). The airflow over mountains. WMO Tech. Note No. 34.

Ramenskiy, A. M., Kononenko, S. M., and Gutman, L. N. (1976). The stationary nonlinear one-dimensional mesoscale problem of the influence of orography on the motion of an air mass. *Atmos. Oceanic Phys.* **12,** 534–535.

Reynolds, R. D., Lamberth, R. L., and Wurtele, M. G. (1968). Investigation of a complex mountain wave situation. *J. Appl. Meteorol.* **7,** 353–358.

Richwien, B. A. (1978). The damming effect of the Southern Appalachians. *Bull. Am. Meteorol. Soc.* **59,** 870. (Abstract)

Riley, J. J., Liu, H.-T., and Geller, E. W. (1975). A numerical and experimental study of stably stratified flow around complex terrain. Flow Research Inc., Washington, D.C., Report No. 58.

Sarker, R. P., and Calheiros, R. V. (1974). Theoretical analysis of lee waves over the Andes as seen by satellite pictures. *Pure Appl. Geophys.* **112,** 301–319.

Sawyer, J. S. (1959). The introduction of the effects of topography into methods of numerical forecasting. *Q. J. R. Meteorol. Soc.* **85,** 31–43.

Sawyer, J. S. (1960). Numerical calculation of the displacements of a stratified airstream crossing a ridge of small height. *Q. J. R. Meteorol. Soc.* **86,** 326–345.

Sawyer, J. S. (1962). Gravity waves in the atmosphere as a three-dimensional problem. *Q. J. R. Meteorol. Soc.* **88,** 412–425.

Schwerdtfeger, W. (1975). Mountain barrier effect on the flow of stable air north of the Brooks Range. *In* "Climate of the Arctic," (G. Weller and S. Bowling, eds.), pp. 204–208. Geophysical Institute University of Alaska, Fairbanks.

Scorer, R. S. (1949). Theory of lee waves of mountains. *Q. J. R. Meteorol. Soc.* **75,**41–56.

Scorer, R. S. (1955). Theory of airflow over mountains: IV. Separation of flow from the surface. *Q. J. R. Meteorol. Soc.* **81,** 340–419.

Scorer, R. S. (1956). Airflow over an isolated hill. *Q. J. R. Meteorol. Soc.* **82,** 75–81.

Scorer, R. S. (1958). Airflow over mountains: Indeterminacy of solution. *Q. J. R. Meteorol. Soc.* **84,** 182–183.

Scorer, R. S. (1978). "Environmental Aerodynamics." Wiley, New York.

Scorer, R. S., and Wilkinson, M. (1956). Waves in the lee of an isolated hill. *Q. J. R. Meteorol. Soc.* **82,** 419–427.

Seginer, I. (1972): Wind break drag calculated from the horizontal velocity field. *Bound.-Layer Meteorol.* **3,** 87–97.

Segur, H. (1971). A limitation on Long's model in stratified fluid flows. *J. Fluid. Mech.* **48,** 161–179.

Serguis, L. A., Ellis, G. R., and Ogden, R. M. (1962). The Santa Ana winds of Southern California. *Weatherwise* **15** (3), 102–105.

Sheppard, P. A. (1956). Airflow over mountains. *Q. J. R. Meteorol. Soc.* **82,** 528.

Smirnova, I. V. (1968). Wave clouds produced by obstacles as observed by satellite. *Gidromet. Tsentr. USSR Tr.* **20,** 30–34.

Smith, R. B. (1976). The generation of lee waves by the Blue Ridge. *J. Atmos. Sci.* **33,** 507–519.

Smith, R. B. (1977). The steepening of hydrostatic mountain waves. *J. Atmos. Sci.* **34,** 1634–1654.

Smith, R. B. (1978). A measurement of mountain drag. *J. Atmos. Sci.* **9,** 1644–1654.

Smith, R. B. (1980). Linear theory of stratified hydrostatic flow past an isolated mountain. *Tellus* (submitted).

Sokhov, T. Z., and Gutman, L. N. (1968). The use of the long-wave method in the nonlinear problem of the motion of a cold air mass over a mountain ridge. *Atmos. Oceanic Phys.* **4,** 11–16.

Soma, S. (1969). Dissolution of separation in the turbulent boundary layer and its applications to natural winds. *Meteorol. Geophys.* **20**(2), 111–174.

Starr, J. R., and Browning, K. A. (1972). Observations of lee waves by high-power radar. *Q. J. R. Meteorol Soc.* **98,** 73–85.

Sterten, A. K. (1963). A further investigation of the mountain and valley wind system in southeastern Norway. Internal Report K-254, Norwegian Defense Research Establishment, Kjeller, Norway.

Stringer, E. T. (1972). "Foundations of Climatology." Freeman, San Francisco.

Taylor, P. A. (1977a). Some numerical studies of surface boundary-layer flow above gentle topography. *Bound.-Layer Meteorol.* **11,** 439–465.

Taylor, P. A. (1977b). Numerical studies of neutrally stratified planetary boundary-layer flow above gentle topography. *Bound.-Layer Meteorol.* **12,** 37–60.

Taylor, P. A., and Gent, P. R. (1974). A model of atmospheric boundary-layer flow above an isolated two-dimensional hill: an example of flow above "gentle topography." *Bound.=Layer Meteorol.* **7,** 349–362.

Taylor, P. A., Gent, P. R., and Keen, J. M. (1976). Some numerical solutions for turbulent boundary-layer flow above fixed, rough, wavy surfaces. *Geophys. J. R. Astron. Soc.* **44,** 177–201.

Trubnikov, B. N. (1959). Prostranstvennaya zadacha obtekaniya vozvyshennosti neogranichennym sverkhu vozdushnym potokom. *Akad. Nauk. Dokl.* **129,** 781–784.

Turner, J. S. (1973). "Buoyancy Effects in Fluids." Cambridge Univ. Press, London and New York.

Urfer-Henneberger, Ch. (1964). Wind- und Temperatur Verhältnisse an ungestörten Schönwettertagen im Dischmatal bei Davos. *Mitt. Schweiz, Anst. Forstl.* Versuchsw. **40** (6), 389–441.

Vergeiner, I. (1971). Operational linear lee wave model for arbitrary basic flow and two-dimensional topography. *Q. J. R. Meteorol. Soc.* **97,** 30–60.

Vergeiner, I. (1975). A numerical model of three-dimensional, mountain-induced gravity wave flow. *Riv. Ital. Geofis.* **I,** 15–31.

Vergeiner, I. (1976). Foehn- and lee-wave-flow in a three-dimensional numerical model. *Ber. Nat. Med. Ver. Innsbruck* **63,** 11–56.

Vergeiner, I., and Lilly, D. K. (1970). The dynamic structure of lee-wave flow as obtained from balloon and airplane observations. *Mon. Weather Rev.* **98,** 220–232.

Viezee, W., Collis, R. T. H., and Lawrence, J. D. (1973). An investigation of mountain waves with lidar observations. *J. Appl. Meteorol.* **12,** 140–148.

Vinnichenko, J. K. *et al.* (1973). Mountain waves. *In* "Turbulence in the Free Atmosphere." Plenum, New York.

Wallington, C. E., and Portnall, J. (1958). A numerical study of the wavelength and amplitude of lee waves. *Q. J. R. Meteorol. Soc.* **84,** 38–45.

Warner, R., Anthes, R., and McNab, A. (1978). Numerical simulations with a three-dimensional mesoscale model. *Mon. Weather Rev.* **106,** 1079–1099.

Wilkins, E. M. (1955). A discontinuity surface produced by topographic winds over the Upper Snake River Plain, Idaho, *Bull. Am. Meteorol. Soc.* **36,** 397–408.

Wurtele, M. (1957). The tree-dimensional lee wave. *Beitr. Phys. Frei. Atmos.* **29,** 242–252.

Yih, C.-S. (1960). Exact solutions for steady two-dimensional flow of a stratified fluid. *J. Fluid Mech.* **9,** 161–174.

Yih, C.-S. (1965). "Dynamics of Nonhomogeneous Fluids." Macmillan, New York.

Yih, C.-S., and Guha, C. R. (1955). Hydraulic jump in a fluid system of two layers. *Tellus* **7,** 359–366.

Yoshino, M. M. (1975). "Climate in a Small Area." Univ. of Tokyo Press.

Yoshino, M. M. (1976). Local Wind Bora." Univ. of Tokyo Press.

Zeytounian, R. Kh. (1969). Study of wave phenomena in the steady flow of an inviscid stratified fluid. RAE Trans. #1404 of ONERA Publ. #126.

Section 3. The Flow near Mesoscale and Synoptic-Scale Mountains

Batchelor, G. K. (1967). "An Introduction to Fluid Dynamics." Cambridge Univ. Press, London and New York.

Blumen, W. (1965). Momentum flux by mountain waves in a stratified rotating atmosphere. *J. Atmos. Sci.* **22,** 529–534.

Bretherton, F. P. (1969). Momentum transport by gravity waves. *Q. J. R. Meteorol. Soc.* **95,** 213–243.

Brinkmann, W. A. R. (1970). The chinook at Calgary (Canada). *Arch. Meteorol. Geophys. Biokl. (B)* **18,** 279–286.

Buzzi, A., and Tibaldi, S. (1977). Inertial and frictional effects on rotating stratified flow over topography. *Q. J. R. Meteorol. Soc.* **103,** 135–150.

Carlson, T. N. (1961). Lee-side frontogenesis in the Rockey Mountains. *Mon. Weather Rev.* **89,** 163–172.

Chung, Y. S., Hage, K. D., and Reinelt, E. R. (1976). On lee cyclogenesis and airflow in the Canadian Rocky Mountains and the east Asian mountains. *Mon. Weather Rev.* **104,** 879–891.

Defant, F. (1951). Local winds. *In* "Compendium of Meteorology" (T. F. Malone, ed.), pp. 655–672. American Meteorological Society.

Egger, J. (1972). Numerical experiments on the cyclogenesis in the Gulf of Genoa. *Bietr. Phys. Atmos.* **45,** 320–346.

Egger, J. (1974). Numerical experiments on lee cyclonesis. *Mon. Weather Rev.* **102,** 847–860.

Eliassen, A. 1951. Slow thermally or frictionally controlled meridional circulation in a circular vortex. *Astrophys. Norv.* **V**(2), 19.

Eliassen, A. (1968). On meso-scale mountain waves on the rotating earth. *Geofys. Publ.* **27,** 1-15.

Eliassen, A., and Palm, E. (1960). On the transfer of energy in stationary mountain waves. *Geofys. Publ.* **22,** 1–23.

Eliassen, A., and Rekustad, J.-A. (1971). A numerical study of meso-scale mountain waves. *Geofys. Publ.* **28,** 1–13.

Hage, K. D. (1961). On summer cyclogenesis in the lee of the Rocky Mountains. *Bull. Am. Meteorol. Soc.* **42,** 20–33.

Haltiner, G., and Martin, F. (1957). "Dynamical and Physical Meteorology." McGraw-Hill, New York.

Hess. S. L. (1959). "Introduction to Theoretical Meteorology." Holt, New York.

Hess, S. L., and Wagner, H. (1948). Atmospheric waves in the northwestern United States. *J. Meteorol.* **5,** 1–19.

Hogg, N. G. (1973). On the stratified Taylor column. *J. Fluid Mech.* **58,** 517–537.

Holton, J. R. (1972). "An Introduction to Dynamical Meteorology." Academic Press, New York.

Jacobs, S. J. (1964). On stratified flow over bottom topography. *J. Mar. Res.* **22,** 223–235.

Janowitz, G. S. (1975). The effect of bottom topography on a stratified flow on a β-plane. *J. Geophys. Res.* **80,** (30), 4163–4168.

Johnson, E. R. (1977). Stratified Taylor Columns on a beta-plane. *Geophys. Astrophys. Fluid Dyn.* **9,** 159–177.

Jones, W. L. (1967). Propagation of internal gravity waves in fluids with shear flow and rotation. *J. Fluid Mech.* **30,** 439–448.

Klein, W. H. (1957). Principal tracks and mean frequencies of cyclones and anti-cyclones

in the Northern Hemisphere. Research Paper No. 40, U.S. Weather Bureau, Washington, D.C.

Manabe, S., and Terpstra, T. B. (1974). The effects of mountains on the general circulation of the atmosphere as identified by numerical experiments. *J. Atmos. Sci.* **31,** 3–42.

Mason, P. J., and Sykes, R. I. (1978). On the interaction of topography and Ekman boundary layer pumping in a stratified atmosphere. *Q. J. R. Meteorol. Soc.* **104,** 475–490.

Merkine, L-O. (1975). Steady finite-amplitude baroclinic flow over long topography in a rotating stratified atmosphere. *J. Atmos. Sci.* **32,** 1881–1893.

Merkine, L. O., and Kalnay-Rivas, E. (1976). Rotating stratified flow over finite isolated topography. *J. Atmos. Sci.* **33,** 908–922.

Newton, C. W. (1956). Mechanisms of circulation change during a lee cyclogenesis. *J. Meteorol.* **13,** 528–539.

Peattie, R. (1936). "Mountain Geography—A Critique and Field Study." Harvard Univ. Press, Cambridge, Massachusetts.

Petterssen, S. (1956). "Weather Analysis and Forecasting" (2nd Ed.), Vol. 1. McGraw-Hill, New York.

Queney, P. (1947). Theory of perturbations in stratified currents with applications of airflow over mountain barriers. Dept. of Meteorology., Univ. of Chicago, Misc. Report No. 23.

Queney, P. (1948). The problem of airflow over mountains: A summary of theoretical studies. *Bull. Am. Meteorol. Soc.* **29,** 16–26.

Radinović, D. (1965a). On forecasting in the West Mediterranean and other areas bounded by mountain ranges by baroclinic model. *Arch. Meteorol. Geophys. Biokl. (A)* **14,** 279–299.

Radinović, D. (1965b). Cyclonic activity in Yugoslavia and surrounding areas. *Arch. Meteorol. Geophys. Biokl. (A)* **14,** 391–408.

Reitan, C. H. (1974). Frequencies of cyclones and cyclogenesis for North America, 1951–1970. *Mon. Weather Rev.* **102,** 861–868.

Robinson, A. R. (1960). On Two-dimensional inertial flow in a rotating stratified fluid. *J. Fluid Mech.* **9,** 321–332.

Smith, R. B. (1979a). The influence of the earth's rotation on mountain wave drag. *J. Atmos. Sci.* **36,** 177–180.

Smith, R. B. (1979b). Some aspects of the quasi-geostrophic flow over mountains. *J. Atmos. Sci.* **36.**

Speraza, A. (1975). The formation of baric depressions near the Alps. *Ann. Geofis. Rome* **28,** 177–217.

Trevisan, A. (1976). Numerical experiments on the influence of orography on cyclone formation with an isentropic primitive equation model. *J. Atmos. Sci.* **33,** 768–780.

Woolridge, G. L. (1972). Effects of internal gravity waves on energy budgets and the vertical transport of angular momentum over mountainous terrain. *Mon Weather Rev.* **100,** 177–188.

Yoshino, M. M. (1975). "Climate in a Small Area." Univ. of Tokyo Press.

Section 4. Orographic Control of Precipitation

Ackerman, B. (1960). Orographic-convective precipitation as revealed by radar. *In* "Physics of Precipitation" (H. Weickmann, ed.), pp. 79–85. Geophys. Monograph No. 5, American Geophysics Union, Washington, D.C.

Andersen, P. (1972). The distribution of monthly precipitation in southern Norway in relation to prevailing H. Johansen weather types. Yearbook for Univ. of Bergen Mat., Naturv. Series, No. 1.

Atkinson, B. W., and Smithson, P. A. (1974). Meso-scale circulations and rainfall patterns in an occluding depression. *Q. J. R. Meteorol. Soc.* **100,** 3–22.

Badar, M. J., and Roach, W. T. (1977). Orographic rainfall in warm sections of depressions. *Q. J. R. Meteorol. Soc.* **103,** 269–280.

Bergeron, T. (1949). The problem of artificial control of rainfall on the globe. II. The coastal orographic maxima of precipitation in autumn and winter. *Tellus* **1**(3), 15–32.

Bergeron, T. (1960a). "Problems and Methods of Rainfall Investigation. Physics of Precipitation," pp. 5–30. American Geophysics Union.

Bergeron, T. (1960b). "Operation and results of "Project Pluvius." Physics of Precipitation," pp. 152–157. American Geophysics Union.

Bergeron, T. (1968). Studies of the oreigenic effect on the areal fine structure of rainfall distribution. Meteorological Institute Uppsala Univ., Report No. 6.

Bergeron, T. (1973). Mesometeorological studies of precipitation. V. Monthly rainfall in the Uppsala field. Meteorological Institute Uppsala Univ., Report No. 38.

Biswas, A. K., and Jayaweera, K. (1976). NOAA-3 satellite observations of thunderstorms in Alaska. *Mon. Weather Rev.* **104,** 292–297.

Bleasdale, A., and Chan, Y. K. (1972). Orographic influences on the distribution of precipitation. *In* "Distribution of Precipitation in Mountainous Areas." WMO/OMM, Report #326, Vol. II.

Bonacina, L. C. W. (1945). Orographic rainfall and its place in the hydrology of the globe. *Q. J. R. Meteorol. Soc.* **71,** 41–55.

Braham, R. R., and Draginis, M. (1960). Roots of orographic cumuli. *J. Meteorol.* **17,** 214–226.

Brinkman, W. A. R. (1971). What is a foehn? *Weather* **26**(6), 230–239.

Browning, K. A., Hill, F. F., and Pardoe, C. W. (1974). Structure and mechanism of precipitation and the effect of orography in a wintertime warm sector. *Q. J. R. Meteorol. Soc.* **100,** 309–330.

Browning, K. A., Pardoe, C., and Hill, F. F. (1975). The nature of orographic rain at wintertime cold fronts. *Q. J. R. Meteorol. Soc.* **101,** 333–352.

Changnon, S. A., Jr., Jones, D. M. A., and Huff, F. A. (1975). Precipitation increases in the low hills of southern Illinois: Part 2. Field investigation of anomaly. *Mon. Weather Rev.* **103,** 830–836.

Chappell, C. F., Grant, L. O., and Mielke, P. W., Jr. (1971). Cloud seeding effects on precipitation intensity and duration of wintertime orographic clouds. *J. Appl. Meteorol.* **10,** 1006–1010.

Chuan, G. K., and Lockwood, J. G. (1974). An assessment of topographic of controls on the distribution of rainfall in the central Pennines. *Meteorol. Mag.* **103,** 275–287.

Colton, D. E. (1976). Numerical simulation of the orographically induced precipitation distribution for use in hydrologic analysis. *J. Appl. Meteorol.* **15,** (12), 1241–1251.

Defant, F. (1951). Local winds. *In* "Compendium of Meteorology" (T. F. Malone, ed.), pp. 655–672. American Meteorological Society, Boston.

Douglas, C. K. M., and Glasspoole, J. (1947). Meteorological conditions in orographic rainfall in the British Isles. *Q. J. R. Meteorol. Soc.* **73,** 11–38.

Elliot, R. D., and Hovind, E. L. (1964). The water balance of orographic clouds. *J. Appl. Meteorol.* **3,** 235–239.

Elliot, R. D., and Shaffer, R. W. (1962). The development of quantitative relationships between orographic precipitation and air-mass parameters for use in forecasting and cloud seeding evaluation. *J. Appl. Meteorol.* **1,** 218–228.

Fosberg, M. A. (1967). Numerical analysis of convective motions over a mountain ridge. *J. Appl. Meteorol.* **6,** 889–904.

Fraser, A. B., Easter, R., and Hobbs, P. (1973). A theoretical study of the flow of air and fallout of solid precipitation over mountainous terrain: Part I. Airflow model. *J. Atmos. Sci.* **30,** 813–823.

Gocho, Y. (1978). Numerical experiment of orographic heavy rainfall due to a stratiform cloud. *J. Meteorol. Soc. Japan* **56,** 405–422.

Gocho, Y., and Nakajima, C. (1971). On the rainfall around the Suzuka Mountains. *Ann. Disaster Prev. Res. Inst.* **14** (B), 103–118.

Grant, L. O., and Elliot, R. D. (1974). The cloud seeding temperature window. *J. Appl. Meteorol.* **13,** 355–363.

Harrold, T. W., English, E. J., and Nicholass, C. A. (1974). The accuracy of radar-derived rainfall measurements in hilly terrain. *Q. J. R. Meteorol. Soc.* **100,** 331–350.

Henz, J. F. (1972). An operational technique of forecasting thunderstorms along the lee slope of a mountain range. *J. Appl. Meteorol.* **11,** 1284–1292.

Hill, G. E. (1978). Observations of precipitation-forced circulations in winter orographic storms. *J. Atmos. Sci.* **35,** 1463–1472.

Hobbs, P. V., Honze, R., Jr., and Matejka, T. (1975). The dynamical and microphysical structure of an occluded frontal system and its modification by orography. *J. Atmos. Sci.* **32,** 1542–1562.

Kuo, J. T., and Orville, H. D. (1973). A radar climatology of summertime convective clouds in the Black Hills. *J. Appl. Meteorol.* **12,** 359–368.

Longley, R. W. (1975). Precipitation in valleys. *Weather* **30,** 294–300.

MacHattie, L. B. (1968). Kananaskis valley winds in summer. *J. Appl. Meteorol.* **7,** 348–352.

Mason, B. J. (1971). "The Physics of Clouds." Oxford, Univ. Press (Clarendon), London and New York.

Mielke, P. W., Grant, L. O., and Chappell, C. F. (1971). An independent replication of the Climax wintertime orographic seeding experiment. *J. Appl. Meteorol.* **10,** 1198–1212.

Myers, V. A. (1962). Airflow on the windward side of a ridge. *J. Geophys. Res.* **67,** 4267–4291.

Nordø, J., and Hjortnaes, K. (1966). Statistical studies of precipitation on local, national, and continental scales. *Geofys. Publ.* **16,** (12).

Orville, H. D. (1968). Ambient wind effects on the initiation and development of cumulus clouds over mountains. *J. Atmos. Sci.* **25,** 385–403.

Petterssen, S. (1940). "Weather Analysis and Forecasting." McGraw-Hill, New York.

Ramage, C. S. (1971). "Monsoon Meteorology." Academic Press, New York.

Raymond, D. J. (1972). Calculation of airflow over an arbitrary ridge including diabatic heating and cooling. *J. Atmos. Sci.* **29,** 837–843.

Reynolds, D. W., and Morris, K. R. (1978). Satellite support to the Sierra Cooperative Pilot Project. *Conf.* Sierra *Nevada Meteorol. Am. Meteorol. Soc. Boston.*

Reynolds, D. W., Vonder Haar, T. H., and Grant, L. O. (1978). Meteorological satellites in support of weather modification. *Bull. Am. Meteorol. Soc.* **59,** 269–281.

Ryden, B. E. (1972). On the problem of vertical distribution of precipitation especially in areas with great height differences. *In* "Distribution of Precipitation in Mountainous Areas," pp. 362–369. Vol. II, WMO/OMM, Report #326.

Sarker, R. P. (1966). A dynamical model of orographic rainfall. *Mon. Weather Rev.* **94,** 555–572.

Sarker, R. P. (1967). Some modifications in a dynamical model of orographic rainfall. *Mon. Weather Rev.* **95,** 673–684.

Sawyer, J. S. (1956). The physical and dynamical problems of orographic rain. *Weather* **11,** 375–381.

Silverman, A. (1960). The effect of a mountain on convection. *In* "Cumulus Dynamics" (C. F. Anderson, ed.), pp. 4–27. Pergamon, Oxford.

Skaar, E. (1976). Local climates and growth climates of the Sognefjord region. *Meteorol. Ann.* **7,** 19–67.

Smebye, S. (1978). A synoptic investigation of a situation with exceptionally heavy precipitation and early snow over southeastern Norway. Unpublished manuscript from Det Norske Meteorologiske Institutt, Blindern, Norway.

Spinnangr, F., and Johansen, H. (1954). On the distribution of precipitation in maritime tropical air over Norway. *Meteorol. Ann.* **3,** (14), 351–424.

Spinnangr, F., and Johansen, H. (1955). On the influence of the orography in southern Norway on instability showers from the sea. *Meteorol. Ann.* **4,** (3), 17–35.

Sterten, A. K. (1963). A further investigation of the mountain and valley wind system in southeastern Norway. Internal Report K-254, Norwegian Defense Research Establishment, Kjeller, Norway.

Storebø, P. B. (1976). Small-scale topographical influences on precipitation. *Tellus* **28,** 45–59.

Storr, D., and Ferguson, H. L. (1972). The distribution of precipitation in some mountainous Canadian watersheds. *In* "Distribution of Precipitation in Mountainous Areas," Vol. II. WMO/OMM, Report #326.

Turner, J. S. (1973). "Buoyancy Effects in Fluids." Cambridge Univ. Press, London and New York.

Utaaker, K. (1963). The local climate of Nes, Hedmark. *Univ. Bergen Skrifter* **28.**

Williams, P., and Peck, E. L. (1962). Terrain influences on precipitation in the intermountain west as related to synoptic situations. *J. Appl. Meteorol.* **1,** 343–347.

Wilson, J., and Atwater, M. (1972). Storm rainfall variability over Connecticut. *J. Geophys. Res.* **77,** 3950–3956.

Yoshino, M. M. (1975). "Climate in a Small Area." Univ. of Tokyo Press.

Young, K. C. (1974a). A numerical simulation of wintertime orographic precipitation: Part I. Description of model microphysics and numerical technique. *J. Atmos. Sci.* **31,** 1735–1748.

Young, K. C. (1974b). A numerical simulation of wintertime orographic precipitation: Part II. Comparison of natural and AgI seeded conditions. *J. Atmos. Sci.* **31,** 1749–1767.

Section 5. Planetary-Scale Mountain Waves

Andrews, D. G., and McIntyre, M. E. (1976). Planetary waves in horizontal and vertical shear: The generalized Eliassen–Palm relation and the mean zonal acceleration. *J. Atmos. Sci.* **33,** 2031–2048.

Beland, M. (1976). Numerical study of the nonlinear Rossby wave critical level development in a barotropic zonal flow. *J. Atmos. Sci.* **33,** 2066–2078.

Bolin, B. (1950). On the influence of the Earth's orography on the character of the westerlies. *Tellus* **2,** 184–195.

Booker, J. R., and Bretherton, F. P. (1967). The critical layer for internal gravity waves in a shear flow. *J. Fluid Mech.* **27,** 513–539.

Charney, J. G., and Drazin, P. G. (1961). Propagation of planetary-scale disturbance from the lower into the upper atmosphere. *J. Geophys. Res.* **66,** 83–109.

Charney, J. G., and Eliassen, A. (1949). A numerical method for predicting the perturbations of the middle latitude westerlies. *Tellus* **1,** (2), 38–54.

Dickinson, R. E. (1968a). On the exact and approximate linear theory of vertically propagating planetary Rossby waves forced at a spherical lower boundary. *Mon. Weather Rev.* **96,** 405–415.

Dickinson, R. E. (1968b). Planetary Rossby waves propagating vertically through weak westerly wind wave guides. *J. Atmos. Sci.* **25,** 984–1002.

Dickinson, R. E. (1969). Vertical propagation of planetary Rossby waves through an atmosphere with Newtonian cooling. *J. Geophys. Res.* **74,** 929–938.

Dickinson, R. E. (1970). Development of a Rossby wave critical level. *J. Atmos. Sci.* **27,** 627–633.

Egger, J. (1978). On the theory of planetary standing waves. *Beitr. Phys. Atmos.* **51,** 1–14.

Geisler, J. E., and Dickinson, R. E. (1975). External Rossby modes on a β-plane with realistic vertical wind shear. *J. Atmos. Sci.* **32,** 2082–2093.

Hirota, I. (1971). Excitation of planetary Rossby waves in the winter stratosphere by periodic forcing. *J. Meteorol. Soc. Jpn* **49,** 439–449.

Holton, J. R. (1975). The dynamic meteorology of the stratosphere and mesosphere. *Meteorol. Monogr.* No. 37, *Am. Meteorol. Soc.*

Holton, J. R. (1976). A semi-spectral numerical model for wave-mean flow interactions in the stratosphere: Application to sudden stratospheric warmings. *J. Atmos. Sci.* **33,** 1639–1649.

Johnson, E. R. (1977). Stratified Taylor columns on a beta-plane. *Geophys. Astrophys. Fluid Dyn.* **9,** 159–177.

Kasahara, A., and Washington, W. M. (1971). General circulation experiments with a six-layer NCAR model, including orography, cloudiness and surface temperature calculations. *J. Atmos. Sci.* **28,** 657–701.

Kasahara, A., Sasamori, T., and Washington, W. M. (1973). Simulation experiments with a 12-layer stratospheric global circulation model. 1. Dynamical effect of the Earth's orography and thermal influence of continentality. *J. Atmos. Sci.* **30,** 1229–1251.

Manabe, S., and Terpstra, T. B. (1974). The effects of mountains on the general circulation of the atmosphere as identified by numerical experiments. *J. Atmos. Sci.* **31,** 3–42.

McNulty, R. P. (1976). Vertical energy flux in planetary-scale waves: Observational results. *J. Atmos. Sci.* **33,** 1172–1183.

Matsuno, T. (1970). Vertical propagation of stationary planetary waves in the winter northern hemisphere. *J. Atmos. Sci.* **27,** 871–883.

Namias, J. (1966). Nature and possible causes of the northeastern United States drought during 1962–1965. *Mon. Weather Rev.* **94,** 543–554.

Queney, P. (1948). The problem of airflow over mountains. A summary of theoretical studies. *Bull. Am. Meteorol. Soc.* **29,** 16–26.

Ratcliffe, R. A. S. (1974). The use of 500mb anomalies in long-range forecasting. *Q. J. R. Meteorol. Soc* **100,** 234–244.

Reiter, E. R. (1963). "Jet Stream Meteorology." Chicago Univ. Press, Chicago.

Saltzman, B. (1965). On the theory of the winter-average perturbations in the troposphere and stratosphere. *Mon. Weather Rev.* **93,** 195–211.

Saltzman, B. (1968). Surface boundary effects on the general circulation and macroclimate: A review of the theory of the quasi-stationary perturbations in the atmosphere. *Meteorol. Monogr.* **8** (30), 4–19.

Sankar-Rao, M. (1965a). Continental elevation influence on the stationary harmonics of the atmospheric motion. *Pure Appl. Geophys.* **60,** 141–159.

Sankar-Rao, M. (1965b). Finite difference models for the stationary harmonics of atmospheric motion. *Mon. Weather Rev.* **93,** 213–224.

Schoeberl, M., and Geller, M. (1976). The structure of stationary planetary waves in winter in relation to the polar night jet intensity. *Geophys. Res. Lett.* **3,** 177–180.

Simmons, A. J. (1974). Planetary disturbances in the polar winter stratosphere. *Q. J. R. Meteorol. Soc.* **100,** 76–108.

Smagorinsky, J. (1953). The dynamical influence of large-scale sources and sinks on the quasi-stationary mean motions of the atmosphere. *Q. J. R. Meteorol. Soc.* **79,** 342–366.

Smith, R. F. T., and Davies, D. R. (1977). A note on some numerical experiments with model mountain barriers. *Tellus* **29,**(2), 97–106.

VanLoon, H., Jenne, R. L., and Labitzke, K. (1973). Zonal harmonic standing waves. *J. Geophys. Res.* **78,** 4463–4471.

Wagner, J. (1977). Past record cold winter explained. *Bull. Am. Meteorol. Soc.* **58,** 109.

White, A. A. (1977). Modified quasi-geostrophic equations using geometric height as vertical coordinate. *Q. J. R. Meteorol. Soc.* **103,** 383–396.